Zintl Ions

DOI: 10.1002/anie.201001630

Zintl Ions, Cage Compounds, and Intermetalloid Clusters of Group 14 and Group 15 Elements

*Sandra Scharfe, Florian Kraus, Saskia Stegmaier, Annette Schier, and Thomas F. Fässler**

Keywords:
cage compounds · Group 14 elements · Group 15 elements · intermetalloid compounds · Zintl ions

In memory of Hans-Georg von Schnering

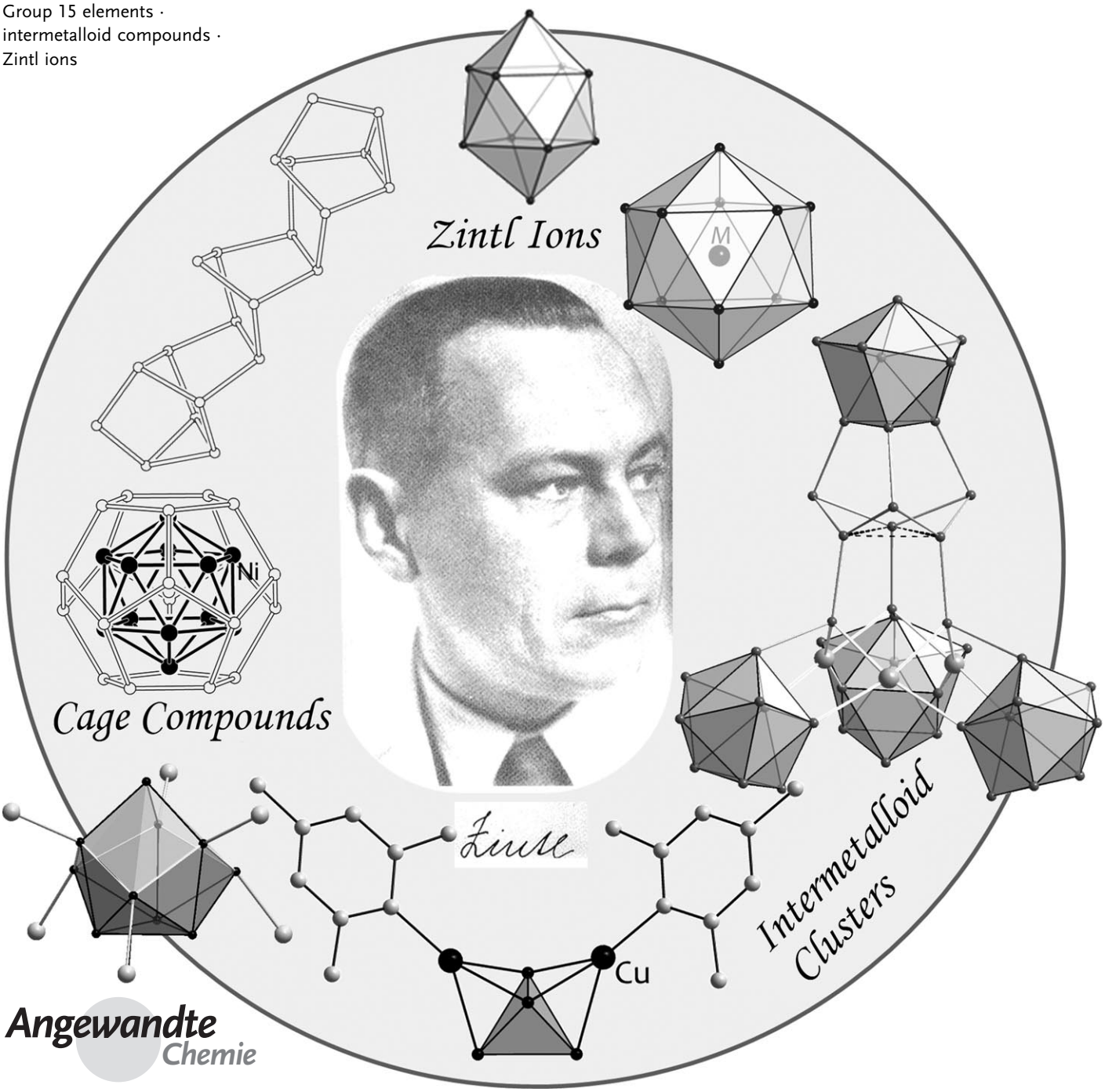

For a long time, Zintl ions of Group 14 and 15 elements were considered to be remarkable species domiciled in solid-state chemistry that have unexpected stoichiometries and fascinating structures, but were of limited relevance. The revival of Zintl ions was heralded by the observation that these species, preformed in solid-state Zintl phases, can be extracted from the lattice of the solids and dissolved in appropriate solvents, and thus become available as reactants and building blocks in solution chemistry. The recent upsurge of research activity in this fast-growing field has now provided a rich plethora of new compounds, for example by substitution of these Zintl ions with organic groups and organometallic fragments, by oxidative coupling reactions leading to dimers, oligomers, or polymers, or by the inclusion of metal atoms under formation of endohedral cluster species and intermetalloid compounds; some of these species have good prospects in applications in materials science. This Review presents the enormous progress that has been made in Zintl ion chemistry with an emphasis on syntheses, properties, structures, and theoretical treatments.

From the Contents

1. Introduction

> *"Die Phantasie kommt hier nicht zu kurz, und abweichende Resultate lassen auch der nächsten Generation noch die Hoffnung auf Neues."*
> Hans-Georg von Schnering[11]

Platonic solids have always impressed mankind, and their realization as homoatomic molecular or ionic cage structures has fascinated chemists and physicists in particular for decades. The discovery of homoatomic carbon fullerenes[1] triggered the development of a captivating research field culminating in the application of nanotubes, and their anions were found to form amazingly simple binary superconducting materials.[2] An improvement of the synthetic approach[3] was, however, necessary to move on from the beauty of the C_{60} polyhedron to research activities in this field towards novel materials.

Gas-phase experiments have revealed the existence of a larger number of homoatomic clusters, which raises questions about the forces that hold the atoms in such structures together and has initiated the search for a synthetic approach to such species. It has been shown that the synthesis and the structural characterization of ligand-stabilized main-group element clusters with up to 84 atoms is possible.[4] In the case of the Group 13 element aluminum, an impressive series of clusters having different nuclearities illustrates that the transition from a small molecule consisting of a few atoms to a metallic solid is possible. These so-called metalloid clusters[5] offer a fantastic possibility to investigate the dependency of the properties of a material from the cluster size. Whereas much attention has been drawn in various Reviews to metalloid Group 13 element clusters,[6] herein we summarize recent developments in the field of Group 14 and 15 element clusters.

Polar intermetallic compounds, that is, compounds consisting of two or three types of metals that have different electronegativities, very often already contain cluster units. If the electronegativity difference of the involved elements is large enough, the resulting intermetallic compound can be described as being salt-like. In compounds with electropositive Group 1 or 2 elements and p-block metals as the more electronegative component, the p-block atoms build clusters and polyanions. In so-called Zintl phases, such element clusters are preformed, and therefore they are good candidates to serve as a source for anionic element clusters, provided that they are soluble so as to achieve a full charge separation.

The transition from generally semiconducting Zintl phases to more or less discrete Zintl anions is possible only for a small number of phases. In case of Group 14 and 15 elements, soluble molecular Zintl polyanions are formed. These homoatomic clusters are not only fascinating because of their aesthetic simplicity and the beauty of their structures, but also because of their enormous synthetic potential. Owing to their versatile chemical reactivity, they can serve as precursors for the synthesis of nanostructured materials or of large intermetalloid clusters. In contrast to Group 13 element clusters, Zintl anions are ligand-free; however, recent research progress has demonstrated that their functionaliza-

[*] Dr. S. Scharfe, Dr. F. Kraus, S. Stegmaier, Dr. A. Schier, Prof. Dr. T. F. Fässler
Department of Chemistry, Technische Universität München
Lichtenbergstrasse 4, 85747 Garching/München (Germany)
Fax: (+49) 89-289-13186
E-mail: thomas.faessler@lrz.tum.de

tion is possible, and thus the fields of Zintl ions and ligand-stabilized main-group-element clusters increasingly merge.

Several Reviews[7–11] have appeared in the field of homoatomic main-group-element clusters, and two recent publications gave an overview of some aspects of Group 14 Zintl anion chemistry.[12,13] Nonetheless, vital developments in the field of Group 14 and 15 element polyanions make it desirable that they are summarized separately and placed in the context of a progressive materials design.

2. A Brief Overview of Zintl Ions

The exploration of the chemistry of polyanions of Group 14 and 15 elements was initiated by the discovery of M. Joannis in 1891, which he described in *Comptes Rendus*: "*Le sodammonium et le potassammonium sont decomposes par divers méteaux, en particulier par le mercure, le plomb et lántimoine. (…) Lorsque l'on met une baguette de plomb pur en excés, en presence du sodammonium, on constate que la liquour mordorée ne trade pas à venir bleue au contact du plomb, puis verde.*"[14] Later, the work of Peck, Smyth, Kraus, and Zintl[15–19] on reactions of alkali metals with p-block elements in liquid ammonia established the perception of the species being highly charged element particles, or homoatomic polyanions. In the report by Joannis, green and deep red solutions were mentioned for the first time, which were observed in the reaction of sodium with lead and antimony, respectively, in liquid ammonia, and later determined to contain $[Pb_9]^{4-}$ and $[Sb_7]^{3-}$ anions. Zintl recognized that the dissolution of binary intermetallic phases such as Na_4Pb_9[20] in liquid ammonia leads to the same solutions. He thus established the close relationship between soluble polyanions and salt-like intermetallic phases. The existence of Group 14 and 15 element polyanions was finally verified by the crystal-structure determination of $[Sn_9]^{4-}$ [21–23] and $[Sb_7]^{3-}$,[24] and has led to a fast growing research field ever since.[7,8] A major step forward towards the isolation and crystallization of compounds containing such Zintl anions was the change of the solvent for the binary phases A_4E_9 and A_3Pn_7 (A = alkali metal, E = Group 14 element, Pn = Group 15 (pnicogen) element) from liquid ammonia to ethylenediamine,[16,25] and many years later to dimethylformamide.[26] To obtain high-quality crystalline materials from Zintl ion-containing solutions, alkali-metal-ion-sequestering agents, such as [2.2.2]crypt,[27] were employed by Corbett.[24] Again it took many years before crown ethers, such as [18]crown-6,[28] and

Thomas F. Fässler studied chemistry and mathematics at the University of Konstanz. After his PhD studies at the University of Heidelberg in the field of organometallic chemistry (Prof. Dr. G. Huttner), he had a stay as a postdoctoral fellow at the University of Chicago working on quantum chemical calculations. He completed his Habilitation in the field of Zintl phases, Zintl ions, and fullerides at ETH Zürich, Switzerland. From 2000 until 2003 he worked as a full professor at the Eduard Zintl Institute of the TU Darmstadt, and took up the chair of Inorganic Chemistry at the TU München in 2003. His research covers solid-state/materials chemistry, main-group-element clusters, fullerenes, and theory.

Sandra Scharfe studied chemistry at the Humboldt University in Berlin (1996—1998) and at the TU München (1998—2001). She received her PhD on Zintl ion chemistry in the group of Prof. Dr. T. F. Fässler (2006—2010).

Florian Kraus studied chemistry at the universities of Regensburg and San Diego (1998–2003). In 2005 he finished his PhD thesis on the reactions of polyphosphides and hydroclosoborates in liquid ammonia under the guidance of Prof. Dr. N. Korber (Regensburg) and Prof. Dr. B. Albert (Hamburg). He was a fellow of the Studienstiftung des Deutschen Volkes and of the Fonds der chemischen Industrie. Since 2006 he has been working on his Habilitation as a Liebig fellow in Professor Dr. T. F. Fässler's laboratories at TU München. Apart from fluorine chemistry, his research is focused on the chemistry of beryllium and uranium.

Saskia Stegmaier studied chemistry at the TU München (2001–2007) and at the University of Oxford (2003/2004). At TU München she joined the Fässler group for her diploma thesis on theoretical and experimental studies of Ge_9 polyanions and received the Jürgen Manchot Studienpreis in 2007. Since 2007, she has been working on her PhD thesis as a fellow of the Studienstiftung des deutschen Volkes in the group of Prof. Dr. T. F. Fässler. Her research is focused on the synthesis and characterization of ternary Zintl phases and on computational studies of intermetalloid cluster anions.

Annette Schier studied chemistry at the TU München (1974—1980) where she also completed her diploma and PhD under the guidance of Prof. Dr. H. Schmidbaur. She was a postdoctoral fellow at the Australian National University at Canberra (1984–1985) and was a Visiting Professor at Chalmers University of Technology, Göteborg, Sweden, in 2004. She is involved in advanced teaching assignments at TU München and was in charge of the organization of several major national and international chemistry conferences.

their derivatives also were successfully used in Zintl ion chemistry: a melt of [18]crown-6 at 40 °C was employed as reaction medium for the elements K/Sn or K/Pb.[29] Later it turned out that different fully and semisequestered cations lead to different products and thus influence the reactivity of Zintl ion solutions.

Discrete atom clusters,[270] and polyanions of Group 14 and 15 elements after a formal electron transfer, also arise in binary or ternary solid-state phases. The smallest polyhedral Group 14 clusters are the tetrahedral $[E_4]^{4-}$ ions, which were observed for the first time for E = Pb in the alloy NaPb in 1953.[30] Only recently, Korber et al. showed that this cluster can be retained in a liquid ammonia solution of Rb_4Pb_4 (binary-phase RbPb).[31] Generally, such 1:1 phases are not soluble, but the larger nine-atom clusters $[E_9]^{4-}$ of Group 14 elements can be easily obtained by dissolution of A_4E_9 phases, which, however, are not available for E = Si. After it was shown that the binary phase Cs_4Ge_9[32] contains the nine-atom cluster $[Ge_9]^{4-}$, the synthesis of nine-atom clusters of the heavier Group 14 elements tin and lead from corresponding alloys became straightforward. Furthermore, it was shown that intermetallic compounds of the general composition $A_{12}E_{17}$ contain $[E_4]^{4-}$ and $[E_9]^{4-}$ polyanions in the ratio 2:1 (A = Na, K, Rb, Cs; E = Si, Ge, Sn), from which the soluble silicon clusters $[Si_4]^{4-}$ and $[Si_9]^{4-}$ became accessible by extraction with liquid ammonia.[33–35] Zintl ions of tin and lead can also be obtained by electrochemical methods when the respective element is used as cathode material.[16,36,37]

Several different approaches have been applied to the synthesis of polypnictides. Reactions of the various modifications of the elemental pnicogens Pn with dissolved or finely dispersed alkali or alkaline earth metals in solution are as common[38] as the congruent dissolution of solid-state phases such as M_3Pn_7 (M = Li–Cs, Pn = P, As; M = Cs, Pn = Sb) or M_3Pn_{11} (M = Na–Cs, Pn = P, As),[39] which already contain the preformed polyanions or the incongruent dissolution. M_4Pn_6 phases (M = K–Cs, Pn = P; M = Rb, Cs, Pn = As) dissolve in liquid ammonia with the formation of $[Pn_4]^{2-}$, $[Pn_5]^{-}$, $[Pn_7]^{3-}$, and $[Pn_{11}]^{3-}$ and other polypnictides.[40–42] In other cases, gaseous and sometimes highly unstable hydrogen compounds of the pnicogens, such as PnH_3 (Pn = P, As, Sb) or P_2H_4, were used as precursors.[43–48]

Haushalter and co-workers presented the first crystal structures of compounds that contain $[E_9]^{4-}$ and $[Pn_7]^{3-}$ clusters as ligands to d-block elements with the form $[(\eta^4\text{-}Sn_9)Cr(CO)_3]^{4-}$[49] and $[(\eta^4\text{-}As_7)Cr(CO)_3]^{3-}$,[50] respectively. The polymeric chain $^1_\infty\{[HgGe_9]^{2-}\}$[51] was the first ligand-free binary polyanion, which can be regarded as an anion formed only by (semi)metals and heralds the field of intermetalloid clusters. It resulted from the reaction of $[Ge_9]^{4-}$ Zintl anions with elemental mercury. Endohedrally filled bimetallic clusters $[As@Ni_{12}As_{20}]^{3-}$[52] and $[Pt@Pb_{12}]^{2-}$ were subsequently obtained.[53] Backing up Schnöckel's term of metalloid clusters,[5] the expression "intermetalloid clusters" was introduced for cluster compounds that consist of atoms of at least two different (semi)metallic elements in low oxidation states and which might even exhibit topological similarities to structural motifs of related intermetallic compounds.[54]

3. Homoatomic Clusters

3.1. Homoatomic Clusters of Group 14 Elements

A summary of polyhedral Group 14 clusters $[E_4]^{4-}$, $[E_5]^{2-}$, $[E_9]^{n-}$, and $[E_{10}]^{2-}$ that have been structurally characterized to date is given in Tables 1 and 6 (see Appendix), and their structures are shown in Figure 1. The polyhedral structures of these $[E_x]^{n-}$ clusters are best described as delocalized electron-deficient systems with a cluster bonding that is analogous to that of the boranes. Wade's rules[55–57] can be applied if the radial B–H bonds are formally substituted by a lone pair of electrons at each cluster vertex.[57] Thus, each Group 14 element contributes two of its four valence electrons to the cluster skeletal bonding. The tetrahedral clusters $[E_4]^{4-}$ therefore possess $2n+4=12$ skeletal electrons. According to Wade's rules, they build a *nido* cluster[*] derived from the trigonal-pyramidal *closo* cage of $[E_5]^{2-}$ clusters, which also comprise 12 skeletal electrons ($2n+2$). The chemical bonding in $[E_4]^{4-}$ tetrahedra can also be explained using the $(8-N)$ rule. Accordingly, each monoanionic Group 14 atom forms three bonds, and a P_4-analogous

Table 1: Structurally characterized homoatomic Group 14 element cluster anions obtained from solutions.

E	$[E_4]^{4-}$	$[E_5]^{2-}$	$[E_9]^{2-}$	$[E_9]^{3-}$	$[E_9]^{4-}$	$[E_{10}]^{2-}$
Si	–[a]	[60]	[61]	[60]	[62]	–
Ge	–[b]	[63, 64]	[65]	[66–68]	[65, 69–72]	[73]
Sn	[31]	[74]	–	[67, 75–78]	[22, 23, 29, 79–84]	–
Pb	[31]	[74, 85]	–	[67, 76, 86]	[80, 86–88]	[89]

[a] Known only as MesCu adduct in $[(Mes\text{-}Cu)_2Si_4]^{4-}$.[35] [b] Observed only in neat solids.

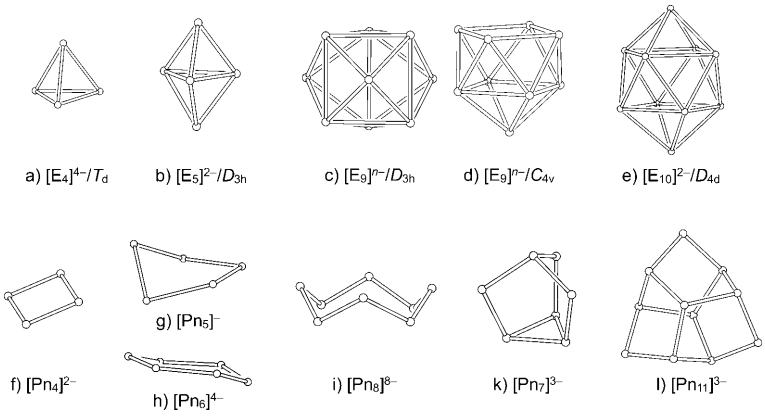

Figure 1. Structures of known homoatomic Group 14 and 15 clusters.

[*] From Wade's rules, a tetrahedron is regarded as a *nido* cluster derived from a trigonal bipyramid with one missing apex atom.

tetrahedral cluster arises. A nine-atom cluster $[E_9]^{n-}$ can build a *closo* deltahedron if $2n+2=20$ skeletal electrons are available for the cluster bonding. Thus, clusters $[E_9]^{2-}$ with a twofold negative charge are appropriate to adopt the *closo* shape of a tricapped trigonal prism (Figure 1c, and **I**, Figure 2a) with point group symmetry D_{3h}. $[E_9]^{4-}$ clusters

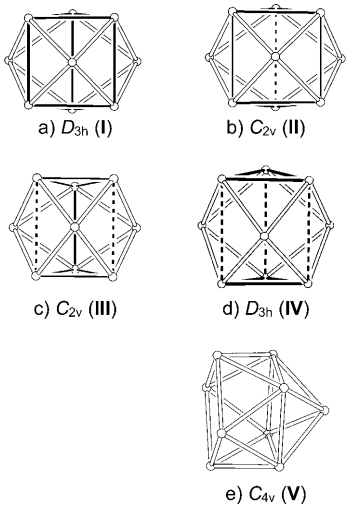

Figure 2. Structure relationships between nine-atom clusters. a) D_{3h}-symmetric tricapped trigonal prism, b) C_{2v} distortion with one long (dashed lines) and two shorter heights of the trigonal prism, c) C_{2v} distortion with two long (dashed lines) and one shorter height of the trigonal prism, d) trigonal prism with three long heights and D_{3h} symmetry, e) elongation of one long height and relaxation of the other atoms leads to the C_{4v}-symmetric monocapped square antiprism.

comprise $2n+4=22$ skeletal electrons that are required for a *nido*-type cluster, and thus form a C_{4v}-symmetric monocapped square antiprism (Figure 1d and **V** in Figure 2e). $[E_9]^{3-}$ clusters possess 21 electrons for their cluster bonding and cannot be described by Wade's rules. Their structure should lie between between structural types **I** and **V**. The HOMO of the C_{4v} cluster $[E_9]^{4-}$ is degenerate, and thus the removal of one electron leads to a Jahn–Teller-type distortion of the cluster framework. In contrast, the LUMO of the D_{3h}-symmetric cluster $[E_9]^{2-}$ is σ-antibonding along the prism height, and when it becomes the SOMO of $[E_9]^{3-}$, a distorted tricapped trigonal prism with either one (**II**, Figure 2b) or two (**III**, Figure 2c) elongated heights results. If the prism heights are equally stretched, the D_{3h} symmetry is retained (**IV**, Figure 2d). Because distortions from the idealized boundary geometries **I** and **IV** are quite common in the solid-state structures of $[E_9]^{n-}$ clusters, their charge cannot reliably be deduced from their crystallographically determined static shape.[58] The very low energy barrier for the intramolecular atom exchange in solution is shown by ^{119}Sn and ^{207}Pb NMR spectroscopy investigations (see Section 6).[59]

For the heavier Group 14 elements (Si–Pb), the smallest clusters $[E_4]^{4-}$ can be obtained from solid-state reactions of the elements with an equimolar amount of an alkali metal A (A = Na, K, Rb, Cs) at higher temperatures. For lead, the ammoniates $Rb_4Pb_4(NH_3)_2$ can be isolated from a liquid ammonia solution of RbPb.[31] The isotypic compounds $A_4Sn_4(NH_3)_2$ have been obtained for A = Rb and Cs from reactions of the alkali metals with Sn and $Sn(C_6H_5)_4$, respectively, in liquid ammonia.[31] The coordination spheres of the tetrahedral anions of the ammoniates show remarkable similarities to those of the corresponding intermetallic 1:1 phases, and many strong anion–cation contacts were found in all of the compounds.

$[E_5]^{2-}$ anions are not formed in regular solid-state reactions, and there is only one report of a five-atom cluster in the solid: the binary phase $K_{70}Sn_{103}$ can be written as $(K^+)_{70}([Sn_4]^{4-})_{11}([Sn_5]^{2-})([Sn_9]^{4-})_6$.[90] Experiments aiming for D_{3h}-symmetric five-atom clusters from solution follow the same procedures as described for nine-atom clusters and involve the dissolution of binary phases. Silicon clusters $[Si_5]^{2-}$ were obtained by extraction of the binary compound $Rb_{12}Si_{17}$ with liquid ammonia in the presence of [2.2.2]crypt and subsequent treatment with triphenylphosphine.[60] Crystalline materials containing the anions $[Ge_5]^{2-}$, $[Sn_5]^{2-}$, and $[Pb_5]^{2-}$ were obtained from ethylenediamine and liquid ammonia solutions of A-E alloys with different ratios under stoichiometric deficiency of [2.2.2]crypt.[63,64,74]

Homoatomic ligand-free Group 14 clusters with six, seven, eight, or more than ten vertices have not yet been detected in solution. Larger cluster anions $[E_n]^{m-}$ and $[AE_n]^{m-}$ were generated and detected in the gas phase, and the latter were interpreted as $A^+[E_9]^{2-}$ Zintl-type anions.[91] Some $[E_n]^{m-}$ anions have been structurally characterized as main-group-element or transition-metal-functionalized species, thereby in some cases following the bonding concepts of Zintl anions (see Section 5.2).

Nine-atom clusters are most prominent in the intermetallic compounds A_4E_9 (A = Na, K, Rb, Cs; E = Ge, Sn, Pb).[32,34,92–95] Extraction of these intermetallic compounds with liquid ammonia, ethylenediamine (en), or dimethylformamide (dmf) is the most common way to yield highly concentrated and intensively colored solutions of nine-atom clusters. However, the crystals often have twinning problems and contain disordered and distorted E_9 clusters.[93]

According to a delocalized description of the chemical bonding in the E_9 cluster framework, E–E distances are in the ranges 2.4–2.7 Å, 2.5–2.9 Å, 2.9–3.3 Å, and 3.0–3.5 Å for E = Si, Ge, Sn, and Pb, respectively, and thus are considerably longer than E–E single bonds: 2.353 Å (α-Si), 2.445 Å (α-Ge), 2.810 Å (α-Sn) and 2.88 Å (twice the Pb valence radius).[96] For E = Sn and Pb, the distances are in the range of the metallic bond length: 3.016 Å and 3.175 Å (β-Sn) and 3.49 (elemental Pb).[96] In both structure types **I** and **V** (Figure 2), the longest E–E contacts occur between E atoms with five nearest neighbors, that is, three long bonds are expected for a tricapped trigonal prism and four for a monocapped square antiprism.

The structures of $[E_9]^{4-}$ clusters in alkali metal crypt or crown ether salts were determined mainly for products obtained from ethylenediamine solutions of the binary phases A_4E_9 for E = Ge, Sn and Pb. Recently, the first two crystal structures of $[Si_9]^{4-}$ salts were presented for compounds obtained from a liquid ammonia solution of $A_{12}Si_{17}$.[35,62] Fourfold negatively charged polyanions $[E_9]^{4-}$

rarely appear as completely isolated units but instead show contacts to the surrounding alkali metal cations either by the cluster vertices, edges, or triangular faces; a η^4 coordination to the open square face of a *nido* cluster has however also been found (Figure 3). In such cases, the A^+ ions are either complexed by less-encapsulating crown ethers or they contain nonsequestered cations.

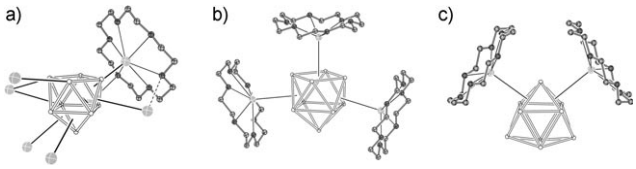

Figure 3. Variation in the number of A-E_9 contacts. a) [Rb([18]crown-6)]$Rb_3[Si_9](NH_3)_4$ with seven contacts,[62] b) $[K([18]crown\text{-}6)]_4[Pb_9]$[87] with three contacts to C_{4v}-symmetric $[Pb_9]^{4-}$, and c) $[K([18]crown\text{-}6)]_3K[Sn_9]$ with two contacts to C_{2v}-symmetric $[Sn_9]^{4-}$.[29]

The $[E_9]^{4-}$ anions in $[K([18]crown\text{-}6)]_4E_9$ are coordinated by two (E = Sn)[29] or three (E = Pb)[87] $[K([18]crown\text{-}6)]^+$ fragments, leading to discrete units of the composition $^0[K_2Sn_9]^{2-}$ and $^0[K_3Pb_9]^-$, respectively. Owing to their unambiguously determined fourfold negative charge, both Zintl clusters have 22 skeletal electrons, and accordingly the $[Pb_9]^{4-}$ cluster in $[K([18]crown\text{-}6)]_4[Pb_9]$ is almost perfectly C_{4v}-symmetric (Figure 3b), whereas for $[Sn_9]^{4-}$, the symmetry is closer to D_{3h} (Figure 3c), which demonstrates the structural flexibility of E_9 cages.

Additional contacts between alkali metals and clusters entail intermetallic structural units. Of course, the number of A-E_9 contacts decreases continuously with increasing contents of solvent and sequestering molecules, and the three-dimensional network typical for the neat solids is opened into layers and chains, as depicted in Figure 4. $[E_9]^{4-}$ clusters without contacts to alkali metal atoms are present only in $[Na([2.2.2]crypt)]_4Sn_9$[22] and in $[Li(NH_3)_4]_4E_9(NH_3)$[80] with

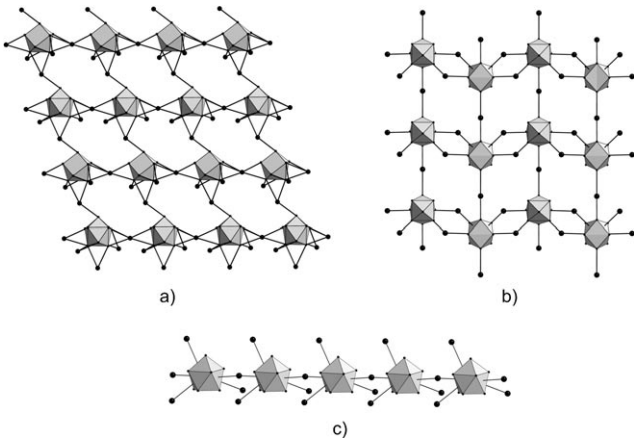

Figure 4. Examples of structures with one- and two-dimensional intermetallic motifs: a) 2D layer $\{^2_\infty[K_4Sn_9]\}$ in $[K([18]crown\text{-}6)]_2K_2[Sn_9](en)_{1.5}$,[82] b) 2D layer $\{^2_\infty[(K_3Ge_9)^-]\}$ in $[K([2.2]crypt)][K_3Ge_9](en)_2$,[70] and c) linear chain $\{^1_\infty[K_4Sn_9]\}$ in $[K([18]crown\text{-}6)]_3K[E_9]$.[29]

E = Sn, Pb, where the coordination spheres of all alkali metal ions are saturated by [2.2.2]crypt or ammonia molecules, respectively.

Uncharged intermetallic chains of $\{^1_\infty[K_4Sn_9]\}$ arise in crystals of $[K([18]crown\text{-}6)]_3K[Sn_9]$, where each Sn_9 cage interacts with five potassium atoms (Figure 4c).[29] The chains are separated by [18]crown-6 molecules. In $[K([2.2.2]crypt)]_3K[E_9]$ (E = Sn, Pb), the E_9 clusters are connected by one potassium atom, leading to anionic chains of $\{^1_\infty[(KE_9)^-]\}$ that are separated by $[K([2.2.2]crypt)]^+$ counterions.[79,86] Two-dimensional substructures $\{^2_\infty[A_4E_9]\}$ (A = K, Rb; E = Sn, Pb) with six A-E_9 contacts and separated by [18]crown-6 molecules were found in the isotypic compounds $[K([18]crown\text{-}6)]_2K_2[E_9](en)_{1.5}$ (E = Sn, Pb)[82,88] and $[Rb([18]crown\text{-}6)]_2Rb_2[Sn_9](en)_{1.5}$ (Figure 4a).[81] Layers of $\{^2_\infty[(K_3Ge_9)^-]\}$ and $\{^2_\infty[(KCs_2Sn_9)^-]\}$ occur in $[K([2.2]crypt)][K_3Ge_9](en)_2$ (Figure 4b)[70] and $[K([2.2]crypt)]_2Cs_2[Sn_9](en)_2$,[83] respectively, which are separated by non-coordinating $[K([2.2]crypt)]^+$ units.[97] Intermetallic double layers $\{^2_\infty[(Cs_7Sn_9Sn_9)^-]\}$ have been found in $[K([2.2.2]crypt)]Cs_7[Sn_9]_2(en)_3$[84] and $\{^2_\infty[(Rb_4Si_9)_2]\}$ in $[Rb([18]crown\text{-}6)]Rb_3[Si_9](NH_3)_4$. In the latter, each almost C_{4v}-symmetric $[Si_9]^{4-}$ anion interacts with seven rubidium atoms (Figure 3a).[62]

Solvates of the binary phases A_4E_9 can be obtained either from ethylenediamine (E = Ge and Sn) or from liquid ammonia solutions (E = Si and Ge). The coordination spheres of the E_9 clusters in the three-dimensional networks of the en solvates $Na_4Sn_9(en)_7$,[22] $Rb_4Ge_9(en)$,[69] and $Cs_4Ge_9(en)$[69] and in the ammoniates $K_4Ge_9(NH_3)_9$, $Rb_4Ge_9(NH_3)$,[71] and $Rb_4Si_9(NH_3)_{4.75}$[62] are similar to those found in the corresponding binary phases A_4E_9 and $Rb_{12}Si_{17}$, respectively.

The only example of a nine-atom Group 14 element cluster with an unequivocal charge of −2 has been obtained from the reaction between $K_{12}Si_{17}$ and Ph_3GeCl in liquid ammonia. The product $[K([18]crown\text{-}6)]_2Si_9(py)$ crystallized from pyridine in the presence of [18]crown-6, and its $[Si_9]^{2-}$ cluster interacts with the two potassium cations by two deltahedral faces. Despite $2n+2=20$ skeletal electrons, the cluster deviates significantly from D_{3h} symmetry and is best described as a distorted tricapped trigonal prism with one elongated height (structure type **II**, Figure 2b).

Nine-atom clusters with a threefold negative charge $[E_9]^{3-}$ (E = Si, Ge, Sn, and Pb) have been exclusively isolated as $[A^+([2.2.2]crypt)]$ salts.[60,66–68,75,76,78,86,98] As these paramagnetic clusters are formed even in the absence of oxidizing agents, solvated electrons and also the reduction of ethylenediamine protons to H_2 are proposed to be involved in this unusual oxidation process. In their crystalline compounds, all of the $[E_9]^{3-}$ units have the shape of a distorted tricapped trigonal prism with approximate C_{2v} symmetry (structure type **II**, Figure 2b), but in some cases, for reasons that are not understood, $[Sn_9]^{3-}$ retains almost perfect D_{3h} symmetry (structure type **IV**, Figure 2d).

The $[K^+([2.2.2]crypt)]$ salts of all paramagnetic $[E_9]^{3-}$ units contain either one or two symmetrically independent E_9 clusters per asymmetric unit and various amounts of solvent molecules. EPR measurements on powdered samples had increasing line widths from Ge to Pb for $[K([2.2.2]crypt)]_6E_9E_9(en)_{1.5}(tol)_{0.5}$ (E = Ge, Sn, Pb; Figure 5a),

Table 2: Molecular homoatomic Group 15 element Zintl ions obtained from synthesis in solution and characterized by single-crystal X-ray structure determination.

Pn	$[Pn_2]^{2-}$	$[Pn_4]^{2-}$	$[Pn_5]^{5-}$	$[Pn_6]^{4-}$	$[Pn_7]^{3-}$	$[Pn_8]^{8-}$	$[Pn_{11}]^{3-}$	$[Pn_{14}]^{4-}$	$[Pn_{21}]^{3-}$	$[Pn_{22}]^{4-}$	$[Pn_{26}]^{4-}$
P	–	[42, 48, 106]	–	–	[42, 111–116]	–	[113, 117–121]	[122, 123]	[124]	[125]	[126]
As	–	[106, 127, 128]	–	[41]	[129–132]	–	[133, 134]	[122]	–	[135]	
Sb	–	[107]	[110]	–	[107]	[136]	[135, 137]	–	–	–	
Bi	[103, 104, 137]	[108, 109]	–	–	–	–	–	–	–	–	

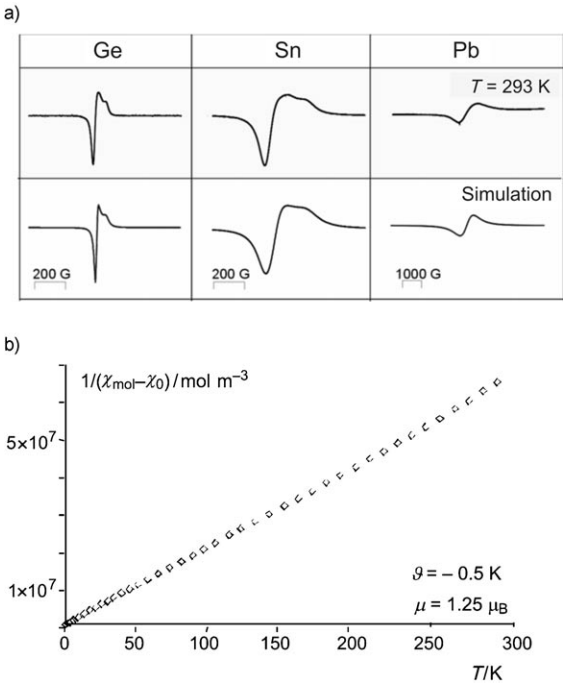

Figure 5. a) EPR spectra of powdered samples of $[K^+([2.2.2]crypt)]$ salts of paramagnetic $[E_9]^{3-}$. The spectra were simulated using two to three *g* tensors.[98] b) Magnetic susceptibility of $[K([2.2.2]crypt)]_6E_9E_9(en)_{1.5}(tol)_{0.5}$ (E = Sn) as a funtion of temperature, showing Curie–Weiss behavior.[98]

which comprise one ordered and one disordered E_9 cluster per asymmetric unit, and they revealed Curie–Weiss paramagnetism for only 50% of the clusters (Figure 5b). For that reason, an uneven electron count and thus a threefold negative charge was attributed to the ordered cluster, and a superposition of diamagnetic $[E_9]^{2-}$and $[E_9]^{4-}$ species was assumed for the disordered case.[68,98] In light of these results, a charge assignment based on structural arguments in the mixed-valent compound $[K^+([2.2.2]crypt)]_6[Ge_9]^{2-}[Ge_9]^{4-}(en)_{2.5}$ containing a $[Ge_9]^{2-}$ cluster is doubtful.[65] However, we repeatedly obtained brown samples that crystallize in the trigonal crystal system[*] and contain strongly disordered $[Ge_9]$ clusters counterbalanced by two $[K^+([2.2.2]crypt)]$ units.[98] The crystal structure of a compound with rather similar cell parameters but having a violet color has been reported to contain strongly disordered $[Ge_{10}]^{2-}$ anions.[73]

A well-ordered ten-atom $[Pb_{10}]^{2-}$ *closo* cluster, obtained as a $[K([2.2.2]crypt)]^+$ salt from an ethylenediamine solution of K_4Pb_9 in the presence of PPh_3Au^ICl and cryptand, which adopts the shape of a bicapped quadratic antiprism in accordance with Wade's rules, is the largest empty Group 14 element cluster isolated in solid state to date.[89] Recently, a $[Ge_{10}]^{2-}$ cluster was finally characterized as a σ-donor ligand to a $[Mn(CO)_4]^-$ fragment in $[Ge_{10}Mn(CO)_4]^{3-}$.[386] Although gas-phase experiments and theoretical investigations predict a remarkable stability for the stannaspherene $[Sn_{12}]^{2-}$ [99] and the plumbaspherene $[Pb_{12}]^{2-}$ cluster anions, these polyanions have not yet been isolated in crystalline form.[100]

3.2. Homoatomic Clusters of Group 15 Element

In contrast to homoatomic E_n cages, deltahedral Pn_n structures are limited to molecular P_4, As_4, and the cationic $[Bi_5]^{3+}$, $[Bi_8]^{2+}$ and $[Bi_9]^{5+}$ species (Table 2). The bismutates were synthesized either by molten-salt routes or by using superacidic systems. Generally, complex anions, such as $[AlCl_4]^-$, $[AsF_6]^-$, and $[HfCl_6]^{2-}$, act as counterions in crystals.[7,57,101,102] According to Wade's rules, the clusters possess $2\times4+4$ (Pn_4), $2\times5+2$ ($[Bi_5]^{3+}$), $2\times8+6$ ($[Bi_8]^{2+}$), and $2\times9+4$ ($[Bi_9]^{5+}$) skeletal electrons, and *closo*-T_d, *nido*-D_{3h}, *arachno*-D_{4d}, and *closo*-D_{3h} clusters, respectively are observed. However, deviations from the expected structures are possible. Pn_4 can also be described by localized covalent bonds. The overall higher tendency of Pn anions to form localized bonds results in a higher abundance of small polyanionic chains and rings (Figure 1). The smallest homoatomic Group 15 element (Pn) polyanion obtained from solution is the dumbbell-shaped $[Bi_2]^{2-}$.[103,104] Cyclic $[Pn_4]^{2-}$ anions have been characterized by NMR spectroscopy (Pn = P)[105] and by X-ray crystal structure analysis on crystals obtained from solution (Pn = P, As, Sb, Bi; Figure 1f).[42,48,106–109] A planar $[Pn_5]^-$ anion has been found for Pn = P in solution by NMR spectroscopy.[105] Five-membered rings were also trapped as ligands in organometallic complexes for Pn = P, As, Sb (see Section 5.3 and Figure 13), but to date they have not been detected in binary phases or in solvate crystals. For Pn = Sb, a non-planar, envelope-shaped $[Pn_5]^{5-}$ cluster is known (Figure 1g).[110] In contrast to the cyclohexaphosphide anion $[P_6]^{4-}$, the binary phases of which dissolve incongruently in liquid ammonia, the corresponding $[As_6]^{4-}$ anion is in a steady-state equilibrium with other polyarsenides in solution and has been characterized as a chair-shaped $[As_6]^{4-}$ anion in $(Rb[18]crown\text{-}6)_2Rb_2[As_6](NH_3)_6$ (Figure 1h).[41]

[*] Cell parameters at 293 K: $a = b = 11.960$ Å, $c = 22.364$ Å, space group: $P\bar{3}c1$.

As with the nine-atom clusters $[E_9]^{4-}$ for Group 14 elements, the heptapnicanortricyclane anions $[Pn_7]^{3-}$ are the most abundant species found in solution for Pn = P, As, Sb (Figure 1k).[42,107,111–116,129–132] The S_8-analogous, crown-shaped $[Pn_8]^{8-}$ unit has been obtained for Pn = Sb in $[K_{17}(Sb_8)_2(NH_2)](NH_3)_{17.5}$ (Figure 1i),[136] and, as can be seen from Tables 2 and 7 (see Appendix), the trishomocubane-shaped (ufosane-like) anions $[Pn_{11}]^{3-}$ (Pn = P, As, Sb) are also common among polypnictides (Figure 1l).[113,117–121,133,134,137]

All of these clusters contain covalently linked Pn atoms. For Pn = P, all of the distances are in the range 2.1–2.3 Å (Figure 10 and Table 3) and compare well with the covalent radius of a phosphorus atom. The formally negatively charged phosphorus atoms form the shortest P–P bonds (*b* and *c* in Figure 10), while the longest (*a*) are between the atoms of the basal triangle. The same holds for Pn = As and Sb.

Table 3: Structural parameters of P_7 nortricyclane clusters and alkylated derivatives (approximate values). For parameters, see Figure 10.

	$[P_7]^{3-}$	$[P_7R_3]$	$[P_7(R_6)]^{3+}$
Height, *h* [Å]	3.00	3.15	3.40
Distance *a* [Å]	2.29	2.22	2.22
Distance *b* [Å]	2.14	2.19	2.22
Distance *c* [Å]	2.19	2.18	2.22
Ratio $Q = h/a$	1.30–1.36	1.42	1.53
Angle γ [deg]	99	102	109
Angle δ [deg]	102	99	92

The aromaticity of the anions $[Pn_4]^{2-}$ and $[Pn_5]^-$ differs from regular hydrocarbon 6π-aromatic systems and was thus called "lone-pair aromatic", as delocalization takes place predominantly outside the ring over the lone pairs and bonds (see Figure 18b in Section 7.3). In hydrocarbons, delocalization is however seen above and below the ring.

3.3. Oxidative Coupling Products of Homoatomic Clusters

The anions with higher nuclearity, $[Pn_{14}]^{4-}$ and $[Pn_{22}]^{4-}$ (Pn = P, As), can be regarded as oxidative coupling products of the monomers $[Pn_7]^{3-}$ and $[P_{11}]^{3-}$, respectively (Figure 6a and c). The intercluster Pn–Pn distances between the $[P_7]^{2-}$ or $[P_{11}]^{2-}$ monomers amount to approximately 2.23 Å and 2.24 Å, respectively, and are in the same range as the P–P distances within the cluster units. The henicosapnictide anion $[P_{21}]^{3-}$ (Figure 6b) is a norbornane-like P_7 unit that is connected to two heptaphosphanortricyclane P_7 cages by two covalent bonds for each. The shortest P–P bonds (less than 2.18 Å) are formed by the formally negatively charged phosphorus atoms, and the intercluster bonds are again just as long as the intracluster bonds of threefold-bonded phosphorus atoms.[138] The $[P_{26}]^{4-}$ anion can be seen as consisting of two heptaphosphanortricyclane P_7 cages that are connected by two covalent bonds to a P_{12} unit, which consists of two edge-sharing norbornane-like P_7 units.[126]

In the case of the nine-atom Group 14 element clusters $[E_9]^{4-}$, radicals $[E_9^{\bullet}]^{3-}$ are quite stable and compete with dimerization reactions. The analogous $[Pn_7^{\bullet}]^{2-}$ radical has not been reported. For germanium and tin, corresponding oxidative coupling products have been reported. In $[Ge_9{-}Ge_9]^{6-}$ (Figure 6d and e) two Ge_9 units are connected by an *exo* bond.[71,139–141] In these dimers, the structure of the Ge_9 cages deviates slightly from a monocapped square antiprism. The open faces of the *nido* clusters are usually rhombohedrally distorted, and one atom of this face forms an *exo* bond to an analogous atom of the second cluster. The intercluster bond is colinear with the shorter diagonal of the open face of each cluster (Figure 6d, conformer **A**), and the clusters are arranged in a transoid conformation. Apart from conformer **A**, $K_6(Ge_9{-}Ge_9)(dmf)_{12}$ contains another dimeric unit with a different structure (Figure 6e, conformer **B**).[26] In **B** both clusters derive from a tri-capped trigonal prism with two strongly elongated prism heights leading to two vertex-sharing rectangular cluster faces according to structure type **III** (Figure 2c). The connecting *exo* bond between the two apex atoms approximately points to the cluster centers. The $Ge_9{-}Ge_9$ *exo* bonds with a mean value of 2.48 Å are only slightly longer than the Ge–Ge single bond in elemental germanium (2.45 Å) and are typically surrounded by four alkali metal atoms bridging the two clusters units.

Recently, the first dimeric $[Sn_9\text{-}Sn_9]^{6-}$ anion was obtained by oxidation of $[Sn_9]^{4-}$ with MesAg (Mes = 2,4,6-$Me_3C_6H_2$) (Figure 6f).[142] Two fused Sn_9 cluster units are further

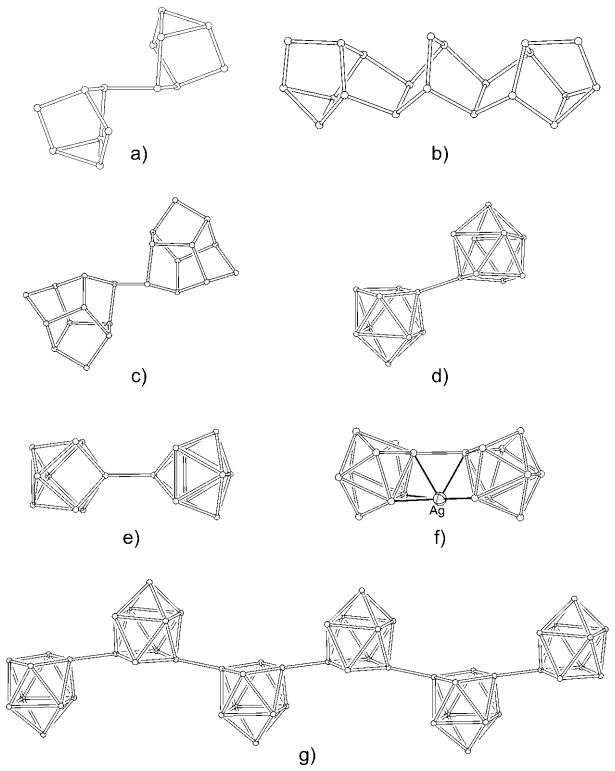

Figure 6. Dimers and polymers with covalent connections: a) Dimeric $[P_7{-}P_7]^{4-}$,[122,123] b) trimeric $[P_7{-}P_7{-}P_7]^{3-}$,[138] c) dimeric $[P_{11}{-}P_{11}]^{4-}$,[125] d) transoid dimeric $[Ge_9{-}Ge_9]^{6-}$,[26] e) a second conformer of $[Ge_9{-}Ge_9]^{6-}$,[26] f) cisoid dimeric $[Sn_9{-}Sn_9]^{6-}$ bonded to Ag^+,[142] and g) polymeric $^1_\infty\{[Ge_9]^{2-}\}$.[144] A complete list of the compounds is given in Tables 6 and 7.

connected to a bridging Ag^+ ion, and the dimer is thereby forced into a cisoid conformation. The Sn–Sn *exo* bond (2.99 Å) is approximately 7% longer than a typical tin single bond, such as in α-Sn (2.80 Å).

Further oxidation of the Ge_9 clusters to formal $[Ge_9]^{2-}$ leads to linear polymers $^1_\infty\{[-Ge-]^{2-}\}$[143–145] with two intercluster bonds per monomer (Figure 6g). Trimers and tetramers of Ge_9 clusters with a mean charge of −2 are formed by nonclassical bond formation between the units. The formation of intercluster bonds between two neighboring atoms of the triangular prism basis planes of the *closo*-shaped clusters results in Ge-Ge-Ge angles of 90° (Figure 7a and b) and in considerably longer intercluster contacts in the range 2.55 Å to 2.75 Å. The individual clusters in $[Ge_9{=}Ge_9{=}Ge_9]^{6-}$[146,147] and $[Ge_9{=}Ge_9{=}Ge_9{=}Ge_9]^{8-}$[148,149] are elongated along their prism heights of the connecting germanium atoms (C_{2v} symmetry; Figure 2b, **II**). It must be assumed that the *exo* bonds participate in a delocalized electronic system that comprises the whole anion (see Section 7.3).

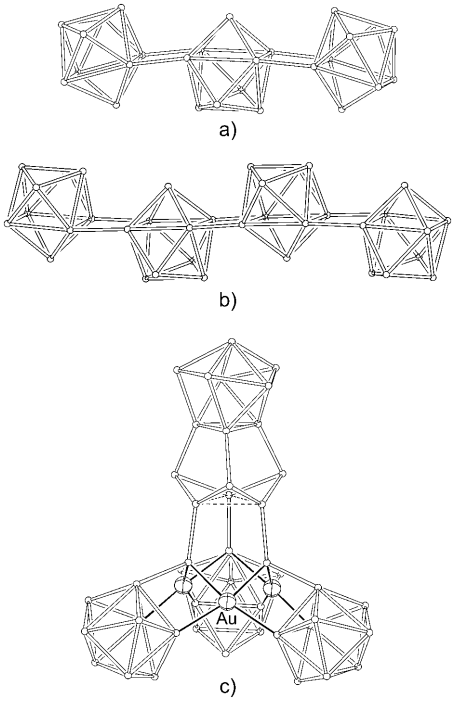

Figure 7. Cluster oligomers, including non-classical connections: a) Trimeric $[Ge_9{=}Ge_9{=}Ge_9]^{6-}$,[147] b) tetrameric $[Ge_9{=}Ge_9{=}Ge_9{=}Ge_9]^{8-}$,[148] and c) pentameric $[Ge_{45}]^{12-}$ attached to three Au^+ ions.[150] A complete list of the compounds is given in Table 6.

A unique cluster oligomerization of five Ge_9 clusters has been realized by oxidation with Au^I compounds. A $[Ge_{45}]^{12-}$ unit was formed in the reaction of an ethylenediamine solution of K_4Ge_9 and Ph_3PAuCl.[150] In this cluster, four Ge_9 polyhedra are retained while the fifth is opened up and covalently links the four intact subunits. The chemical bonding in the resulting 45-atom germanium cluster is rather complex and ranges from covalent two-center two-electron *exo* cluster bonds to delocalized multicenter bonds in the deltahedral subunits. Furthermore, long Ge–Ge contacts within a triangle of five-coordinate germanium atoms are involved (shown as dashed lines in Figure 7c), which correspond to a three-center two-electron bond. The anion even has five-membered germanium faces, which are typical structural motifs of three-dimensional solids, such as alkali- and alkaline-earth-metal germanides with clathrate structures that are indeed formed by oxidation of $[Ge_9]^{4-}$ clusters (see Section 8).[151] Similar to the coordination of the $[Sn_9{-}Sn_9]^{6-}$ dimer to an Ag^+ ion described above, the Ge_{45} unit coordinates to three Au^+ ions, and the resulting cluster anion has the composition $[Au_3Ge_{45}]^{9-}$.

4. Ligand-Stabilized (Functionalized) Homoatomic Clusters

The description of the term cluster given by von Schnering[11] emphasizes the regions of homonuclear bonding. The consideration of the homonuclearly bonded regions of Group 14 and 15 element clusters as quasi-isolated, bare units irrespective of attached ligands allows the research fields of functionalized Zintl ions and of main-group element-rich molecules or ions to be merged. Even though the synthetic approaches are rather different, the resulting products have great structural similarities and comparable bonding situations. Formal addition of R^+ to $[E_4]^{4-}$, $[E_9]^{4-}$, and $[Pn_7]^{3-}$ clusters leads to the alkylated species $[E_4R_m]^{(4-m)-}$, $[E_9R_m]^{(4-m)-}$, and $[Pn_7R_m]^{(3-m)-}$, respectively. $[Si_4(SiMeDis_2)_3]^-$ ($Dis = CH(SiMe_3)_2$)[152] and $E_4(tBu_3Si)_4$ (E = Si,[153] Ge[154]) and also P_7Me_3[191] are illustrative examples. While both fields have been recently summarized separately,[12,13,155,156] an overview with emphasis on the similarities of the two fields is given here.

4.1. Group 14 Element Clusters with exo-Bonded Ligands

Oligomerization and polymerization of $[Ge_9]^{4-}$ clusters as described in Section 3.3 already provide a strong indication that the functionalization of Zintl polyanions by the introduction of *exo*-bonded ligands should be possible. If covalent *exo* bonds are formed under simultaneous reduction of the negative cage charge, the number of skeletal electrons remains unchanged, and even the structure of a bare Zintl cluster might be retained, as found for example for the cage $[Ge_9R_3]^-$ (Figure 8e), which has not been synthesized by a Zintl anion route. Remarkably, uncharged molecules Ge_9R_4 have not been reported to date, but we have no doubt that they exist.

The experimental realization of functionalized Zintl clusters starting from solutions of binary A_4E_9 phases (Zintl anion approach) is not as easy, owing to the strong reducing power of the $[E_9]^{4-}$ species. Alternative reactions for the synthesis of homoatomic Group 14 element cage compounds include the reduction of $ER_{4-n}X_n$, (R = alkyl, aryl; X = hal) and the formation of ligand-free E atoms by ligand stripping,[157] the reduction of low-valent molecules $E^{II}R'_2$ (R′ being either amyl or halide),[158–160] or the disproportionation of Ge^I and Sn^I subhalides, which are available through co-

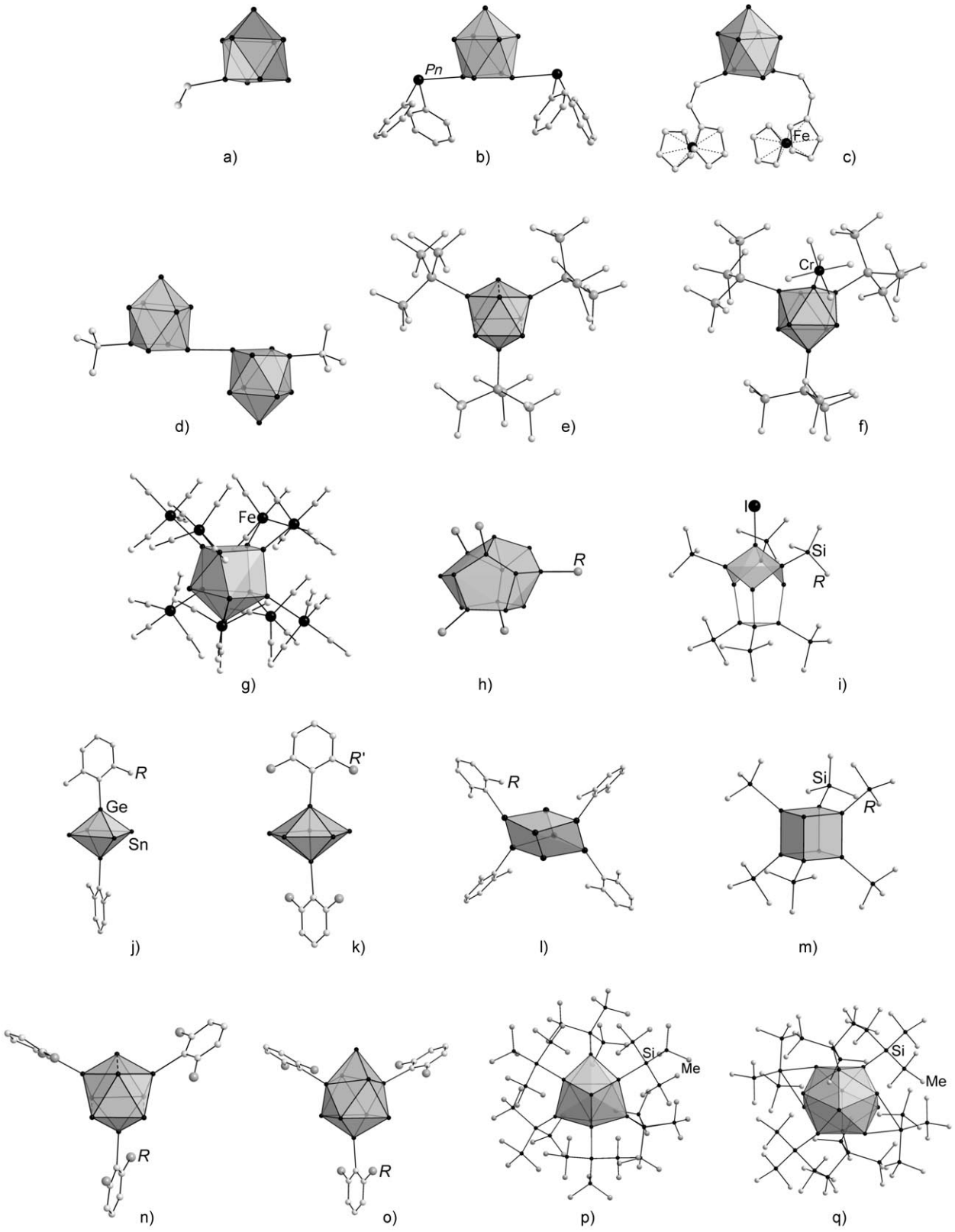

Figure 8. Examples of homoatomic ligand-stabilized clusters. a) $[Ge_9(CH{=}CH_2)]^{3-}$,[170] b) $[Ge_9\{Sb(C_6H_5)_2\}_2]^{2-}$,[162] c) $[Ge_9(CH{=}CH\text{-}Fc)_2]^{2-}$,[169] d) $[(Ge_9tBu)_2]^{4-}$,[165] e) $[Ge_9\{Si(SiMe_3)_3\}_3]^-$,[171] f) $[\eta^1\text{-}Ge_9\{Si(SiMe_3)_3\}_3Cr(CO)_5]^-$,[172] g) $[Ge_{10}(Fe(CO)_4)_8]^{6-}$,[173] h) $[Ge_{14}\{Ge(SiMe_3)_3\}_5]^{3-}$,[174] i) $[Ge_{10}(SitBu_3)_6I]^+$,[175] j) $\{2,6\text{-}(2,6\text{-}iPr_2C_6H_3)_2C_6H_3\}_2Ge_2Sn_4$,[176] k) $Sn_7\{2,6\text{-}(2,6\text{-}iPr_2C_6H_3)_2C_6H_3\}_2$,[177] l) $Sn_8\{C_6H_3\text{-}2,6\text{-}(2,4,6\text{-}Me_3C_6H_2)_2\}_4$,[178] m) $[Sn_8(SitBu_3)_6]^{2-}$ [159] and the related $[Ge_8\{N(SiMe_3)_2\}_6]$,[179] n) $Sn_9\{2,6\text{-}(2,4,6\text{-}iPr_3C_6H_2)_2C_6H_3\}_3$,[158] o) $[Sn_{10}\{2,6\text{-}(2,4,6\text{-}iPr_3C_6H_2)_2C_6H_3\}_3]^+$,[158] p) $Pb_{10}\{Si(SiMe_3)_3\}_6$,[180] and q) $Pb_{12}\{Si(SiMe_3)_3\}_6$.[180] A complete list of the compounds is given in Table 6.

condensation of the monohalide together with suitable solvent mixtures, as described by Schnepf.[161]

Using the Zintl anion approach, up to two ligands can be attached to $[E_9]^{4-}$ clusters, and numerous mono- and difunctionalized Ge_9 clusters have been obtained by this method, examples of which are shown in Figure 8a–c. Functionalized dimers may also occur, as shown in Figure 8d. Even though the mechanism of formation is not entirely understood, a nucleophilic attack at the cluster atoms is more likely than an electrophilic attack.[155] The oxidation of $[Ge_9]^{4-}$ with $SbPh_3$ and $BiPh_3$ leads to $[Ph_2Sb–Ge_9–SbPh_2]^{2-}$ and $[Ph_2Bi–Ge_9–BiPh_2]^{2-}$, respectively, with two *exo*-bonded main-group fragments (Figure 8b),[162] and it is assumed that during the reaction the phenylpnictides are reduced to give the anions $[PnPh_2]^-$, which in a following step react with the oxidized Ge_9 cages. Analogous reactions with the lighter homologues PPh_3 and $AsPh_3$, however, resulted in the formation of the oxidation product $[Ge_9{=}Ge_9{=}Ge_9]^{6-}$. Such oxidative coupling reactions between the cluster units must be considered as an alternative reaction for all $PnPh_3$ species, and the formation of the dimeric ions $[Ph_2Sb–Ge_9–Ge_9–SbPh_2]^{4-}$ [163] and $[Ph_3Sn–Ge_9–Ge_9–SnPh_3]^{4-}$ [164] demonstrates that a combination of both reactions is also possible. As in the case of pure Ge_9 clusters, monomeric paramagnetic $[Ge_9–SnR_3]^{3-}$ clusters (R = Ph, Me) can alternatively be formed.[164] For the formation of the phenyl- and alkyl-substituted clusters $[Ph\text{-}Ge_9\text{-}SbPh_2]^{2-}$ [163] and $[t\text{Bu-}Ge_9\text{-}Ge_9\text{-}t\text{Bu}]^{4-}$,[165] a radical mechanism was considered. Recently, the cluster $[Ge_9–Mes]^{3-}$ was obtained from the reaction of MesAg with $[Ge_9]^{4-}$,[166] the formation of which is probably initiated by a homolytic dissociation of the Ag–C bond.

To date, the vinylation of Ge_9 and Sn_9 units using alkynes is the best-studied derivatization reaction of these clusters, but again, different reaction mechanisms have been proposed depending on the stability of the reactive species, which can either be a radical or an anion, and also the solvent ethylenediamine seems to play a major role.[167] The reaction of the clusters with $Me_3Si–C{\equiv}C–SiMe_3$ or $H–C{\equiv}C–Ph$ proceeds by the loss of the ligands Me_3Si or Ph followed by the hydrogenation of the triple bond to a double bond.[168] Among the large number of disubstituted Ge_9 clusters, there are also species that carry common organic or organometallic functional groups (for example, $[Ge_9(CH{=}CH–Fc)_2]^{2-}$,[169] Fc = ferrocenyl; Figure 8c). The only monovinylated Ge_9 cage characterized in solid state to date is depicted in Figure 8a and was obtained from the reaction of K_4Ge_9 with $Me_3Si–C{\equiv}C–SiMe_3$ after the addition of KCp (Cp = cyclopentadienyl).[166,170]

In the case of the $[Sn_9]^{4-}$ cage, however, vinylation leads exclusively to monosubstituted cluster anions $[Sn_9–CH{=}CHR]^{3-}$ (R = H, Ph), independent of the applied stoichiometry.[181] Anions $[Sn_9–R]^{3-}$ (R = *t*Bu, *i*Pr$_3$, SnCy$_3$) have been obtained from reactions of K_4Sn_9 with RCl in ethylenediamine solution.[182] Recently, Eichhorn et al. investigated the dynamic behavior of functionalized $[Sn_9–i\text{Pr}]^{3-}$ and $[Sn_9–SnCy_3]^{3-}$ clusters in solution by ^{1}H, ^{13}C, and ^{119}Sn NMR spectroscopy and proposed two different ligand-exchange mechanisms. In case of $[Sn_9–SnCy_3]^{3-}$, a migration of the $SnCy_3$ group along the cluster surface occurs, whereas for the *i*Pr-substituted cage, a rearrangement of the eight bare tin atoms within the Sn_9 framework leads to an exchange of the ligand position. The first mechanism is supported by the fact that in the solid-state structure, the *exo*-bonded tin atom shows two weak contacts to neighboring cluster atoms (3.66 Å) along with the covalent bond (2.91 Å).[182] A similar trend to a three-center two-electron bond between the *exo*-bonded tin atom and a cluster triangular face has been observed for the two monosubstituted anions $[Ge_9–SnPh_3]^{3-}$ and $[Ge_9–SnMe_3]^{3-}$.[164] The *exo* bonds between the ligands and the atoms of the open square of the E_9 *nido* clusters are mostly regular covalent two-center two-electron bonds, analogous to the well-understood B–H bonds in deltahedral boranes. The *exo* bonds are oriented colinearly to the diagonal of the open square. As in cluster dimers, this diagonal is shortened, and the *nido* structure is distorted toward a C_{2v}-symmetric cage.

Vinylation was also used to functionalize the first mixed Group 14 atom Zintl anions, and different species of the general formula $[Ge_nSn_{(4-n)}\text{-}(CH{=}CHR)_m]^{(4-m)-}$ (n, $m = 1, 2$; R = H, *c*Pr (cyclopropanyl), Ph) were obtained.[183] In all these anions the ligands are carried by the germanium atoms, which are localized at the prism basal planes.

Even though an experimental approach from Zintl ions to an $[E_9]^{4-}$ cluster with more than two ligands has not yet been realized, the formation of $[Ge_9R_3]^-$ products or fully alkylated molecules E_9R_4 can be imagined and is completely in line with $[Ge_9R_2]^{2-}$. A nine-atom germanium cluster with three *exo*-bonded ligands can be obtained by the reduction of low-valent germanium compounds. The deltahedral cluster $[Ge_9\{Si(SiMe_3)_3\}_3]^-$ [171] with 22 skeletal electrons (Figure 8e) appears as a D_{3h}-symmetric cage of type **IV**, while the undistorted C_{4v}-symmetric cluster of type **V** is retained in $[\eta^1\text{-}Ge_9\{Si(SiMe_3)_3\}_3Cr(CO)_5]^-$ [172] (Figure 8f). Functionalized germanium clusters with higher nuclearity transform from deltahedral structures to cages with four- and five-membered rings. In $[Ge_{10}\{Fe(CO)_4\}_8]^{6-}$,[173] three- and four-membered rings are found (Figure 8g), and with an increasing number of germanium atoms, four- and five-membered rings become the dominant structural features, as shown for $[Ge_{14}\{Ge(SiMe_3)_3\}_5]^{3-}$ in Figure 8h.[174] Regarding $[Ge_{10}\{Fe(CO)_4\}_8]^{6-}$ as a $[Ge_{10}]^{6-}$ anion that is coordinated by eight $Fe(CO)_4$ units, a 26-electron cluster results. The $2n + 6$ electron Wade cluster ($n = 10$) corresponds to an *arachno* cluster with some longer Ge–Ge contacts. Interestingly, a cluster of a rather similar topology has been observed in the case of a Sn_{14} unit in the Zintl phase $Na_{29}Zn_{24}Sn_{32}$. The Na^+-encapsulating Sn_{14} enneahedron consists of three square faces and six pentagons with nearly equal edge lengths and almost planar faces. As eight tin atoms covalently bind to the Sn/Zn framework, the Sn_{14} cage can be described as a $[(3b\text{-}Sn^-)_8(4b\text{-}Sn^0)_6)]$ unit with entirely localized two-center two-electron Sn–Sn bonds.[90,328] Recently a mixed cluster $[Eu@Sn_6Bi_8]^{4-}$ having the same framework has been described.[362] The cation $[Ge_{10}(Si\text{t}Bu)_6I]^+$ (Figure 8i) and the structurally related anion $[Ge_{10}\{Si(SiMe_3)_3\}_4\{SiMe_3\}_2Me]^-$ still possess one deltahedral face, but also three squares and three five-membered rings, which form a concave cage.[175,184] Most interestingly, the same connectivity of nine of the ten germanium atoms in Figure 8i

is found in the Ge_{45} unit shown in Figure 7c, where the upper germanium triangle is part of a nine-atom cluster.[150] Even the three-center two-electron bond indicated as dashed lines in Figure 7c is present in both structures, with Ge–Ge distances ranging from 3.25 to 3.26 Å in $[Ge_{10}(Si\mathit{t}Bu)_6I]^+$ and from 2.79 to 2.83 Å in $[Au_3Ge_{45}]^{9-}$. Regarding these dashed lines as three-center two-electron bonds, both species are electron-precise valence compounds.[150]

In the case of functionalized tin clusters, deltahedral structures are known for $n = 6$ (mixed-atom polyhedron), 7, 9, and 10 (Figure 8j,k,n, and o, respectively).[158,176,177] Owing to the ligands, the ideal deltahedra appear distorted, but their skeletal electron numbers strictly follow Wade's rules. The trialkylated 21 skeletal-electron cluster $[Sn_9R_3]^0$ (Figure 8n), which has been synthesized by the thermolysis of $\{ArTrip_2Sn\text{-}(\mu\text{-}H)\}_2$ (Trip = 2,4,6-iPr$_3$C$_6$H$_2$) in hot toluene, is paramagnetic, and its structure shows a distortion towards D_{3h} symmetry (type **IV**), in a rather similar fashion to that found for the isovalence-electronic radical $[Sn_9]^{3-}$.[158] The corresponding ten-vertex *closo* cluster $[Sn_{10}R_3]^+$ has also been characterized in solid state, and its structure agrees perfectly with Wade's rules (Figure 8o). In contrast, the ten-atom cluster $[Sn_{10}(Si(SiMe_3)_3)_6]$ is isoelectronic to the above-mentioned 26 skeletal-electron cluster $[Ge_{10}(Fe(CO)_4)_8]^{6-}$ and has a structure with more rectangular than triangular faces.[185]

Eight-atom clusters exist either with four ligands as neutral $[Sn_8(2,6\text{-}Mes_2C_6H_3)_4]$ species[178] or with six ligands as dianionic $[Sn_8(Si\mathit{t}Bu_3)_6]^{2-}$ species (Figure 8l and m, respectively).[159] Whereas the Sn–Sn distances are very similar in the neutral molecule, the dianion and the related germanium species $[Ge_8\{N(SiMe_3)_2\}_6]$[179] have significantly different E-E distances. Interestingly, deltahedral eight-atom Zintl anions are not yet known.

In the case of lead, two larger polyhedral ligand-stabilized lead clusters are also known. $[Pb_{10}(Si\{SiMe_3\}_3)_6]$ and $[Pb_{12}(Si\{SiMe_3\}_3)_6]$ are shown in Figure 8p and q, respectively. They have been obtained by the reaction of $Pb(Si\{SiMe_3\}_3)_2$ with CuH and phosphane, respectively.[180] Formally, $[Pb_{10}(Si\{SiMe_3\}_3)_6]$ can be described as a Pb^{2+} cation coordinated to a deltahedral cluster $[Pb_3(PbR)_6]^{2-}$ ($R = Si\{SiMe_3\}_3$) which comprises 26 skeletal electrons ($3\times2+6\times3+2$) and therefore has the expected *hypho* structure. The Pb–Pb distances within the *hypho* Pb_9 unit vary from 3.1 to 3.2 Å and are in the expected range for delocalized bonds in a Zintl anion framework. The Pb^{2+} cation is located in an apex-like position and forms three significantly shorter bonds to the Pb_9 cage, indicating a lesser degree of delocalization.[180] Despite of some disorder, a distorted Pb_{12} icosahedron with six ligand-free lead atoms has been revealed in the solid-state structure of $[Pb_{12}(Si\{SiMe_3\}_3)_6]$ in which Pb–Pb separations in the range 3.1 to 3.4 Å support a delocalized bonding situation.

4.2. Clusters of Group 15 Elements with exo-Bonded Ligands

P_4 is the only deltahedral phosphorus cage known so date. While a large number of transition-metal complexes with degraded or aggregated phosphorus units resulting from P_4 activation have been discovered,[186] the functionalization of P_4 with main-group-element fragments is a less-developed field. More common are framework extensions by insertion of for example $[SiR_2]$[187] or $[PPh_2]^+$[188] units into up to three P–P bonds of P_4 leading to the species $[R_2Si{\subset}P_4]$ (Figure 9a),

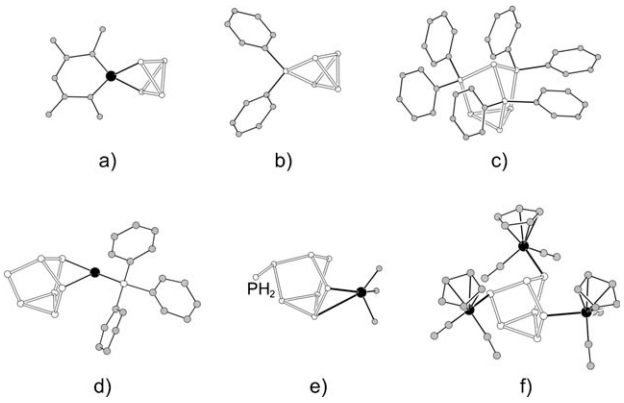

Figure 9. Molecular structures of functionalized pnictide cages. a) $[P_4(Si\text{-aminosilyl})]$[a],[187] b) $[Ph_2P{\subset}P_4]^+$[188], c) $[(Ph_2P)_3{\subset}P_4]^{3+}$,[188] d) $[(Pn_7H)Pt(PPh_3)]^{2-}$ (Pn = P, As),[196,197] e) $[Nb(OC[^2Ad]Mes)_3\text{-}(P_7PH_2)]$,[198] and f) $P_7[FeCp(CO)_2]_3$.[199] [a] The bis-inserted $[P_4(Si\text{-aminosilyl})_2]$ is also known. A complete list of the compounds is given in Table 7.

$[Ph_2P{\subset}P_4]^+$ (Figure 9b), $[(R_2Si)_2{\subset}P_4]$, $[(Ph_2P)_2{\subset}P_4]^{2+}$, and $[(Ph_2P)_3{\subset}P_4]^{3+}$ (Figure 9c). The latter shows a typical nortricyclane (tricyclo[2.2.1.0^{2,6}]heptane) skeleton and is thus reminiscent of a formal six-fold addition of R^+ to $[P_7]^{3-}$. Interestingly, the reaction of thallium organyls with P_4 leads to organyl-functionalized catena-P_4 or bicyclo-P_4 units with relatively short P–P bonds, which is indicative of some double-bond character.[189] A neutral P_7Me_3 species has been obtained by direct methylation of Li_3P_7 by Baudler in the course of their seminal work on polyphosphanes, hydrogenpolyphosphides, and organo-substituted phosphides,[190] and $P_7(MMe_3)_3$ (M = Si, Ge, Sn, Pb) was obtained by von Schnering et al.[191] Partially alkylated or hydrogenated polypnictides seem to be rare; the few known examples include $[HP_7]^{2-}$, $[R_2P_7]^-$ (R = Bn, H), and $[Bn_2As_7]^-$.[192–195]

The P–P bond lengths of the P_7 cage change significantly upon alkylation: Bare $[P_7]^{3-}$ shows P–P distances of about 2.29 Å in the basal plane (*a*), while the bonds from this plane to the formally negatively charged phosphorus atoms are about 2.14 Å long (*b*), and the distances between the formally negatively charged phosphorus atoms to the apical phosphorus atom are approximately 2.19 Å (*c*) (Figure 10). In $[P_7(EMe_3)_3]$ (E = Si, Ge, Sn, Pb) the bonds are about 2.22 Å (*a*), 2.19 Å (*b*), and 2.18 Å (*c*). In $[P_7Ph_6]^{3+}$, all of the P–P bonds have rather similar lengths (ca. 2.22 Å). Whereas in the anion $[P_7]^{3-}$ the angle γ is found to be smaller than the angle δ, the reverse is true for substituted species.[200] The ratio Q of the cluster height h and the mean basal

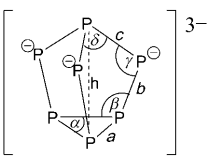

Figure 10. The $[P_7]^{3-}$ cage with bonds and angles labeled (for parameters, see text and Table 3).[200]

bond lengths *a* gives an estimate of the bonding situation of the phosphorus atoms: *Q* values of between 1.30 and 1.36 are indicative of an ionic $[P_7]^{3-}$ unit, while values of 1.40 and higher show that covalent bonding to ligands is involved, as found for example in $[P_7(SiMe_3)_3]$ (Table 3).[200] Upon alkylation, the height *h* of the cluster increases by about 0.4 Å. The P–P bonds in the basal plane are longest for the anionic species and are similar in neutral and cationic P_7 units.

The heptapnicanortricyclane $[P_7]^{3-}$ and $[As_7]^{3-}$ units remain unchanged when acting as a protonated chelating ligand $[(Pn_7)PtH(PPh_3)]^{2-}$ (Figure 9d).[196,197] $[Nb(OC[^2Ad]Mes)_3(P_7PH_2)]$ shows coordination of the transition metal with two shorter bonds to the two-connected phosphorus atoms and two longer bonds to the three-connected phosphorus atoms of the trigonal base (Figure 9e),[198] and a triple functionalization of the formally negatively charged phosphorus atoms of the P_7 cage is realized in $P_7[FeCp(CO)_2]_3$ (Figure 9f).[199] It is interesting to note that in all of these functionalizations of the P_7 cage, the basal triangular plane is retained.

The simplest functionalized polypnictides are the hydrogen polypnictides. However, owing to the instability of polypnictides towards acids, only a few protonated hydrogen polyphosphides are known. While the P–P bond lengths in the catenapolyphosphides $[P_3H_2]^{3-}$ and $[P_3H_3]^{2-}$ are similar and comparable to regular P–P single bonds (ca. 2.2 Å), protonation (or alkylation) of polyphosphide clusters such as $[P_7]^{3-}$ or $[P_{11}]^{3-}$ at the formally negatively charged phosphorus atoms leads to an increase of the P–P bond lengths.[118,194,201,202]

5. Heteroatomic and Intermetalloid Clusters

5.1. Heteroatomic Clusters of Group 14 and Group 15 Elements

The existence of mixed Ge/Sn, Sn/Pb, and Tl/Sn clusters was known from early NMR investigations,[59,203] and some of them were recently trapped in the solid state as ligand-stabilized anions $[Ge_nSn_{(4-n)}\text{–}(CH{=}CHR)_m]^{(4-m)-}$ ($n, m = 1, 2$; R = H, *c*Pr, Ph).[183] The synthesis of heteroatomic Group 14 and Group 15/13 deltahedral clusters of main-group elements generally follows the approach to dissolve ternary phases containing Group 14 and Group 15/13 elements, but Sevov and co-workers showed by using ESI-MS techniques that E_9 cages of different Group 14 elements are able to exchange atoms in some solvents.[183] The clusters $[Sn_2Bi_2]^{2-}$, $[Pb_2Sb_2]^{2-}$, $[InBi_3]^{2-}$, and $[GaBi_3]^{2-}$ were structurally characterized. They are valence-isoelectronic to P_4 and $[E_4]^{4-}$ anions and adopt tetrahedral structures.[204,205] Only a few larger ligand-free clusters have been reported, such as the *nido*-type nine-vertex cages $[In_4Bi_5]^{3-}$and $[TlSn_8]^{3-}$ and the *closo*-type $[TlSn_9]^{3-}$.[206] Unfortunately, all of these structures suffer from atom disorder. $[In_4Bi_5]^{3-}$, which has 22 skeletal electrons, adopts the shape of a *nido* cluster **IV**. Most of the anions follow classical bonding principles. Surprisingly, there is also only one heteroatomic cluster molecule that contains exclusively Group 15 elements: AsP_3 has been structurally characterized as a ligand in an organometallic complex and has the shape of a distorted tetrahedron, with P–P and P–As bonds of about 2.18 and 2.3 Å, respectively.[207,208] The large number of known Group 15/16 clusters exceed the scope of this Review and are thus not included.

5.2. Homoatomic Group 14 Element Clusters as Ligands

Structural units with less than nine Group 14 element atoms rarely serve as ligands for d-block elements. The octahedral subunits $[E_6]^{2-}$ were first reported in the anions $[\{ECr(CO)_5\}_6]^{2-}$ for E = Ge[209] and Sn[210] in which they are stabilized by $Cr(CO)_5$ fragments coordinating to each cluster vertex (Figure 11a). Later the $[\{EM(CO)_5\}_6]^{2-}$ family was extended to M = Mo and W.[211] The clusters are formed in the reaction of $Na_2[M_2(CO)_{10}]$ with GeI_2 or $SnCl_2$.

An anionic planar five-membered Pb_5 ring has been found in $[Pb_5\{Mo(CO)_3\}_2]^{4-}$, which was obtained as $K_2[K([2.2]\text{-crypt})]_2[Pb_5\{Mo(CO)_3\}_2](en)_3$ from an ethylenediamine solution of $[Pb_9]^{4-}$ and $[(\eta^6\text{-mesityl})Mo(CO)_3]$ in the presence of [2.2]-crypt (Figure 11b).[212] The Pb_5 ring binds to two $\{Mo(CO)_3\}$ fragments in a η^5 fashion, similar to *cyclo*-Pn_5 units in their transition-metal complexes (Section 5.3). DFT calculations support a formal description of the anion as an aromatic 2π electron system $[Pb_5]^{2-}$, which is coordinated to two $[Mo(CO)_3]^-$ moieties. This result is a surprise, because the bare $[Pb_5]^{2-}$ unit with the same number of skeletal electrons adopts the expected *closo*-D_{3h}-symmetric trigonal-bipyramidal structure as mentioned in Section 3.1 (Figure 1).[74] This example shows how two-dimensional π aromaticity and a three-dimensional electron delocalization compete in bare element cluster anions.

The Zintl anion $[Sn_6]^{12-}$ is isoelectronic with cyclohexene or the sulfur modification S_6. It was crystallized in the complex $[Sn_6\{Nb(\eta^6\text{-tol})\}_2]^{2-}$ from a solution of K_4Sn_9 and $[Nb(\eta^6\text{-tol})_2]$ in ethylenediamine (Figure 11c). The Sn–Sn distances in the corrugated ring agree well with those for covalent single bonds.[213]

Reactions of nine-atom Zintl ions with transition-metal compounds were studied in 1988 when Haushalter and Eichhorn discovered the anion $[Cr(\eta^4\text{-}Sn_9)(CO)_3]^{4-}$ as the first non-borane transition-metal–main-group-element deltahedral cluster,[49] which was formed in a ligand-exchange reaction starting from $[(\eta^6\text{-mesityl})Cr(CO)_3]$. Subsequently the syntheses of other complexes $[M(E_9)(CO)_3]^{4-}$ (E = Sn, Pb; M = Cr, Mo, W) of this series have been attained (Figure 11d).[214–217] The *nido*-shaped E_9 coordinates to the transition metal mainly by means of the open square face in a η^4 fashion, but the crystal structures of two η^5-E_9 complexes $[W(\eta^5\text{-}Sn_9)(CO)_3]^{4-}$[216] and $[Mo(\eta^5\text{-}Pb_9)(CO)_3]^{4-}$[217] showed that the heteroatom can just as well occupy a vertex of the square antiprism (Figure 11e). The resulting η^5 coordination is rather similar to that found in $[Pb_5\{Mo(CO)_3\}_2]^{4-}$ described above (Figure 11b). $[Cr(\eta^5\text{-}Ge_9[Si(SiMe_3)_3]_3)(CO)_3]^-$[172] (Figure 11f) is an example of a ligand-stabilized transition-metal–Ge_9 *closo* cluster with the $Cr(CO)_3$ group attached to five germanium atoms. A number of other complexes involving d-block elements in a η^4 coordination to the open square of an E_9 *nido* cluster have been isolated in the last few years: $[Ir(\eta^4\text{-}$

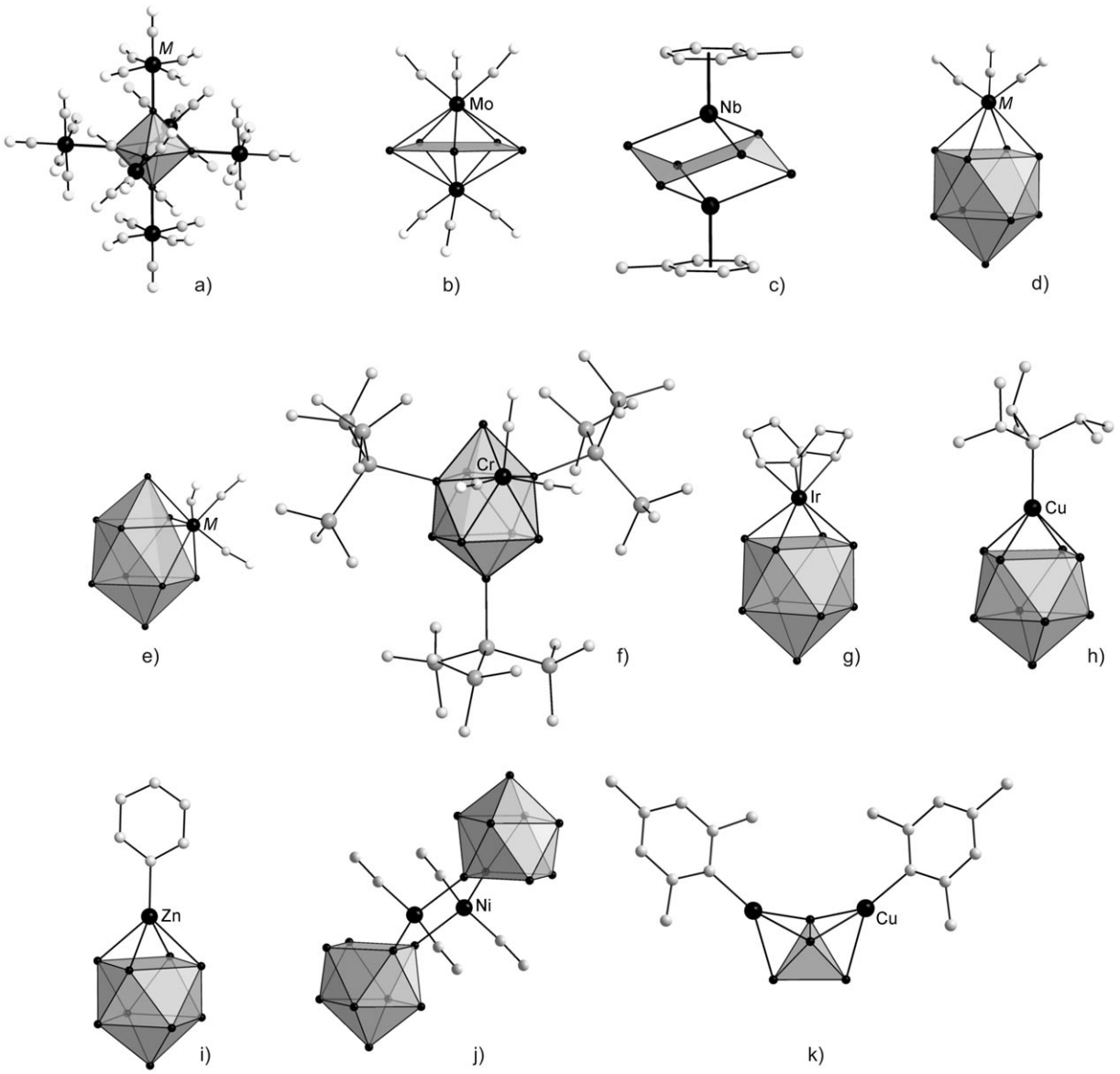

Figure 11. Coordination compounds with Zintl ions. a) $[\{EM(CO)_5\}_6]^{2-}$ (E = Ge, Sn, M = Cr, Mo, W),[209] b) $[(CO)_3Mo(\eta^5\text{-}Pb_5)Mo(CO)_3]^{4-}$,[212] c) $[Sn_6\{Nb(\eta^6\text{-}Tol)\}_2]^{2-}$,[213] d) $[M(\eta^4\text{-}E_9)(CO)_3]^{4-}$ (E = Sn, Pb; M = Cr, Mo, W),[49,214–217] e) $[M(\eta^5\text{-}E_9)(CO)_3]^{4-}$ (M = W: E = Sn; M = Mo: E = Pb),[216,217] f) $\{Cr(\eta^5\text{-}Ge_9[Si(SiMe_3)_3]_3)(CO)_3\}^-$,[172] g) $[Ir(\eta^4\text{-}Sn_9)(cod)]^{3-}$,[219] h) $[Cu(\eta^4\text{-}Ge_9)(P\mathit{i}Pr_3)]^{3-}$,[221] i) $[Zn(\eta^4\text{-}Ge_9)(C_6H_5)]^{3-}$,[222] j) $[(Si_9)\{\mu^2\text{-}Ni(CO)_2\}_2\text{-}(Si_9)]^{8-}$,[226] and k) $[(MesCu)_2Si_4]^{4-}$.[35] A complete list of the compounds is given in Table 6.

$E_9)(cod)]^{3-}$ (E = Sn, Pb[218,219] (Figure 11 g), $[Ni(\eta^4\text{-}Ge_9)(CO)]^{3-}$,[220] $[Cu(\eta^4\text{-}Ge_9)(P\mathit{i}Pr_3)]^{3-}$[221] (Figure 11 h), $[Zn(\eta^4\text{-}E_9)(R)]^{3-}$ (R = C_6H_5,[222] E = Si–Pb; R = *i*Pr, Mes,[223] E = Ge–Pb) (Figure 11 i), $[Pd(\eta^4\text{-}Ge_9)(PPh_3)]^{3-}$,[224] $[Cd(\eta^4\text{-}E_9)(C_6H_5)]^{3-}$,[225] and $[Cd(\eta^4\text{-}Sn_9)(Sn\mathit{n}Bu_3)]^{3-}$.[225]

According to the isolobal concept, $M(CO)_3$ fragments with M = Cr, Mo, and W and also $Ir(cod)^+$, $CuPR_3^+$ (R = *i*Pr, Cy) and $M'R'^+$ (M′ = Zn, Cd and R′ = C_6H_5, *i*Pr, Mes and $Sn(alkyl)_3$) units act as zero-electron building blocks for deltahedral clusters. Therefore, the electron count of the cluster remains unchanged upon the addition of the transition-metal fragment, and in accordance with the Wade/Mingos rules, the cluster expansion corresponds to the transformation of a nine-atom *nido* cluster ($2n+4=22$ skeletal electrons with $n=9$) to a ten-atom electron-precise *closo* cluster ($2n+2=22$ skeletal electrons with $n=10$).

Recently, the complex $[(Si_9)\{\mu^2\text{-}Ni(CO)_2\}_2(Si_9)]^{8-}$ was characterized in which two $Ni(CO)_2$ fragments bridge two $[Si_9]^{4-}$ units (Figure 11 j).[226] Furthermore, the first transition-metal-functionalized tetrahedral $[E_4]^{4-}$ cluster was obtained as $[(CuMes)_2Si_4]^{4-}$ from a liquid ammonia solution of $Rb_6K_6Si_{17}$ and CuMes (Figure 11 k).[35]

The reaction of K_4Ge_9 with elemental mercury in ethylenediamine[51] or *N*,*N*-dimethylformamide[227] led to the isolation of the first ligand-free transition-metal complex of an E_9 cluster in form of the polymer structure $^1_\infty\{[HgGe_9]^{2-}\}$. A similar chain was reported in the oligomeric anion $[Hg_3(Ge_9)_4]^{10-}$, which is formed when $HgPh_2$ is used as starting

material.[228] In these chains, the mercury atoms are covalently connected to the Ge_9 cages, which are subsequently formally oxidized to a dianion. The mercury atom is shifted however towards the midpoint of a triangular face of each adjacent cluster (η^3 coordination), as indicated by the dashed lines in Figure 12c.

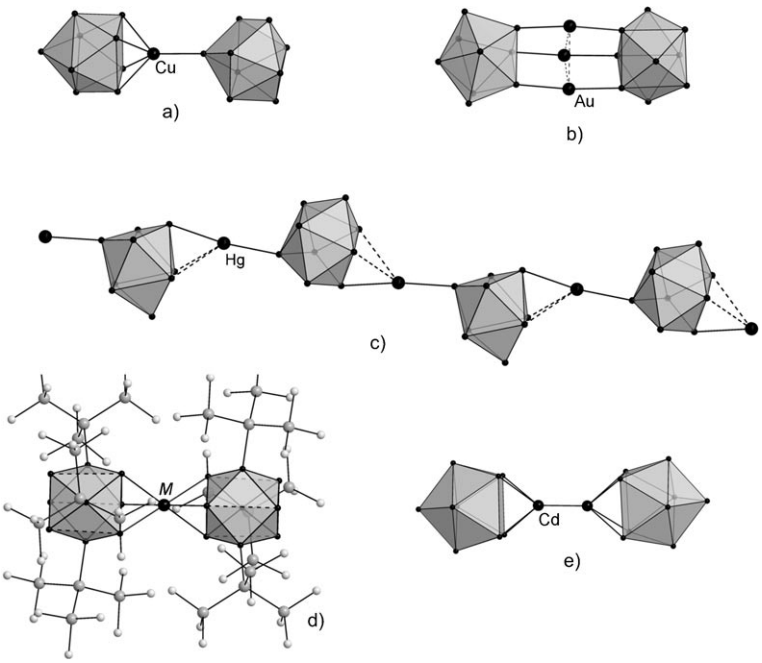

Figure 12. Zintl ions with ligand-free d block metal atoms. a) $[Cu(\eta^4\text{-}Ge_9)(\eta^1\text{-}Ge_9)]^{7-}$,[221] b) $[(Ge_9)Au_3(Ge_9)]^{5-}$,[229] c) $\{^1_\infty[(HgGe_9)]^{2-}\}$,[51] d) $[M(Ge_9\{Si(SiMe_3)_3\}_3)_2]^-$ (M = Cu, Ag, Au),[230,231] and e) $[(Pb_9)Cd\text{–}Cd(Pb_9)]^{6-}$.[233] A complete list of the compounds is given in Table 6.

The anion $[Cu(\eta^4\text{-}Ge_9)(\eta^1\text{-}Ge_9)]^{7-}$[221] (Figure 12a) arises from the complex $[Cu(\eta^4\text{-}Ge_9)(P\mathit{i}Pr_3)]^{3-}$ (Figure 11h) after substitution of the phosphane ligand by a second $[Ge_9]^{4-}$ unit. $[Cu(\eta^4\text{-}Ge_9)(\eta^1\text{-}Ge_9)]^{7-}$ is therefore another rare example where a lone pair of a homoatomic E_9 cluster becomes chemically relevant and acts as a two-electron σ donor as in $[Cr(\eta^1\text{-}Ge_9\{Si(SiMe_3)_3\}_3)(CO)_5]$[172] (Figure 8f) and $[\{SnCr(CO)_5\}_6]^{2-}$ (Figure 11a).[210] Thereby the transition metal atoms reach the 18-electron configuration. The reactions starting from the analogous gold compound Ph_3PAu^ICl led to the cluster $[(Ge_9)Au_3(Ge_9)]^{5-}$[229] (Figure 12b) in which three singly positively charged gold atoms in a triangular arrangement bridge two Ge_9 clusters by deltahedral germanium faces in a face-to-face orientation.[229] Rather short gold–gold contacts hint for aurophilic interactions. The positive charge of the gold atoms has been confirmed by DFT calculations.[229] The reaction of Ph_3PAu^ICl with the three-fold-functionalized Group 14 element cluster $[Ge_9\{Si(SiMe_3)_3\}_3]^-$ led to the formation of the anion $[M(Ge_9\{Si(SiMe_3)_3\}_3)_2]^-$ with M = Au,[230] and the analogous clusters with M = Cu and Ag[231] were obtained from $[M(Al(OC_4F_9)_4]$ (Figure 12d). In these anions, the transition-metal atoms interconnect two Ge_9R_3 cluster units in an η^3 fashion by their triangular prism basal planes, which results in an almost undistorted trigonal antiprismatic coordination sphere at Cu, Ag, and Au, respectively, and thus resembles the coordination of Hg and Ge_9 Zintl anions in Figure 12c. The same coordination was found in their uncharged analogues $[M(Ge_9\{Si(SiMe_3)_3\}_3)_2]$, which were synthesized from $[Ge_9\{Si(SiMe_3)_3\}_3]^-$ and MCl_2 for M = Zn, Cd, and Hg in tetrahydrofuran. The vertices along the transition-metal-capped faces are elongated, and as expected, these neutral molecules dissolve very well in non-polar solvents such as pentane.[232]

The above-mentioned anion $[Ag(Sn_9)_2]^{5-}$ (Figure 6f) and the recently found $[(Pb_9)Cd\text{–}Cd(Pb_9)]^{6-}$[233] (Figure 12e) are the first representatives of E_9 clusters containing ligand-free d-block elements and E = Sn and Pb, respectively. In $[(Pb_9)Cd\text{–}Cd(Pb_9)]^{6-}$, the Pb_9 cages stabilize a covalent cadmium–cadmium bond, which is ascribed to the electronic properties of the Group 14 atom clusters.

5.3. Homoatomic Clusters of Group 15 Elements as Ligands

Organometallic complexes of Group 15 element clusters are more frequent than those of Group 14 elements. Neutral P_4 and As_4 molecules acting as ligands have been comprehensively summarized in the literature[186,234] and thus are not further discussed herein. Recently, the coordination of Cu^I to two tetrahedral P_4 molecules in $[Cu(P_4)_2]^+$ has been reported in the presence of weakly coordinating counteranions. The Cu^+ ion bridges two P_4 molecules in an η^2,η^2 fashion.[235] Most frequent are derivatives of $[Pn_7]^{3-}$ Zintl anions, and some complexes with intact P_7 cages were already discussed in Section 4.2. One bond of the triangular base of the P_7 unit is opened upon the reaction of K_3P_7 with $[Ni(CO)_2(PPh_3)_2]$, and a $[Ni(\eta^4\text{-}P_7)(CO)]^{3-}$ unit is formed (Figure 13a).[196] The bond length of the former basal phosphorus atoms to the formally negatively charged phosphorus atoms decreases by 0.1 Å in this process to 2.13 Å, which might suggest some P–P double-bond character. Interestingly, in the analogous reaction of K_3Sb_7 with $[Ni(CO)_2(PPh_3)_2]$, the nortricyclane-like Sb_7 cage is transformed into the ten-vertex *nido* cluster $[(Sb_7)(Ni(CO))_3]^{3-}$ with 24 skeletal electrons (Figure 13b).[236] The reaction of P_4 with samarocene leads to a realgar-type homoatomic $[P_8]^{4-}$ unit in $[(Cp^*_2Sm)_4(P_8)]$ ($Cp^* = C_5Me_5$) with P–P bond lengths between 2.18 and 2.29 Å (Figure 13c).[237] In $[(Ni(PBu_3)_2)_4P_{14}]$, two P_7 clusters are coupled, and the resulting $[P_{14}]^{8-}$ anion formally consists of two norbornane-like units covalently connected by their apical phosphorus atoms and following the 8–*N* rule (Figure 13d).[199]

In the complex $[Co(\eta^3\text{-}\mathit{cyclo}\text{-}As_3)(CO)_3]$ (Figure 13e), a *cyclo*-As_3 unit coordinates to the Co atom,[238] whereas $[(\mu^2\text{-}M)_2(\eta^2\text{-}Bi_3)(CO)_6]^{3-}$ (M = Cr, Mo) (Figure 13f) contains a bent, ozone-like $[Bi_3]^{3-}$ unit coordinating to two neutral $M(CO)_3$ moieties.[239] Including further contacts, the resulting

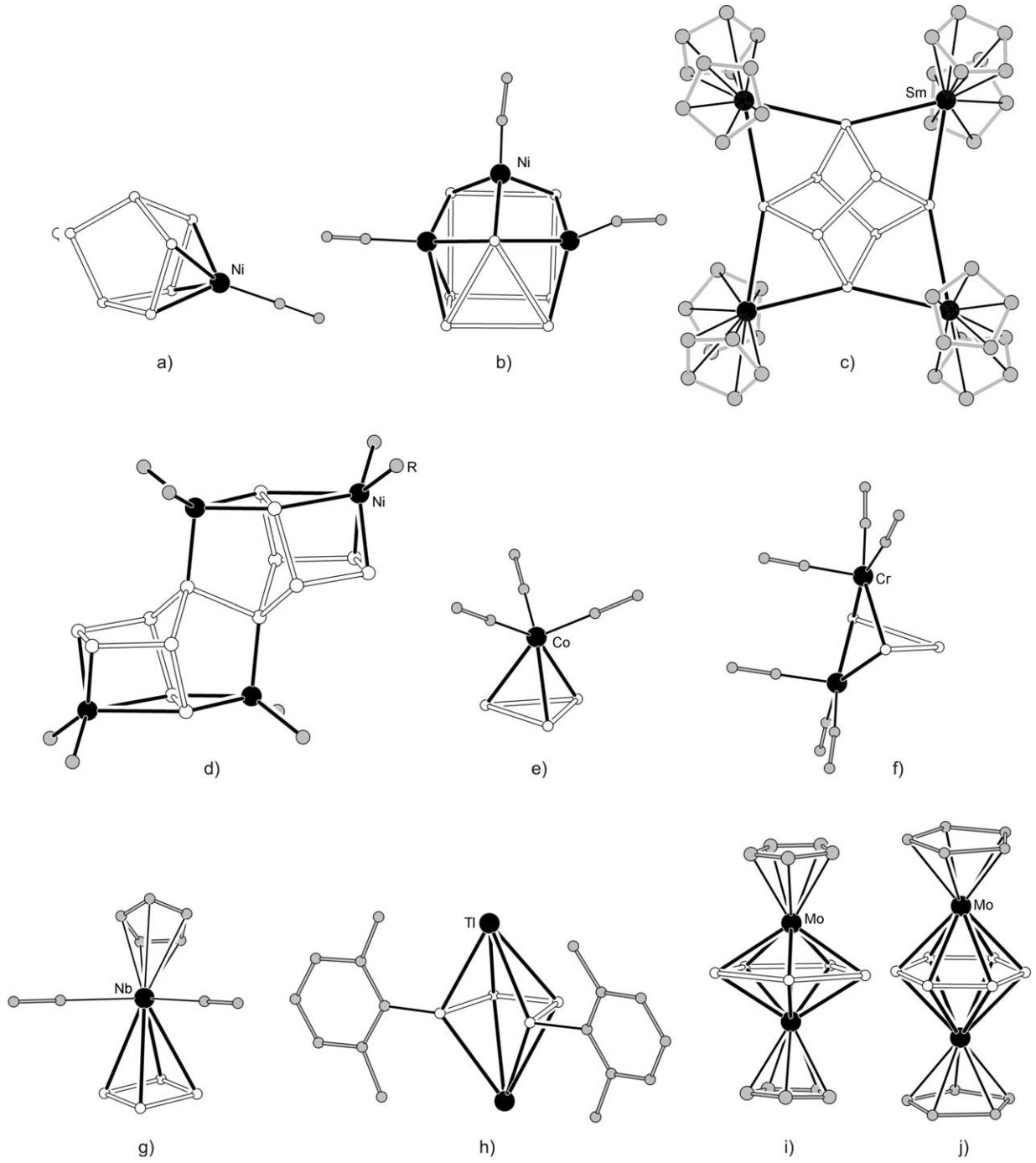

Figure 13. Structures of Pn cluster complexes and intermetalloid clusters. a) $[Ni(P_7)(CO)]^{3-}$,[196] b) $[(Sb_7)\{Ni(CO)\}_3]^{3-}$,[236] c) $[(Cp^*{}_2Sm)_4(P_8)]$,[237] d) $[\{Ni(PBu_3)_2\}_4(P_{14})]$,[199] e) $[Co(As_3)(CO)_3]$,[238] f) $[M_2(Bi_3)(CO)_6]^{3-}$ (M = Cr, Mo),[239] g) $[Cp^*Nb(CO)_2(P_4)]$,[241] h) $[Tl_2(ArDipp_2)_2(P_4)]$,[189] i) $[(CpMo)_2(\eta^5\text{-}cyclo\text{-}As_5)]$,[244] and j) $[(Cp^*Mo)_2(\eta^6\text{-}cyclo\text{-}P_6)]$ (R = Me, *t*Bu groups omitted).[246] A complete list of the compounds is given in Table 7.

cluster is described to be isosteric to $[E_5]^{2-}$ (E = Ge, Sn, Pb) and $[Bi_5]^{3+}$.[239] The P_3 ligand coordinates in an η^3 fashion to $[W\{N(i\text{Pr})Ar\}_3]$ and η^1 to $[W(CO)_5]$ in the trigonal-pyramidal metal cluster $[W(CO)_5(P_3)W\{N(i\text{Pr})Ar\}_3]$.[238–240] Lone-pair-aromatic square-planar $[Pn_4]^{2-}$ anions acting as 6π ligands in transition-metal complexes have not yet been encountered. To date, only distorted P_4 rings have been found, for example in $[Cp^*Nb(CO)_2(P_4)]$ (Figure 13 g), and a square-planar P_4 ring has been observed as a 12-electron donor in $[(CO)_4W(P_4)\{W(CO)_5\}_4]$.[241,242] A planar but ring-opened P_4 unit is coordinated in $[Tl_2(ArDipp_2)_2(P_4)]$ ($ArDipp_2 = C_6H_3$-2,6-(C_6H_2-2,6-$i\text{Pr}_2$)$_2$; Figure 13 h),[189] and a Bi_4 tetrahedron is present in $[Fe_4(Bi_4)(CO)_{13}]^{2-}$ in which three faces are capped by $Fe(CO)_3$ moieties, and a $Fe(CO)_5$ unit is attached to the apical bismuth atom.[243] Remarkable is the series of triple-decker sandwich complexes $[(CpMo)_2(\eta^5\text{-}cyclo\text{-}As_5)]$,[244] $[(Cp'Mo)_2(\eta^5\text{-}cyclo\text{-}Sb_5)]$[245] ($Cp' = C_5H_2R_3$, R = Me, *t*Bu), and $[(Cp^*Mo)_2(\eta^6\text{-}cyclo\text{-}P_6)]$[246] that contain *cyclo*-Pn_5 and

cyclo-Pn_6 units (Figure 13i and j, respectively), and have a remarkable similarity to Pn_5 and Pb_5 complexes (Figure 11b).

5.4. Endohedrally Filled Group 14 Clusters

An impressive number of endohedrally filled Group 14 atom clusters has been synthesized in the last few years (Figure 14; Table 4). These anions appear to form from transition-metal complexes that have released their organic ligands. The smallest transition-metal-filled Zintl clusters are

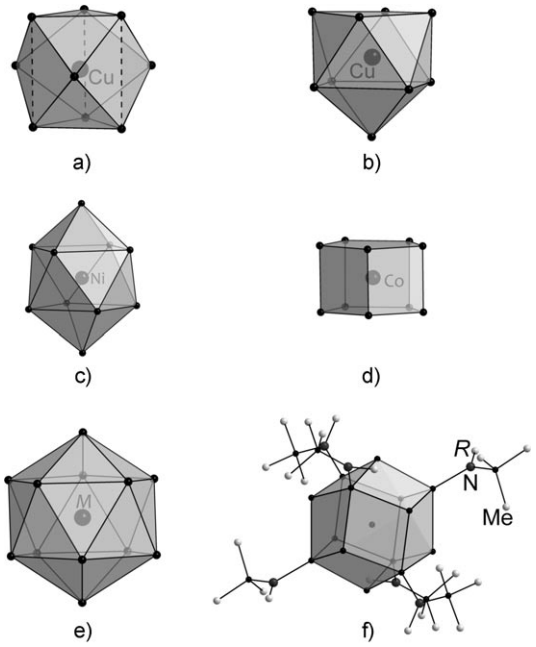

Figure 14. Representative Zintl ions with one endohedral metal atom: a) $[Cu@E_9]^{3-}$ (E = Sn, Pb) with D_{3h} symmetry,[248] b) $[Cu@E_9]^{3-}$ (E = Sn, Pb) with C_{4v} symmetry,[258] c) $[Ni@Pb_{10}]^{2-}$,[251] d) $[M@Ge_{10}]^{3-}$, (M = Co, Fe),[249,250] e) $[Ir@Sn_{12}]^{3-}$[219] and $[M@Pb_{12}]^{2-}$ (M = Ni, Pd, Pt),[53,252] and f) $[Sn@\{Sn_8[SnN(2,6\text{-}iPr_2C_6H_3)(SiMe_3)]_6\}]$.[260] A complete list of the compounds is given in Table 6.

Table 4: Endohedral Group 14 element clusters.

$M_n@E_m$ $E_m \rightarrow M\downarrow$	E_9	E_{10}	E_{12}	E_{17}	E_{18}
□	$[Si_9]^{2-,3-,4-}$[a] $[Ge_9]^{3-,4-}$[a] $[Sn_9]^{3-,4-}$[a] $[Pb_9]^{3-,4-}$[a]	$[Pb_{10}]^{2-}$[229]			
Fe		$[Fe@Ge_{10}]^{3-}$[249]			
Co		$[Co@Ge_{10}]^{3-}$[250]			
Ir			$[Ir@Sn_{12}]^{3-}$[219]		
Ni	$[Ni@Ge_9]^{3-}$[220,247]	$[Ni@Pb_{10}]^{2-}$[251]	$[Ni@Pb_{12}]^{2-}$[252]	$[Ni_2@Sn_{17}]^{4-}$[253]	$[Ni_3@Ge_{18}]^{4-}$[247]
Pd			$[Pd@Pb_{12}]^{2-}$[252]		$[Pd_2@Ge_{18}]^{4-}$[254] $[Pd_2@Sn_{18}]^{4-}$[255,256]
Pt			$[Pt@Pb_{12}]^{2-}$[53]	$[Pt_2@Sn_{17}]^{4-}$[257]	
Cu	$[Cu@Sn_9]^{3-}$[248,258] $[Cu@Pb_9]^{3-}$[248,258]				

[a] See Table 1 for references. □ = vacant site.

$[Ni@Ge_9]^{3-}$,[220,247] obtained from an ethylenediamine solution of K_4Ge_9 and $[Ni(cod)_2]$, and $[Cu@E_9]^{3-}$ (E = Sn and Pb) formed in dimethylformamide solutions of MesCu and the Zintl phase K_4E_9.[248] In these clusters, a transition metal is incorporated into an E_9 skeleton. According to EPR measurements, the endohedral nickel complex is paramagnetic and thus can be described as $[Ni^0@(Ge_9)^{3-}]$, while for the copper-containing cages, sharp ^{119}Sn, ^{207}Pb, and ^{63}Cu NMR signals indicate the presence of diamagnetic $[Cu^+@(E_9)^{4-}]$ units. The charge of Cu^I was also confirmed by DFT calculations.

The structure refinement of $[Ni@Ge_9]^{3-}$ suffers from significant disorder.[220,247] In the well-ordered $[Cu@E_9]^{3-}$ anions (Figure 14a), the cage atoms form an elongated tricapped trigonal prism with almost-perfect D_{3h} symmetry. Recently a second conformer of the $[Cu@E_9]^{3-}$ anions has been found with the shape of an endohedral *nido* cluster with almost perfect C_{4v} symmetry for E = Sn, Pb (Figure 14b).[258] In the latter case, the bonds between the fivefold-coordinate tin or lead atoms at the vertices of the E-capped square are significantly elongated by the incorporation of the copper atom. NMR spectroscopy experiments illustrate well the structural flexibility of the E_9 cages of the $[Cu@E_9]^{3-}$ units in solution, which reflects the observation of different cluster shapes in the crystals (Section 6, Figure 17).[248]

The endohedral ten-vertex cluster $[Ni@Pb_{10}]^{2-}$ (Figure 14c) was obtained from the reaction of $[Ni(cod)_2]$ with K_4Pb_9 in ethylenediamine.[251] The Ni^0 atom occupies the center of a bicapped square antiprism, as was predicted from DFT calculations for the neutral cluster $[Ni@Pb_{10}]^0$.[259] The process of formation of the ten-vertex clusters remains unclear to date. During the redox reaction, the cod ligand is reduced to cyclooctene, which was detected by GC-MS measurements.[252] The icosahedral cluster $[Ni@Pb_{12}]^{2-}$ was found as a minor by-product of the reaction of $[Ni(cod)_2]$ with K_4Pb_9 (Figure 14e).[252] The isostructural clusters $[Pd@Pb_{12}]^{2-}$ and $[Pt@Pb_{12}]^{2-}$ of the heavier Group 10 homologues were obtained from the reactions of K_4Pb_9 with $[Pd(PPh_3)_4]$ and $[Pt(PPh_3)_4]$, respectively.[53,252] In these reactions, the oxidation of the cluster atoms was ascribed to PPh_3, but no concluding reaction is given. The cluster structures strictly follow Wade's rules, which predict a *closo* structure for a unit with twelve vertices and $2n+2=26$ electrons. A comparison of the three solid-state structures of $[M@Pb_{12}]^{2-}$ confirms that the smaller the transition metal, the stronger the distortion of the Pb_{12} skeleton.[252] While the interstitial platinum atom is surrounded by an almost-perfect icosahedron with virtually equal Pb–Pb and Pt–Pb distances, the Pb–Pb contacts and the M–Pb distances in the cages with interstitial palladium and nickel atoms are distributed over a larger range with increasing variances. The arising anisotropy of the cluster certainly indicates the instability of the clus-

ters with small endohedral atoms, and for M = Ni the ten-vertex cluster is clearly favored.

An analogous germanium compound with a metal-atom-centered Ge_{12} cluster has not been reported to date, but recently an endohedral twelve-atom tin cluster $[Ir@Sn_{12}]^{3-}$ was obtained.[219] It is formed in a stepwise reaction that starts from an ethylenediamine solution of K_4Sn_9 and $[IrCl(cod)]_2$ (Scheme 1). In the first step, the Ir(cod)-capped Sn_9 cluster

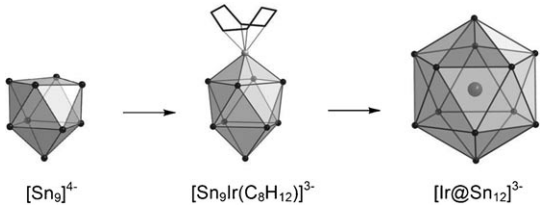

Scheme 1.

(Figure 11 g) is formed. Upon heating the ethylenediamine solution of this ten-vertex cluster to 80 °C, it is transformed into $[Ir@Sn_{12}]^{3-}$ with the loss of the cod ligand and the oxidation of the cluster skeleton. The reaction is accelerated by the addition of dppe (1,2-bis(diphenylphosphino)ethane), whichs act as an oxidizing agent as shown by NMR spectroscopy. According to DFT calculations, the iridium atom is negatively polarized, and the formal charge allocation $[Ir^{1-}@(Sn_{12})^{2-}]$ accounts for a *closo* cluster endohedrally filled with an atom with d^{10} configuration (see Section 7.3, Figure 18 a).[219]

The range of endohedral atoms was recently extended to electron-poorer d-block elements with $[Co@Ge_{10}]^{3-}$ (Figure 14 d).[250] The anion is the first example of a non-deltahedral structure without any triangular faces. Instead, D_{5h}-symmetric pentagonal prisms occur, indicating that neither the electron count nor the framework bonding follow conventional rules, and the encountered coordination sphere of the transition metal atoms in these clusters is more typical of an intermetallic phase. Thus $[Co@Ge_{10}]^{3-}$ has been the subject of DFT calculations and NBO analyses, the results of which are discussed in detail in Section 7. The isosteric cluster $[Fe@Ge_{10}]^{3-}$ was reported shortly thereafter. The expected paramagnetic behavior has not yet been verified.[249]

$[Sn@\{Sn_8[SnN(2,6\text{-}iPr_2C_6H_3)(SiMe_3)]_6\}]$ is a remarkable example of an endohedrally filled metalloid molecule (Figure 14 f).[260] A tin atom is encapsulated in a cage that consists of eight ligand-free and six *exo*-bonded tin atoms, thus the central tin atom possesses a coordination number of 14. This high coordination number of the central tin atom causes remarkably long Sn–Sn contacts, which are more common in solid-state compounds such as $BaSn_5$, where the tin atoms are encapsulated in hexagonal prisms of twelve tin atoms.[261] An alternative Sn_{14} polyhedron encapsulating Na^+ has however been described in Section 4.1.[90]

Interestingly, the same starting materials used for the synthesis of $[M@Pb_{12}]^{2-}$ gave clusters of different sizes when they were reacted with Sn_9 clusters. Three clusters of higher nuclearity, $[Ni_2@Sn_{17}]^{4-}$,[253] $[Pt_2@Sn_{17}]^{4-}$,[257] and $[Pd_2@Sn_{18}]^{4-}$,[255,256] were obtained from ethylenediamine solutions of K_4Sn_9 and $[Ni(cod)_2]$, $[Pt(PPh_3)_4]$, and $[Pd(PPh_3)_4]$, respectively (Figure 15 c,e, and f, respectively). Again, cluster formation proceeds by the partial oxidation of the Sn_9 clusters and the reduction of cyclooctadiene; the solvent ethylenediamine also seems to be involved in the redox process. In $[Ni_2@Sn_{17}]^{4-}$, two $[Ni@Sn_9]^{2-}$ subunits share one apex-like, central tin atom.[253] The clusters deviate significantly from deltahedral structures and have the same widely opened shape as the Ge_9 cages in conformer **B** of the anion $[Ge_9–Ge_9]^{6-}$ (Figure 6 e). In fact, $[Ge_9\text{-}Ge_9]^{6-}$ in conformation **B** and $[Ni_2@Sn_{17}]^{4-}$ both display D_{2d} point group symmetry, and the central tin atom of the Sn_{17} framework is surrounded by a pseudo-cube of eight tin atoms as it is the Ge–Ge dumbbell in Figure 6 e. The dynamic behavior of the tin cluster was examined by temperature-dependent ^{119}Sn NMR experiments in dmf solutions (see Section 6).[253] The isovalence-electronic cluster $[Pt_2@Sn_{17}]^{4-}$ (Figure 15 e) has however a completely different solid-state structure, with a closed polyhedron of 17 tin atoms surrounding two platinum atoms, which can be ascribed to the higher steric demands of the larger endohedral atoms.[253] Again these two clusters have an interesting antagonist among the ligand-stabilized clusters.

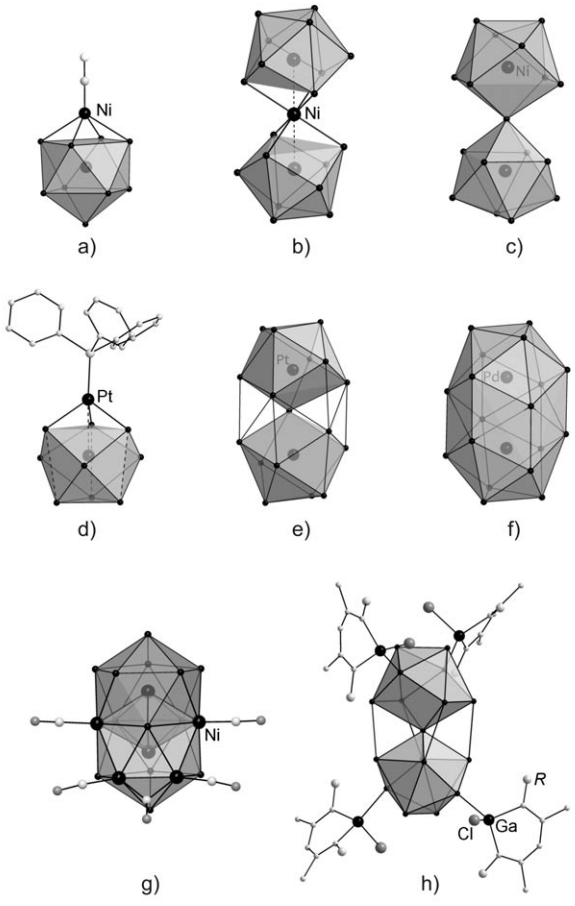

Figure 15. Representative Zintl ions with one or two endohedral metal atoms: a) $[(Ni@Sn_9)Ni(CO)]^{3-}$,[263] b) $[Ni_2@Sn_{17}]^{4-}$,[253] c) $[Ni_3@Ge_{18}]^{4-}$,[247] d) $[(Pt@Sn_9)Pt(PPh_3)]^{3-}$,[263] e) $[Pt_2@Sn_{17}]^{4-}$,[257] f) $[Pd_2@E_{18}]^{4-}$ (E = Ge, Sn),[254–256] g) $[Ni_6Ge_{13}(CO)_5]^{4-}$,[262] and h) $[Sn_{17}\{GaCl(ddp)\}_4]$.[160] A complete list of the compounds is given in Table 6.

The tin skeleton of $[Sn_{17}\{GaCl(ddp)\}_4]$[160] (ddp = $HC(CMeNC_6H_3\text{-}2,6\text{-}iPr_2)_2$; Figure 15h) adopts a rather similar structure to $[Ni_2@Sn_{17}]^{4-}$, although its two subunits are not filled with a transition metal. All of the presented Sn_{17} clusters can be considered as valence-isoelectronic species, as $[Sn_{17}\{GaCl(ddp)\}_4]$ has four *exo*-bonded {GaCl(ddp)} ligands, each increasing the number of skeletal electrons by one, whereas the Group 10 atoms do not contribute electrons to the fourfold negatively charged $[M_2@Sn_{17}]^{4-}$ anions.

An ellipsoidal shape was found for the isostructural clusters $[Pd_2@Ge_{18}]^{4-}$[254] and $[Pd_2@Sn_{18}]^{4-}$ (Figure 15f).[255,256] These units are the largest endohedral Group 14 atom clusters with a completely closed cluster shell discovered to date. In both clusters, 18 Group 14 atoms form a prolate deltahedral cage that encloses two Pd^0 atoms located in the ellipse foci. The Pd–Pd distance (2.831 Å) is significantly shorter in the smaller germanium cage[254] than in the larger tin cage (3.384 Å),[255] but no bonding Pd–Pd interactions must be considered in both cases.[254]

The structure of the intermetalloid cluster $[Ni_3@Ge_{18}]^{4-}$ (Figure 15b) in which a linear nickel atom trimer bridges to two widely opened D_{3h}-symmetric Ge_9 clusters, is related to the E_{18} polyhedra.[247] Thus, the two separate Ge_9 units feature the same structure as that of the two E_9 subunits found in $[Pd_2@E_{18}]^{4-}$ (Figure 15f). Although the germanium atoms of the two cluster units are in direct contact, the relative orientation of the six atoms of the open prism bases is already staggered as it is required for an 18-vertex cage.[254]

A closed deltahedral cluster that is filled with two transition-metal atoms is also realized in $[Ni_6Ge_{13}(CO)_5]^{4-}$ (Figure 15g).[262] The cluster consists of two interpenetrating icosahedrons that share a central, pentagonal bipyramidal Ge_3Ni_3 unit. The cage is defined by 13 germanium atoms and 4 Ni(CO) fragments. Owing to the high Ni:Ge atom ratio, this cluster has intermetalloid character.

The mechanism of the formation of endohedral clusters with nine or more skeleton atoms still remains unexplained.[255,256] However, observations made during the syntheses of several empty transition-metal-capped E_9 clusters give evidence for a possible reaction path. So does the appearance of the anions $[Cu(\eta^4\text{-}Ge_9)(P\mathit{i}Pr_3)]^{3-}$ and $[Cu(\eta^4\text{-}Ge_9)(\eta^1\text{-}Ge_9)]^{7-}$ (Figure 12a) that both were obtained from reactions of K_4Ge_9 with $CuCl(P\mathit{i}Pr_3)$ in liquid ammonia, but at different temperatures.[221] The Cu–P bond remains intact at a reaction temperature of −70 °C, and salts of $[Cu(\eta^4\text{-}Ge_9)(P\mathit{i}Pr_3)]^{3-}$ crystallize from these solutions. However, upon storage of these solutions at −40 °C, the anion $[Cu(\eta^4\text{-}Ge_9)(\eta^1\text{-}Ge_9)]^{7-}$ forms in which the phosphane ligand is substituted by a σ-donating $[\eta^1\text{-}Ge_9]^{4-}$ unit. Therefore, the ligand of the transition metal can be released from the capping transition-metal atom. Two reaction paths are then possible: a) the transition-metal atom can slip into the E_9 cluster, as happens in $[Cu@E_9]^{3-}$ and $[Ni@Ge_9]^{3-}$; or b) the empty coordination site of the d-block metal can be filled by a second cluster under formation of anions such as $[Cu(\eta^4\text{-}Ge_9)(\eta^1\text{-}Ge_9)]^{7-}$, which can then rearrange into an endohedral cluster with a higher number of cage atoms depending on the nature of the heteroatom and the overall reaction conditions. Certainly the formation of endohedral clusters can in principle also occur by a fragmentation of the Sn_9 framework and reordering at the copper atom.

Hints for the formation of larger assemblies comprising 17 or 18 Group 14 atoms are given by a series of E_9 clusters that are filled and simultaneously capped by a transition metal, such as the anions $[(Ni@Sn_9)Ni(CO)]^{3-}$[263] and $[(Pt@Sn_9)Pt(PPh_3)]^{3-}$[263] (Figure 15a and d, respectively), and by the modified Ge_9 clusters $[(Ni@Ge_9)Ni(R)]^{n-}$ (R = CO, C≡C-Ph, en)[220] and $[(Ni@Ge_9)Pd(PPh_3)]^{2-}$.[220] However, there still remain some open questions; for example, it is not understood why a nickel atom builds a ten-vertex cluster during the reaction with the Pb_9 unit, while nine much smaller germanium atoms are able to suitably enclose the same transition metal. It is also noteworthy that endohedral clusters obtained from solution chemistry are formed in a completely different way as in gas-phase experiments in which the Group 14 atoms apparently assemble step-by-step around the doping element.[224,264]

5.5. Heteroatomic Intermetalloid Group 15 Clusters

The coordination chemistry of Group 15 elements to bare transition metals forming intermetalloid-like systems traces back to $[Nb(As_8)]^{3-}$ from von Schnering et al., which can be described as an Nb^V cation complexed by a cyclic $[As_8]^{8-}$ anion (Figure 16a).[265] A similar unit, $[Mo(As_8)]^{2-}$, contains an Mo^{VI} cation in the center of the $[As_8]^{8-}$ ring.[266] In both cases, the transition metal resides in the center of a crown-shaped ring of arsenic atoms. If each arsenic atom in the $[As_8]^{8-}$ anion acts as a two-electron σ donor, 16-electron complexes would result, but von Schnering and co-workers suggested additional π donation from the $[As_8]^{8-}$ unit to the metal, which leads to stable 18-electron complexes. In $[(P_5)_2Ti]^{2-}$, two $[P_5]^-$ rings coordinate in a ferrocene-like fashion to a Ti^0 atom, leading to a 16-electron complex (Figure 16b).[267] Intermetalloid clusters with intact heptapnicanortricyclane anions $[Pn_7]^{3-}$ (Pn = P, As) are frequently observed as in $[(As_7)Sn(As_7)]^{4-}$, $[(P_7)Cu_2(P_7)]^{4-}$, $[(P_7)Zn(P_7)]^{4-}$, and $[(P_7)Cd(P_7)]^{4-}$ (Figure 16c–f) in which the $[Pn_7]^{3-}$ anions coordinate to M^{2+}, and in one case to a Cu_2^{2+} dumbbell.[135,268] In $[(As_7)Pd_2(As_7)]^{4-}$, one bond of each nortricyclane unit is broken. Assuming two-bonded arsenic atoms as As^-, the resuling norbornane-shaped anions are connected to a Pd_2 dumbell with a formal charge of +6 (Figure 16g).[269] A complete rearrangement of the $[As_7]^{3-}$ anion is found in the palladium-rich anion $[Pd_7As_{16}]^{4-}$ in which a Pd_7 core with the topology of a distorted singly capped trigonal prism is coordinated by two $[As_5]^-$ rings (electronically equivalent to aromatic $C_5H_5^-$), two $[As_2]^{2-}$ dumbbells, and two isolated As^{3-} atoms (Figure 16h). Assuming the charges of the arsenic atoms, the palladium prism can be described as consisting of six Pd^I and one square-planar-coordinated Pd^{II} cation.[269] Eichhorn and co-workers also succeeded in the synthesis of a unique endohedral Group 15 element cluster. In $[As@Ni_{12}@As_{20}]^{3-}$ (Figure 16i), the central arsenic atom is icosahedrally surrounded by 12 nickel atoms, forming an $[Ni_{12}(\mu_{12}\text{-}As)]$ cluster. The latter is surrounded by a pentagon dodecahedron of 20 arsenic

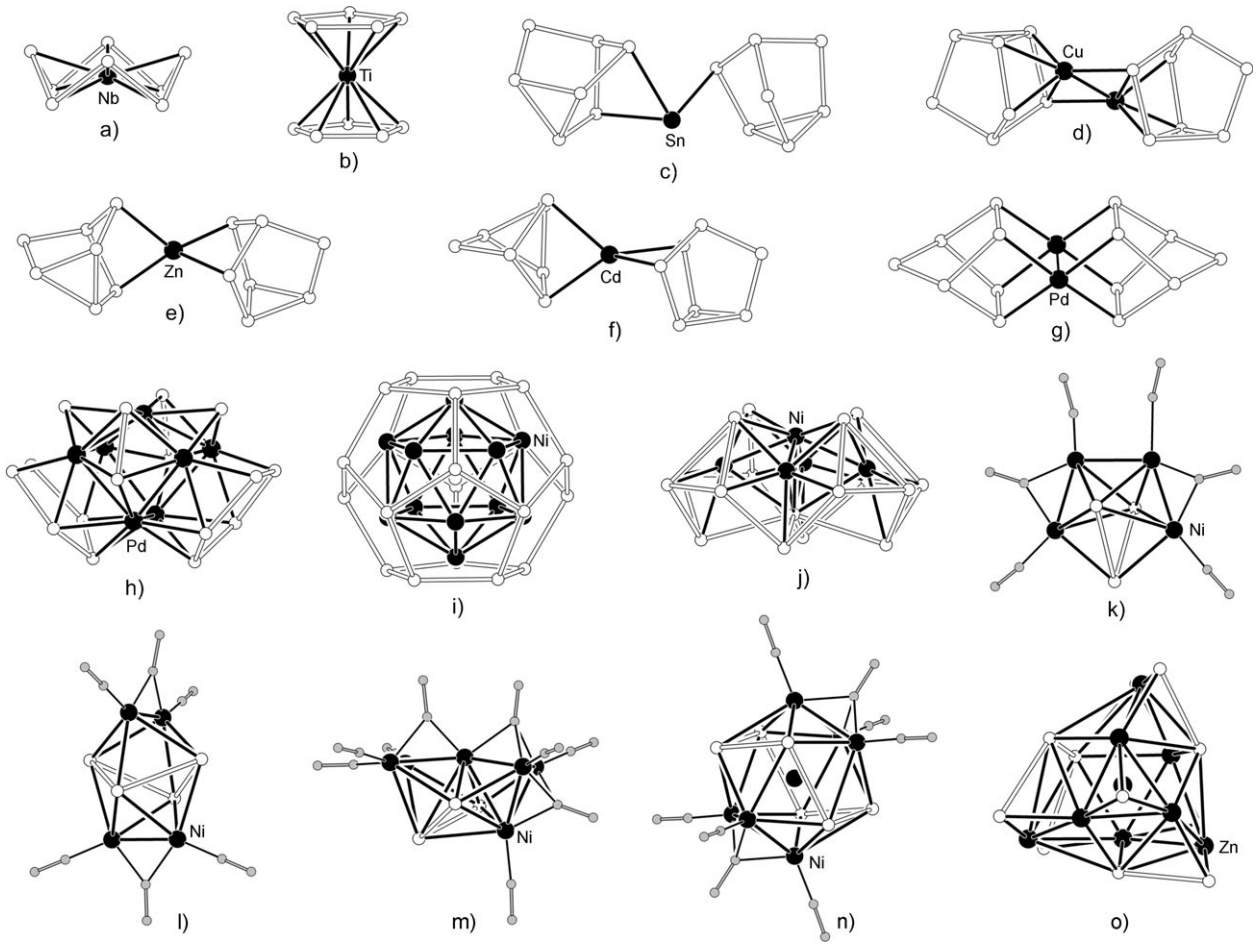

Figure 16. a) $[M(As_8)]^{3-}$ (M = Nb,[265] Mo[266]), b) $[Ti(P_5)_2]^{2-}$,[267] c) $[(As_7)Sn(As_7)]^{4-}$,[135] d) $[(P_7)Cu_2(P_7)]^{4-}$,[268] e) $[(P_7)Zn(P_7)]^{4-}$,[268] f) $[(P_7)Cd(P_7)]^{4-}$,[268] g) $[(As_7)Pd_2(As_7)]^{4-}$,[269] h) $[Pd_7As_{16}]^{4-}$,[269] i) $[As@Ni_{12}@As_{20}]^{3-}$,[270] j) $[Ni_5Sb_{17}]^{4-}$,[271] k) $[Ni_4Pn_3(CO)_6]^{3-}$ (Pn = Sb, Bi),[272] l) $[Ni_4Bi_4(CO)_6]^{2-}$,[272] m) $[Ni_6Bi_3(CO)_9]^{3-}$,[272] n) $[Ni_x@Bi_6Ni_6(CO)_8]^{4-}$,[272] and o) $[Zn@Zn_8Bi_4@Bi_7]^{5-}$[273]. A complete list of the compounds is given in Table 7.

atoms.[270] To the best of our knowledge, the only known bare intermetalloid cluster of tin is $[Ni_5Sb_{17}]^{4-}$ (Figure 16j). The central Ni_5 unit has a similarity to five of the seven palladium atoms in Figure 16h. Although the anion with 139 valence electrons should be paramagnetic, no EPR signal is obtained.[271] In the anion $[Sb_3Ni_4(CO)_6]^{3-}$, the Ni:Pn ratio is close to one and the anion contains a pentagonal bipyramidal Sb_3Ni_4 skeleton with two antimony atoms in the apical positions. From the structure and the electron count, the cluster is a *closo* deltahedron with 16 skeletal electrons (Figure 16k).[272]

As expected, the heavier congener of antimony, bismuth, has a higher tendency to form intermetalloid clusters, but most of its intermetalloid compounds contain CO-coordinated transition metals, such as pentagonal-bipyramidal $[Ni_4Bi_3(CO)_6]^{3-}$ (Figure 16k), bisphenoidal $[Ni_4Bi_4(CO)_6]^{2-}$ (Figure 16m), truncated icosahedral $[Ni_6Bi_3(CO)_9]^{3-}$ (Figure 16m), and filled icosahedral $[Ni_x@Bi_6Ni_6(CO)_8]^{4-}$ (Figure 16n) ($x = 0.33$).[272] A ligand-free endohedral cluster has been found in the anion $[Zn@Zn_8Bi_4@Bi_7]^{5-}$, which may be seen as a zinc-centered, distorted Zn_8Bi_4 icosahedron capped by seven bismuth atoms (Figure 16o). The Zn_8Bi_4 icosahedron shows the same electron count as an icosahedron of Group 13 elements, such as Al_{12} or Ga_{12}, and thus it contributes 36 electrons to the cluster skeleton. Together with the two electrons from the zinc atom, and another five electrons from the cluster charge, 43 electrons are available for the cluster skeleton. The remaining seven electrons required for a *closo* species with 50 skeletal electrons seem to stem from the seven bismuth atoms, which are considered by the authors to act as single-electron ligands.[273] A structurally related ternary intermetalloid cluster anion, $[Zn@Zn_5Sn_3Bi_3@Bi_5]^{4-}$, was recently found. Assuming the composition $Zn_6Sn_3Bi_8$ in the strongly disordered cluster, the observed *nido* cluster has the required 48 skeletal electrons if the five bismuth atoms are again regarded as one-electron-donor ligands.[274] The examples show that in Group 15, owing to the transition between localized covalent bonds and delocalizied skeletal bonding, the description of the bonding situation is sometimes rather difficult as it remains unclear how many electrons are donated by pnictide atoms such as bismuth to a cluster framework.

6. NMR Spectroscopy

Among Group 14 atom clusters, NMR experiments have been reported for the elements tin and lead, which both possess magnetically active spin-1/2 nuclei, ^{119}Sn and ^{207}Pb, with high natural abundance and sufficient NMR receptivity.[275,276] Si NMR data of polyhedral silicon clusters have not yet been reported.

Rudolph and co-workers were the first to explore the structural properties of $[Sn_9]^{4-}$ and $[Pb_9]^{4-}$ in solution using NMR techniques.[59] They dissolved different alloys of the systems Na-Sn-Pb and K-Sn-Pb in an appropriate solvent in the absence of any cryptand molecules. The ^{119}Sn NMR spectrum of the deep-orange ethylenediamine solution of $NaSn_{2.25}$ at −40 °C displayed only one signal for the $[Sn_9]^{4-}$ unit with a chemical shift of $\delta = -1230$ ppm and line splitting owing to ^{119}Sn–^{117}Sn coupling of 256–293 Hz.[59] A single resonance at $\delta = -4098$ ppm was also observed for the $[Pb_9]^{4-}$ cluster extracted from corresponding lead phases in the ^{207}Pb NMR spectrum, showing that the three magnetically nonequivalent E atoms of the static C_{4v}-symmetric structure rapidly exchange on the NMR timescale in solution.[23] The exchange process involves a bond-making step across the open square face of the C_{4v}-symmetric *nido* cluster (**V**, Figure 2e) and leads to the interconversion to the D_{3h}-symmetric *closo* cluster (**I**, Figure 2a) via a C_{2v}-symmetric transition state (**II** or **III**, Figure 2).[65,277]

The existence of the Zintl clusters $[Sn_{(9-n)}Pb_n]^{4-}$ ($n = 0$–9) has also been shown by NMR experiments on ethylenediamine extracts of ternary Na-Sn-Pb alloys.[59] The ^{119}Sn NMR signals of these clusters are gradually highfield-shifted by $\Delta\delta(^{119}\text{Sn}) = 31$–60 ppm for each additional lead atom, while the ^{207}Pb NMR signals are shifted downfield by $\delta = 185$ ppm per additional tin atom. It was pointed out that the substitution of tin by germanium atoms has a considerably smaller effect on the ^{119}Sn NMR shifts of the anionic clusters, and for clusters of the compositions $[Sn_{(8-y)}Pb_yTl]^{5-}$ the ^{119}Sn NMR signals are shifted to higher field by about 45 ppm per additional lead atom.[203] Results of NMR studies are available for a large number of cluster species, for example for $[Sn_4]^{2-}$ ($\delta = -1895$ ppm) and $[Sn_2Bi_2]^{2-}$ ($\delta = -1674$ ppm).[59] An overview is given in Table 5.[278]

Hints for the existence of Zintl ion complexes were also first given on the basis of NMR experiments. Clusters of the type $[E_9\{M(PPh_3)\}_2]^{4-}$ (M = Pt, Pd) were suggested as products of the reactions between $[E_9]^{4-}$ with $[Pt(PPh_3)_4]$[279] and $[Pd(PPh_3)_4]$, respectively.[280] The ^{119}Sn NMR spectrum of a solution of K_4Sn_9 and $[Pt(PPh_3)_3]$ in ethylenediamine displayed one signal at $\delta(^{119}\text{Sn}) = -736$ ppm that was split into a triplet of quintuplets, where the triplet was assigned to the coupling between ^{119}Sn and ^{195}Pt ($J(^{119}\text{Sn}–^{195}\text{Pt}) = 1544$ Hz) and the quintet to the ^{119}Sn–^{117}Sn coupling along the cluster skeleton bonds ($J(^{119}\text{Sn}–^{117}\text{Sn}) = 79$ Hz). In the ^{207}Pb NMR spectrum of the corresponding lead cluster a triplet at $\delta = -2988$ ppm occurred with lines separated by 4122 Hz as a result of ^{207}Pb–^{195}Pt coupling. For the cluster $[Sn_9\{Pd(PPh_3)\}_2]^{4-}$, one ^{119}Sn NMR signal was observed with a chemical shift of $\delta = -755$ ppm and a ^{119}Sn–^{117}Sn coupling of 39 Hz.[280] All Group 14 element clusters were found to be fluxional in solution even after the addition of a transition metal fragment.

20 years later, Eichhorn reinvestigated the reactions of $[E_9]^{4-}$ with $[Pt(PPh_3)_4]$ and $[Pd(PPh_3)_4]$, but this time in the presence of [2.2.2]crypt, and the NMR spectra of the solutions showed the resonances observed by Rudolph but with very low intensities. The main ^{119}Sn NMR signals of the solutions containing $[Sn_9]^{4-}$ and $[M(PPh_3)_4]$ were generated by the clusters $[Pt@Sn_9H]^{3-}$ ($\delta = -368$ ppm),[257] $[Pt_2@Sn_{17}]^{4-}$ ($\delta = -742$ ppm),[257] and $[Pt@Sn_9Pt(PPh_3)]^{2-}$ [263] ($\delta = -862$ ppm) for M = Pt and by $[Pd_2@Sn_{18}]^{4-}$ [255] ($\delta = -730$ ppm) for M = Pd. Only one resonance was detected for each species, indicating again the fluxional behavior of the cluster frameworks in solution. The ^{207}Pb NMR resonances of $[Ni@Pb_{12}]^{2-}$ ($\delta = +1167$ ppm), $[Pd@Pb_{12}]^{2-}$ ($\delta = +1520$ ppm), $[Pt@Pb_{12}]^{2-}$ ($\delta = +1780$ ppm), and $[Ni@Pb_{10}]^{2-}$ ($\delta = -996$ ppm) obtained from solutions containing $[Pb_9]^{4-}$ and $[M(PPh_3)_4]$ or $[Ni(cod)_2]$ have also been established.[252]

Table 5: ^{119}Sn and ^{207}Pb NMR data for Group 14 element clusters in solution.

Polyanion	^{119}Sn, δ [ppm] [$J(^{119}\text{Sn}-^{117}\text{Sn})$/Hz] (solvent)			Polyanion	^{207}Pb, δ [ppm] (solvent)
$[Sn_9]^{4-}$	−1230 [260] (en)			$[Pb_9]^{4-}$	−4098 (en)
$[(PPh_3)_2PtSn_9]^{4-}$	−736 [79] (en)			$[(PPh_3)_2PtPb_9]^{4-}$	−2988 (en)
$[(PPh_3)Pt_2Sn_9]^{4-}$	−862 (dmf)			$[Pt@Pb_{12}]^{2-}$	+1780 (dmf)
$[Pt@Sn_9H]^{3-}$	−368 [160] (en/tol)			$[Pd@Pb_{12}]^{2-}$	+1520 (dmf)
$[Pt_2@Sn_{17}]^{4-}$	−742 [170] (dmf)			$[Ni@Pb_{12}]^{2-}$	+1167 (dmf)
$[(PPh_3)_2PdSn_9]^{4-}$	−755 [39] (en)			$[Ni@Pb_{10}]^{2-}$	−996 (dmf)
$[Pd_2@Sn_{18}]^{4-}$	−730(dmf); −751(en) [<120]				
$[Ni_2@Sn_{17}]^{4-}$	1713, −1049, −1010, +228 (dmf)				
$[Cu@Sn_9]^{3-}$	−1431 [85] (dmf) −1458 [60] (en) −1440 [85] (acn)			$[Cu@Pb_9]^{3-}$	−4144 (dmf)
$[(CO)_3M\text{-}Sn_9]^{4-}$ [a]	Sn_{ap} [d]	$Sn_{M\ c\text{-}s}$ [d]	$Sn_{Sn\ c\text{-}s}$ [d]	$[(CO)_3MoPb_9]^{4-}$	Pb_{ap}, $Pb_{Mo\ c}$, $Pb_{Pb\ c}$ [d]
M = Cr	2493	−213	−521		
Mo	2125	−402	−681		27, −1934, −3450 (NH_3)
W	2448	−496	−735		
	[129 to 1048] (NH_3)				
$[i\text{Pr-}Sn_9]^{3-}$ [b]	−1413 [c] [170] (dmf)				
$[Cy_3Sn\text{-}Sn_9]^{3-}$ [b]	−1172 [155] (dmf)				

[a] Measurements were also carried out in en. [b] Coupling constants between the exchanging tin atoms are 115 Hz and 295 Hz for $[i\text{Pr}(Sn_9)]^{3-}$ and $[Cy_3Sn(Sn_9)]^{3-}$, respectively. The *exo* tin atom couples with $^1J(^{119}\text{Sn}–^{119}\text{Sn}) = 1331$ Hz and $^1J(^{119}\text{Sn}–^{117}\text{Sn}) = 1272$ Hz to the Sn_9 cluster. $^1J(^{119}\text{Sn-}^{119}\text{Sn})$ and $^1J(^{119}\text{Sn}–^{117}\text{Sn})$ coupling constants of 1876 Hz and 1793 Hz, respectively, occur between the alkyl-bonded tin atom and the remaining eight tin atoms in $[i\text{Pr}(Sn_9)]^{3-}$. [c] Multiplet. [d] ap = apical, c = capped, c-s = capped square.

At a temperature of −64 °C, the anion $[Ni_2@Sn_{17}]^{4-}$ generates four different ^{119}Sn resonances at $\delta_1 = -1713$ ppm, $\delta_2 = -1049$ ppm, $\delta_3 = -1010$ ppm, and $\delta_4 = +228$ ppm with relative intensities of approximately 4:8:4:1.[253] Thus, the Zintl cluster is rigid in solution under these conditions, and on the basis of its solid-state structure (Figure 15c), δ_2 can be assigned to the eight magnetically equivalent tin atoms connected to the central tin atom and δ_4 to the central tin atom itself. At 60 °C, only one signal is observed at −1167 ppm, indicating again fast atom-to-atom exchange processes at elevated temperatures.

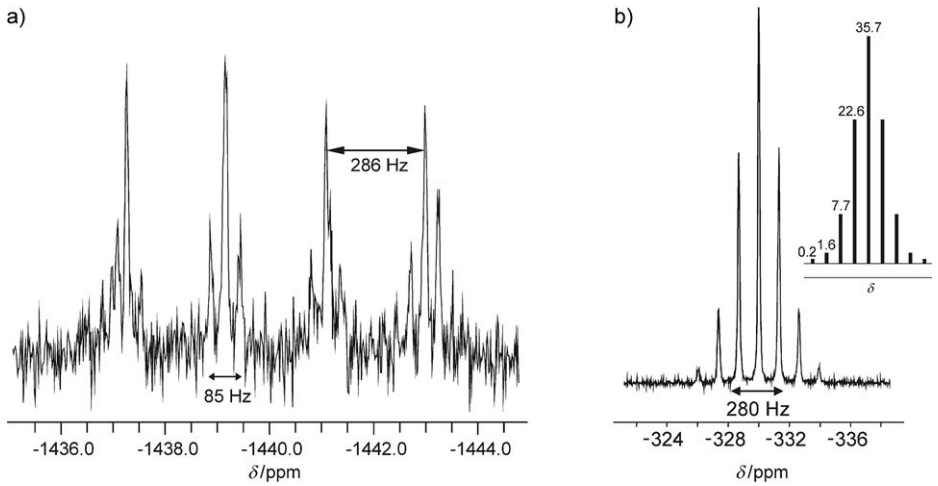

Figure 17. NMR spectra of $[Cu@Sn_9]^{3-}$: a) Experimental ^{119}Sn NMR spectrum ($\delta = -1440$ ppm, 1:1:1:1 quartet, $J(^{119}Sn–^{63/65}Cu) = 286$ Hz, two satellites with $J(^{119}Sn–^{117}Sn) = 85$ Hz), b) experimental ($\delta = -332$ ppm, $J(^{119}Sn–^{63}Cu) = 280$ Hz) and simulated ^{63}Cu NMR spectrum (inset). The spectra were recorded in acetonitrile at room temperature. Simulations account for coupling to various $^{119/117}Sn$ isotopomers $[Cu@^{119/117}Sn_xSn_{(9-x)}]^{3-}$ (with $x = 0, 1, ..., 4$).[248]

For $[Sn_9M(CO)_3]^{4-}$ (M = Cr, Mo, W) and $[Pb_9Mo(CO)_3]^{4-}$, three resonances are observed in their NMR spectra with a ratio of 4:4:1 and with the chemical shifts given in Table 5, indicative of a rigid C_{4v}-symmetric E_9 skeleton with the lowest-intensity signal assigned to the apical Group 14 atom.[214,216] The remaining two signals are generated by the two sets of four magnetically equivalent Group 14 atoms in the square planes of the clusters, with the more shielded resonances assigned to the atoms bound to the transition metal. The tin atoms receive through-bond and through-space coupling interactions, and it is assumed that the direct interaction causes larger coupling constants than the indirect one.[214]

The ^{119}Sn and ^{207}Pb NMR spectra of the endohedral clusters $[Cu@E_9]^{3-}$ (E = Sn, Pb) in dmf solution again show a fluxional behavior of the cage atoms down to −60 °C with single resonances at $\delta = -1431$ ppm[248] and $\delta = -4144$ ppm,[258] respectively. The highfield shifts of the cage signals compared to that of the empty $[E_9]^{4-}$ clusters is attributed to an enhanced electron density at the Group 14 atoms in these endohedral clusters.

As both NMR-active copper nuclei ^{63}Cu and ^{65}Cu have a spin of 3/2 and thus a strong quadrupole moment, the linewidth of the NMR signals strongly depends on the symmetry of the copper coordination sphere. An cubic environment at least is required to decrease the linewidth of the ^{63}Cu NMR resonance to the point that it can be detected. Owing to the highly dynamic E_9 framework, which causes an environment of spherical symmetry for the endohedral copper atom in $[Cu@E_9]^{3-}$, the corresponding copper signals could readily be detected at $\delta = -287$ ppm (E = Sn) and $\delta = +258$ ppm (E = Pb), with exceptionally narrow linewidths of 9 and 8 Hz, respectively (Figure 17).[248]

Recently, the first NMR studies of functionalized clusters have been reported. For $[i\text{Pr}(Sn_9)]^{3-}$, one ^{119}Sn resonance at $\delta = 170$ ppm was assigned to the tin atom that binds to the alkyl group, while the remaining eight tin cluster atoms generate a multiplet at $\delta = -1413$ ppm.[182] The ^{119}Sn NMR spectrum of $[Cy_3Sn(Sn_9)]^{3-}$ displayed one signal at $\delta =$ 155 ppm caused by the *exo* tin atom and a second signal at $\delta = -1172$ ppm corresponding to the scrambling of the Sn_9 cage.

The results of NMR investigations carried out on Group 14 element clusters indicate that the chemical shift of the Group 14 atoms strongly depends on the ratio of cluster charge to the number of cluster vertices. A reduced charge per Group 14 atom causes a downfield shift of the signal, which is also observed when the cluster atom participates in coordinative bonding to form of a ten-vertex cluster with a transition metal in a capping position or when a ligand is *exo*-bonded. Accordingly, the signal of a cluster atom appears at higher field when the number of its bonds is reduced or when the bond lengths are significantly elongated.

The surprisingly small $^{119}Sn–^{117}Sn$ coupling constants in transition-metal-filled Sn_x clusters ($x = 9$, 17, 18) indicate a hindered direct coupling when the cluster center is occupied. The very early NMR studies on Group 14 element Zintl ions showed that the flexibility of these clusters also reduces the coupling constants. Clusters like $[Sn_2Ge_7]^{4-}$ display larger coupling which is assigned to direct Sn-Sn contacts, and in $[(Sn_9)SnCy_3]^{3-}$ a much larger coupling arises between the *exo*-bonded tin atom and the cluster atoms than between the tin atoms within the cluster.[182] In $[(Sn_9)M(CO)_3]^{4-}$ (M = Cr, Mo, W), the most intensive coupling was found between the apical tin atom and the tin atoms of the adjacent plane.[214] Thus, the coupling constant increases when static bonds occur. Eichhorn further proposed that the tin–tin coupling decreases with both an increasing number of cluster atoms and enlarged bond lengths within the cluster structure.

Among the Group 15 elements, ^{31}P is an excellent nucleus for NMR spectroscopy owing to its 100% abundance, its nuclear spin of $^1/_2$, and a sensitivity of 6.6% compared to that of ^1H. ^{31}P resonances cover a range of approximately $\delta =$ 1000 ppm between $\delta = -488$ ppm for P_4 and $\delta = +600$ ppm in organo-substituted diphosphenes. Baudler and co-workers used ^{31}P NMR spectroscopy to analyze very complex mixtures

of open-chain, cyclic, and polycyclic phosphanes, hydrogenpolyphosphides, and polyphosphides in solution.[281,282] Precise ^{31}P chemical shifts depend on the concentration, the temperature, the counterions in ionic compounds, and the solvent. Open-chain, cyclic, and polycyclic phosphanes show signals over a range from approximately $\delta = +50$ to -200 ppm.[188,281,282] The polycyclic $[P_7]^{3-}$ anion shows three well-separated groups of signals at low temperatures with shifts of $\delta = -50$, -100, and -160 ppm, which coalesce at higher temperatures to give one signal at $\delta = -120$ ppm owing to valence tautomerism.[48,281] Baudler and co-workers also succeeded in unambigously identifying the polyphosphides $[P_{21}]^{3-}$ and $[P_{26}]^{4-}$ using one- and two-dimensional NMR techniques. $[P_{21}]^{3-}$ has eight different groups of signals in the range from $\delta = +72$ to -169 ppm, and the $[P_{26}]^{4-}$ anion has a similar spectrum with nine different groups of signals in the range from $\delta = +84$ to -169 ppm.[283,284]

The polyphosphides $[P_5]^-$ and $[P_4]^{2-}$ are found as characteristic downfield singlets at approximately $\delta = +468$ ppm and $+340$ ppm, respectively, thus indicating the aromaticity of these anions.[42,48,281] Alkylation, arylation, or substitution with transition-metal fragments leads to a downfield shift of the signals. In the anion $[Et(P_7)W(CO)_3]^{2-}$, three groups of signals are observed in the range $\delta = +142$ to -180 ppm,[285] and the cations $[P_7R_2]^+$, $[P_7R_4]^{2+}$, and $[P_7R_6]^{3+}$ have signals between $\delta = +115$ and -280 ppm.[188]

In the last 30 years, magic angle spinning (MAS) NMR spectroscopy has developed to an invaluable tool for the structural characterization especially of amorphous and disordered solids. However, ^{31}P MAS NMR spectroscopy suffers from limited resolution owing to ^{31}P–^{31}P dipole–dipole interactions, which are not completely averaged even at high spinning rates.[286]

To the best of our knowledge, solid-state ^{31}P MAS NMR spectroscopy on isolated molecular polyphosphides is limited to the cyclic $[P_6]^{4-}$ anion. This study confirmed that the anion is not aromatic,[287] as the spectrum of Rb_4P_6 shows two signals in a 2:1 ratio at $\delta = -55$ and -68 ppm, and the spectrum of Cs_4P_6 has only one very broad signal at $\delta = -19$ ppm. LiP_5, with its three-dimensional infinite anionic phosphorus network, has been analyzed very carefully by one- and multidimensional solid-state NMR spectroscopy. The chemical shifts range from $\delta = +2$ to -128 ppm.[286]

7. Theoretical Investigations

7.1. Wade's Rules, Shell Models, Spherical Aromaticity, and Cluster MOs

Whereas Group 15 element polyanions can readily be described by the $8-N$ rule (including multiple bonds), the deltahedral Group 14 element clusters require a more extended description of their bonding characteristics.

Various concepts have been applied in the discussion of the structure and chemical bonding of Zintl anion clusters. Of note, none of them had originally been developed for Zintl clusters, instead they were applied to Zintl anions after it was established that they give a useful description of those species they were primarily designed for, following a general prospect in cluster chemistry that a unified conceptual treatment of many different types of clusters might be possible.[288,289] Most attractive to chemists are those concepts which establish a correlation between structure and electron count or at least lead to counting rules with "magic numbers" associated with special stability.

Wade's rules[55,56,290] are clearly the most commonly used counting rules for the rationalization of Group 14 element cluster structures. Primarily developed for boranes, they were subsequently found to apply also to deltahedral structures of other main-group element clusters. The four valence electrons of each atom in homoatomic Group 14 element clusters are regarded as one lone pair (pointing radially to the outside of the cluster in analogy to the external B–H bonds in boranes) and two electrons that take part in the skeletal bonding. According to Wade's rules, $n+1$ skeletal bonding molecular orbitals result for a closed deltahedral (*closo*) cluster structure with n vertices. Application of Wade's rules to an n-atom dianionic cluster $[E_n]^{2-}$ (E = Si, Ge, Sn, and Pb) thus leads to an n-vertex *closo* cluster ($2n+2$ skeletal electrons) analogous to the series $[B_nH_n]^{2-}$. The number of bonding skeletal molecular orbitals does not depend on whether all vertices of the deltahedral structure are occupied or not. Consequently, n-atom *nido* and *arachno* clusters (with structures derived from *closo* deltahedra by removal of one or two vertices) require $2n+4$ and $2n+6$ skeletal electrons, resulting in $[E_n]^{4-}$ and $[E_n]^{6-}$ anions, respectively. Notably, the cluster charge is constant independent of cluster size n for Group 14 element clusters, as each vertex atom contributes two electrons for cluster bonding. In contrast, charges of Group 15 element *closo* deltahedra $[Pn_n]^{(n-2)+}$ increase linearly with cluster size.[54]

Wade's rules are most valuable for the established correlation between electron count and structure. Several other models which are occasionally used to rationalize Zintl clusters, such as the Jellium model,[291,292] tensor surface harmonic (TSH) theory,[293–295] and the $2(N+1)^2$ rule[296,297] ($N = 1, 2, 3, \ldots$), can be categorized as "spherical-shell" models. They provide magic numbers of electrons that are required for especially stable clusters, independent of the exact positions of the atomic cores and of the number of atoms that constitute the cluster. These concepts include some sort of approximation in which the cluster is represented by a sphere, and the electrons move in a spherical potential. The resulting cluster wavefunctions may be described as spherical harmonics, and they can be labeled using radial and angular quantum numbers N and L, respectively. These cluster wavefunctions are not unlike atomic orbitals, and the ordering of the energy levels leads to a shell structure, which however is different from that for atomic energy levels. Special stability results when a shell closure, namely a magic number of electrons, is reached. Naturally, the applicability of such spherical models to real systems which do not show spherical symmetry is limited, and some of these concepts have been developed further to account for the actual shape of the cluster.[298,299]

In recent theoretical studies, the electronic structure of anionic Zintl clusters is usually analyzed by means of density

functional or ab initio molecular orbital calculations. Energy-level diagrams and molecular orbital contour plots obtained from these computations are frequently depicted, and MOs are usually labeled following a terminology that is employed for the spherical models.[248,291,297,300,301] An inspection of the MO plots shows the resemblance to representations of atomic orbitals, and the labels S, P, D… can be assigned to MOs with none, one, two… angular nodes. The first series of cluster S, P, D… orbitals can be labeled as 1S, 1P, 1D… . These MOs do not have a radial nodal surface, and alternative notations are S^+, P^+, D^+…, or (s,σ), (p,σ), (d,σ)… . The corresponding symbols for the second series of cluster MOs are 2S, 2P, 2D…, S^-, P^-, D^-… and (s,π), (p,π), (d,π)… . The cluster surface (defined by the vertices) represents a radial nodal surface for the 2S, 2P, 2D… MOs. Generally, for a cluster with n vertices, there are n MOs that predominantly comprise atomic s orbitals. These MOs are referred to as "s block", and they are associated with the lone pairs. Accordingly, there is also a "p block" of MOs which is mainly based on atomic p orbitals, with a further differentiation between principally radial and primarily tangential (with respect to the cluster surface) atomic p orbitals. The p block MOs can also be referred to as the skeletal bonding MOs. For their characterization, terms such as "core bonding", "surface (on-sphere) bonding", and "lone-pair character" are employed. Principally, the participation of radially oriented atomic p orbitals leads to core bonding and lone-pair character, tangential atomic p orbitals constitute surface bonding MOs. The fully symmetric 2S cluster MO is radially core bonding. The 2P cluster MOs are also generally based on radial p orbitals and show some lone-pair character. The other p block MOs can be described as mainly surface (on-sphere) bonding or surface bonding with some lone-pair character. Labels σ and π have also been used for MOs with lone-pair or surface-bonding character, respectively. Of course, the higher the symmetry and the more spherical the shape of the clusters, the more straightforward the use of these notations.

Another concept that is often employed relating to Zintl cluster anions is "spherical or three-dimensional aromaticity",[302,303] which is a term that has been defined in various ways. There have been attempts to classify homoatomic deltahedral anions according to a concept of three-dimensional aromaticity first suggested for fullerenes, which is commonly referred to as the $2(N+1)^2$ rule mentioned above.[296,297] Currently, the most commonly used aromaticity criterion for Group 14 element cluster anions is the so-called nucleus-independent chemical shift (NICS).[304,305] In a NICS analysis, the absolute magnetic shielding at special points of molecular space is calculated. The NICS(0) value is the NICS value at the center of the cluster. By convention, the sign of the calculated NICS values is changed so as to correspond to the familiar NMR scale. Aromatic clusters exhibit negative (diatropic) NICS(0) values, whereas antiaromaticity is shown by positive (paratropic) NICS(0) values.

7.2. Empty $[E_n]^{2-}$ Cluster Dianions with $n = 10, 12$

$[Pb_{10}]^{2-}$[89] is the only $[E_n]^{x-}$ Zintl cluster of a Group 14 element with $n > 9$ that has been characterized by single-crystal XRD as a bare empty cluster, but the most prominent representatives are $[Sn_{12}]^{2-}$ and $[Pb_{12}]^{2-}$, which have been identified in gas-phase experiments.[91,99,100] As they resemble the C_{60} fullerene in size and symmetry (I_h), they have been named stannaspherene and plumbaspherene, respectively. In this and the following section, the discussion will center on results obtained for empty ten- and twelve-vertex dianions $[E_n]^{2-}$ ($n = 10$, 12) and endohedral intermetalloid clusters $[M@E_n]^q$ with $n = 9$, 10, 12 (M = metal atom, q = charge), respectively.

Applying Wade's rules to an $[E_{12}]^{2-}$ anion (E = Si, Ge, Sn, or Pb) leads to an icosahedral (I_h) *closo* cluster ($12 \times 2 + 2 = 26$ skeletal electrons $= 2n + 2$, for $n = 12$), analogous to $[B_{12}H_{12}]^{2-}$ for all members of the homologous series. However, the results of various quantum-chemical calculations show that the analogy between the borane and the Group 14 element clusters has some limits, and considerable differences occur within the series.

The 25 highest occupied molecular orbitals of the icosahedral $[E_{12}]^{2-}$ clusters[300,306,307] can be divided into a group of 12 s block and a group of 13 p block MOs. The latter have a_g, g_u, t_{1u}, and h_g symmetry and can be labeled as 2S, 1F, 2P, and 1G cluster orbitals. A comparison of the valence MOs of the icosahedral $[E_{12}]^{2-}$ clusters with those of $[B_{12}H_{12}]^{2-}$[99,307] shows that the molecular orbitals of the Group 14 element Zintl anions $[E_n]^{2-}$ indeed are very similar to those of the valence-isoelectronic boranes $[B_nH_n]^{2-}$ with the MOs of $[E_n]^{2-}$ that show lone-pair character corresponding to $[B_nH_n]^{2-}$ MOs with B–H bonding character, but the relative energetic order of the molecular orbitals is generally different. For the boranes, surface bonding valence MOs are higher in energy than valence B–H bonding orbitals, whereas the highest occupied MOs of the $[E_n]^{2-}$ clusters exhibit lone-pair character. The HOMO of $[B_{12}H_{12}]^{2-}$ is the surface bonding g_u set,[99,307] for the $[E_{12}]^{2-}$ anions the HOMO is the h_g (E = Si,[307] Ge,[308] Sn[99,309]) or the t_{1u} (E = Pb[100,300,310]) set with lone-pair character.

It is worth mentioning that such an orbital scheme is actually not sufficient to account for the observed photoelectron spectra of stannaspherene and plumbaspherene, as spin–orbit coupling has to be taken into account for these species.[99,100] Spin–orbit-coupled MO schemes for the 13 skeletal bonding MOs of $[Sn_{12}]^{2-}$ and $[Pb_{12}]^{2-}$ show the splitting of each of the degenerate g_u, t_{1u}, and h_g MO sets into two levels, which leads to a substantially different MO pattern, and these spin–orbit-coupled levels are in qualitative agreement with the observed photoelectron spectra.[99,100]

Structure optimizations for the $[E_{12}]^{2-}$ anions, E = Si,[306,307,311,312] Ge,[306,308,312] Sn,[99,306,312,313] and Pb,[100,300,306,313] revealed that the expected icosahedron (I_h) corresponds to a ground state for all $[E_{12}]^{2-}$ clusters, but it represents the global minimum only for $[Sn_{12}]^{2-}$ and $[Pb_{12}]^{2-}$, whereas in the case of $[Ge_{12}]^{2-}$, structure optimizations led to several energetically almost equal minima, and the lowest-energy structure has not been determined unambiguously. The icosahedron is one of

the candidates; others are structures based on the motif of a tricapped trigonal prism, and another can be described as two stacked six-membered rings in chair conformation. Such less-symmetrical structures, and especially those based on the tricapped trigonal prism, are clearly favored for $[Si_{12}]^{2-}$.

Differences between the icosahedral $[E_{12}]^{2-}$ clusters for E = Si, Ge, Sn, and Pb also became apparent in NICS aromaticity studies, which revealed a change down the group from antiaromatic $[Si_{12}]^{2-}$ to aromatic $[Pb_{12}]^{2-}$.[306] Icosahedral $[Si_{12}]^{2-}$ was found to exhibit a large positive (paratropic) NICS(0) value (reported values lie between $\delta = +46.6$ ppm and $\delta = +56.4$ ppm)[306,307,311,312] indicative of antiaromaticity, in contrast to $[B_{12}H_{12}]^{2-}$, which is regarded as strongly aromatic with a large negative (diatropic) NICS(0) value of $\delta = -27.3$ ppm.[307] Positive (paratropic) NICS(0) values have also been obtained for the I_h-symmetric $[Ge_{12}]^{2-}$ cluster (reported values of $\delta = +11.8$ ppm[312] and $\delta = +14.2$ ppm[306]). The aromaticity of icosahedral stannaspherene $[Sn_{12}]^{2-}$ has been subject to some debate, as depending on the size of the basis sets and the pseudopotentials employed, the NICS(0) values range from $\delta = +2.6$ ppm to $\delta = -5.0$ ppm,[306,312,313] whereas plumbaspherene $[Pb_{12}]^{2-}$ is clearly aromatic with NICS(0) values between $\delta = -10.8$ ppm and $\delta = -20.7$ ppm.[300,306,313,314]

Concerning the discussion of aromaticity, it is worth mentioning that the $[E_{12}]^{2-}$ (E = Si, Ge, Sn, Pb) anions with 50 electrons occupying 25 orbitals do not comply with the $2(N+1)^2$ rule with $N = 4$.[300] That is because the σ and π shells (the first and the second series of cluster energy levels) are to be considered separately in this concept. The electron count for the $[E_{12}]^{2-}$ clusters is thus 42 + 8. With 42 electrons ($1S^2$ $1P^6$ $1D^{10}$ $1F^{14}$ $1G^{10}$), an open-shell situation arises for the first series because the 1G orbitals of g_g symmetry remain unoccupied. For the second series (2S, 2P, 2D, …), however, the $2(N+1)^2$ rule is met with $N = 1$, owing to the closed-shell ($2S^2$ $2P^6$) configuration with 8π electrons. This example illustrates well that some care has to be taken when magic numbers deduced from shell models, such as the $2(N+1)^2$ rule or the Jellium model, are employed for the description of more complex Zintl anions.

DFT calculations for the $[E_{10}]^{2-}$ anions (E = Si,[306,315] Ge,[250,306,316] Sn,[306] Pb[306,317]) have shown that the expected ten-vertex *closo* structure, that is, the D_{4d}-symmetric bicapped square antiprism, is a minimum in all cases. The most comprehensive structure optimization studies have been reported for $[Ge_{10}]^{2-}$.[250,316] While the bicapped square antiprism (D_{4d}) is the global minimum according to all accounts, it depends on the methods employed for the calculations whether the pentagonal prism (D_{5h}) corresponds to a minimum or not. A C_{3v}-symmetric *isocloso* structure has been found as a triplet ground state, while the D_{5d}-symmetric pentagonal antiprism is not a minimum for $[Ge_{10}]^{2-}$.

According to the calculated NICS(0) values, all D_{4d}-symmetric *closo* $[E_{10}]^{2-}$ cluster anions (E = Si,[306,307] Ge,[306] Sn,[306] Pb[306,314,317]) are highly aromatic, and in contrast to the $[E_{12}]^{2-}$ series, $[Si_{10}]^{2-}$ exhibits the largest negative NICS(0) value (reported values of $\delta = -61.9$ ppm[307] and $\delta = -68.0$ ppm[306]) and the diatropicity decreases down the group.[306]

7.3. Intermetalloid Endohedral $[M@E_n]^q$ Clusters with n = 9, 10, and 12

Gas-phase and related computational studies on metal-doped Group 14 element clusters ME_n^q (M = metal atom, q = charge) cover a wide range of cluster sizes n, but are mostly limited to neutral or singly positively or singly negatively charged species, whereas all intermetalloid endohedral Group 14 element clusters $[M@E_n]^q$ obtained from solution are anionic species with a two- or three-fold negative charge and a cluster size of $n = 9$, 10, or 12. The following discussion will focus on $[M@E_n]^q$ clusters with $n = 9$, 10, and 12. As far as nine-vertex clusters are concerned, the discussion will be limited to structurally characterized species. Both known and hypothetical examples will be considered for ten- and twelve-vertex endohedral intermetalloid clusters $[M^z@(E_n)^{2-}]$ ($n = 10$ or 12; z = charge) where M^z is a main group, d block or f block metal with s^0p^0, d^{10}, or f^6 electron configuration.

Centered ten- and twelve-vertex clusters with deltahedral cages that have been structurally characterized by single-crystal X-ray crystallography are the icosahedral clusters $[M@Pb_{12}]^{2-}$ (M = Ni,[252] Pd,[252] Pt[53,252]) and $[Ir@Sn_{12}]^{3-}$ (Figure 4e),[219] and the bicapped square antiprismatic anion $[Ni@Pb_{10}]^{2-}$ (Figure 14c).[251,252] These clusters can be rationalized as $[M^z@(E_n)^{2-}]$ species that contain $2n+2$ skeletal electron $[E_n]^{2-}$ ($n = 10$, 12) units with *closo* structures, and a central M^z atom with an electron configuration that does not change the skeletal electron count. The required closed-shell d^{10} configuration of the d block metal is obviously met when M is a Group 10 transition metal ($M^z = Ni^0$, Pd^0, or Pt^0), but it is also reached for $M^z = Ir^-$, Co^-, and Cu^+ (Table 6). The formal description of $[Ir@Sn_{12}]^{3-}$ as $[Ir^-@(Sn_{12})^{2-}]$ is supported by the calculated natural charge of −1.07 for Ir.[219] $[Co@Ge_{10}]^{3-}$,[250] although valence isoelectronic with $[Ni@Pb_{10}]^{2-}$, exhibits a non-deltahedral pentagonal prismatic structure. A natural charge of −1.05 was calculated for the cobalt atom, thus also indicating a d^{10} configuration.[250]

Among the known nine-vertex endohedral clusters, $[Ni@Ge_9]^{3-}$ [220,247] is not well characterized, and as mentioned above, $[Cu@E_9]^{3-}$ (E = Sn, Pb)[248] can adopt a D_{3h}-symmetric and a C_{4v}-symmetric structure (Figure 14a and b). These known $[M@E_9]^q$ clusters do not relate to $2n+2$ skeletal electron $[E_9]^{2-}$ *closo* clusters. But again, quantum-chemical calculations support the assumption of a d^{10} configuration for the encapsulated d block metal and thus suggest a notation as $[Cu^+@(E_9)^{4-}]$ (E = Sn, Pb).[248]

Although the enclosed metal atom does not contribute electrons to the skeletal electron count of the cluster, it provides orbitals that interact with the cluster orbitals of the $[E_n]^{x-}$ cage. This interaction is held responsible for an overall stabilization of the cluster, and the main contribution to this effect is attributed to the mixing of empty s and p orbitals of the central metal atom with suitable cage orbitals.[53,220] This has been shown e. g. by an orbital interaction diagram for the D_{3h}-symmetric $[Cu@Sn_9]^{3-}$.[248] Although all copper orbitals are included in the interaction, the stabilization results from the mixing of Cu s and p orbitals with the respective S and P cage orbitals. The same arguments hold for the D_{4d}-

symmetric $[M^z@(E_{10})^{2-}]$ and I_h-symmetric $[M^z@(E_{12})^{2-}]$ cluster units.

The valence electron count of an $[E_{12}]^{2-}$ cluster is also unchanged by an enclosed main group metal M^z with s^0p^0 electron configuration. Indeed, it has been shown that the valence MOs of $[M@Pb_{12}]^+$ (M = B, Al, Ga, In, Tl) are similar to those of $[Pb_{12}]^{2-}$.[300] However, the energetic order is different: the 2S and 2P orbitals (a_g and t_{1u}) are lowered in energy in the filled cluster.

DFT calculations have also been carried out for the d-block-metal-centered clusters $[Cu@Sn_{12}]^-$[309] and $[Ir@Sn_{12}]^{3-}$.[219] Apart from the insertion of an h_g MO set that represents the Cu 3d shell, the energetic sequence of the MOs of $[Cu@Sn_{12}]^-$ is consistent with that of the corresponding orbitals of $[Sn_{12}]^{2-}$. However, as observed for $[M@Pb_{12}]^+$ (M = B, Al, Ga, In, Tl), the a_g (2S) and t_{1u} (2P) MOs are considerably lower in energy for the filled cluster. With spin–orbit coupling taken into account, each degenerate orbital is split into two levels.

A molecular orbital diagram (without spin–orbit coupling) with the 18 highest occupied MOs of $[Ir@Sn_{12}]^{3-}$ is shown in Figure 18a. In icosahedral symmetry, s orbitals transform as a_g, p orbitals as t_{1u}, d orbitals have h_g symmetry, f orbitals are split into g_u and t_{2u} sets, and g orbitals into h_g and g_g sets. Thus, the s and p (and f) orbitals of a central atom can only mix with cage S, or P (or F) orbitals. The d orbitals of a central metal, however, are not only allowed to interact with cage D orbitals, but also with the h_g set of the cage G orbitals. These principles are well-illustrated by the depicted MOs of $[Ir@Sn_{12}]^{3-}$. The HOMO set for example is of h_g symmetry and mainly cluster 1G in character but also shows some admixing of the Ir d orbitals. A detailed MO analysis has also been reported for $[Pu@Pb_{12}]$, which can be rationalized as $[Pu^{2+}@(Pb_{12})^{2-}]$.[310]

For many of the $[M^z(E_{12})^{2-}]$ clusters, the I_h-symmetric endohedral structure was found to correspond to the global minimum, but for some, and especially for the silicon clusters, non-endohedral structures have been reported to be energetically favored. Selected results are summarized as follows. Structure optimizations led to I_h-symmetric ground-state structures for $[Ir@Sn_{12}]^{3-}$[219] and for the $[M@Pb_{12}]^{2-}$ clusters with M = Ni,[306] Pd,[306] and Pt.[252,306] The optimized interatomic distances agree well with those obtained from solid-state structure determinations. Compared to the optimized structure of the empty $[E_{12}]^{2-}$ cluster, the calculated Sn–Sn and Pb–Pb distances are elongated by less than 1% and 4% (for $[Pt@Pb_{12}]^{2-}$[252]), respectively.

$[Cu@Sn_{12}]^-$ and $[Au@Sn_{12}]^-$[309] have been characterized in gas-phase experiments, and calculations confirmed the transition-metal-centered icosahedral structure as the global minimum for $[Cu@Sn_{12}]^-$. In both cases, simulated photoelectron spectra based on spin–orbit-coupled calculations agree well with the experimental data.

The most prominent example of a main-group-metal-centered $[M^z@(E_{12})^{2-}]$ cluster is the above-mentioned $[Al@Pb_{12}]^+$.[314] For the AlE_{12}^+ clusters, the icosahedral structure with a central aluminum atom, I_h-$[Al@E_{12}]^+$, is energetically favored for E = Ge,[306] Sn,[306] and Pb.[306] I_h-$[Al@Si_{12}]^+$ is a local minimum, but less symmetrical non-

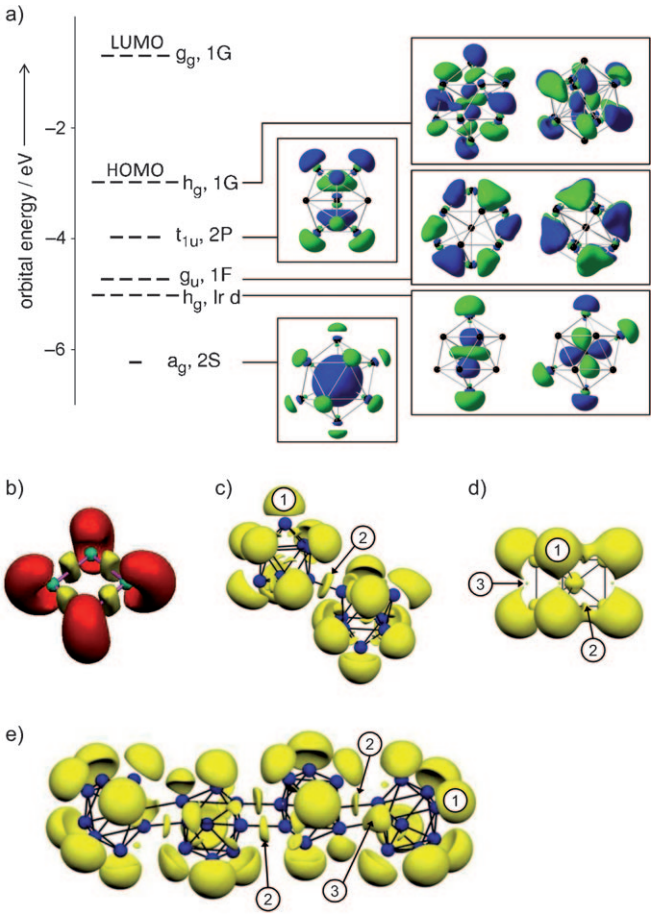

Figure 18. Molecular orbital (MO) and electron localization function (ELF) representations of several Group 14 and 15 polyanions: a) Skeletal bonding MOs of $[Ir@Sn_{12}]^{3-}$ (representative MOs of degenerate sets are shown),[219] b) ELF of $[P_4]^{2-}$[48] ($\eta(r) = 0.78$; core basins are green, disynaptic valence basins yellow, and monosynaptic basins red), c) ELF of $[Ge_9{-}Ge_9]^{6-}$ ($\eta(r) = 0.81$),[329] d) ELF of $[Co@Ge_{10}]^{3-}$ ($\eta(r) = 0.635$),[250] and e) ELF of $[Ge_9{=}Ge_9{=}Ge_9{=}Ge_9]^{8-}$ ($\eta(r) = 0.72$).[328,329]

endohedral structures are lower in energy.[306] The icosahedral structure has been found to be the most stable for all other $[M@Pb_{12}]^+$ clusters filled with Group 13 elements (M = B, Al, Ga, In, Tl).[300] The neutral clusters $[Be@E_{12}]$ (E = Ge, Sn),[318] $[Mg@E_{12}]$ (E = Ge,[318] Sn,[318] Pb[319,320]), $[Ca@Sn_{12}]$,[318] $[Zn@E_{12}]$ (E = Ge,[318,321,322] Sn[318]), and $[Cd@E_{12}]$ (E = Ge,[318] Sn[318,321]) also adopt I_h symmetry, whereas $BaPb_{12}$ and $SrPb_{12}$[319] prefer non-endohedral structures. In gas-phase experiments, no evidence for an enhanced stability of $ZnGe_{12}$ was found, but $ZnSn_{12}$ and $ZnPb_{12}$ were detected abundantly,[323] and for magnesium-doped $[Pb_{12}]^{2-}$ there is even some experimental evidence for the I_h-symmetric magnesium-centered icosahedral structure $[Mg@Pb_{12}]$ in the gas phase.[324] For doped silicon clusters, I_h-symmetric $[M^z@(Si_{12})^{2-}]$ structures correspond only to local minima for $M^z = Li^+$,[306] Na^+,[306] Be^{2+},[306,321] Mg^{2+},[306] Zn^{2+},[325] B^{3+},[306] and Al^{3+}.[306] Calculated ground-state structures are also available for lanthanoid- or actinoid-doped Pb_{12} clusters $[M@Pb_{12}]^q$ with q varying from +2 to −4.[310]

The notation $[M^z@(E_n)^{2-}]$ remains somewhat formal for the clusters with $n = 12$, as to date no empty $[E_{12}]^{2-}$ unit has

been isolated and structurally characterized in the solid state. For the ten-vertex clusters, however, this has been realized, and $[Pb_{10}]^{2-}$ [89] and $[Ni@Pb_{10}]^{2-}$ [251,252] are the only pair of an empty $2n+2$ skeletal electron Group 14 element *closo* cluster anion and its endohedral derivative that has been structurally characterized. As expected according to Wade's rules, both 22 skeletal electron clusters adopt the D_{4d}-symmetric bicapped square antiprismatic structure. The Pb–Pb distances in the endohedral cluster are only slightly elongated (max. 3%) compared to those in the empty cage. Although the expansion of the cluster is not isotropic, the filled cage displays an almost spherical shape as it was also observed for the above mentioned $[Cu@E_9]^{3-}$ anion (E = Sn, Pb).

The centered D_{4d}-symmetric bicapped square antiprism has been found as a ground-state structure for $[Ni@E_{10}]^{2-}$ (E = Ge, Sn, Pb), and for $[Pd@Sn_{10}]^{2-}$, $[Pd@Pb_{10}]^{2-}$, and $[Pt@Pb_{10}]^{2-}$.[306] The structures of $[M@Ge_{10}]^{2-}$ (M = Ni,[250,326,327] Pd,[327] Pt[327]) have been studied in more detail, and the centered D_{4d}-symmetric bicapped square antiprism was reported to be the energetically most favorable structure for $[Ni@Ge_{10}]^{2-}$ and a local minimum for $[Pd@Ge_{10}]^{2-}$. A centered pentagonal prism (D_{5h}) which corresponds to a local minimum for $[Ni@Ge_{10}]^{2-}$ is discussed as the lowest-energy structure for $[Pd@Ge_{10}]^{2-}$ and $[Pt@Ge_{10}]^{2-}$.

DFT calculations for $[Co@Ge_{10}]^{3-}$ [250] have revealed that the centered non-deltahedral D_{5h}-symmetric pentagonal prism is indeed a stable structure, whereas the centered D_{4d}-symmetric deltahedral cage is not a ground or a transition state, but the related energy differences are small. The D_{5h}- and D_{4d}-symmetric stationary states of the isoelectronic anions $[Ni@Ge_{10}]^{2-}$ and $[Co@Ge_{10}]^{3-}$ differ by 5.33 and 13.3 kcal mol^{-1}, respectively.[250] In spite of the different electron count, $[Fe@Ge_{10}]^{3-}$ was reported to be isostructural to $[Co@Ge_{10}]^{3-}$. This is surprising, as $[Co@Ge_{10}]^{3-}$ features a degenerate (e_2'') HOMO set, and it is therefore not straightforward that a species with one electron less adopts the same undistorted D_{5h}-symmetric pentagonal prismatic structure. However, no calculation of the open-shell system and no magnetic measurements on (paramagnetic) $[Fe@Ge_{10}]^{3-}$ are available yet.

Other ME_{10}^{q} clusters have been detected in gas-phase studies, which show high abundances of AlE_{10}^{+} (E = Ge, Sn, and Pb),[306] and $MgPb_{10}$ has also been found in gas-phase experiments.[324] The centered D_{4d}-symmetric bicapped square antiprism has been reported to be the global minimum structure for these clusters ($[Al@E_{10}]^{+}$, E = Ge,[306] Sn,[306] Pb;[306] $[Mg@Pb_{10}]$[319]) and for $[Zn@Si_{10}]$,[325] $[Zn@Ge_{10}]$,[326] and $[Cu@Ge_{10}]^{-}$,[326] while non-endohedral structures were found to be more favorable for $SrPb_{10}$ and $BaPb_{10}$.[319] For $AlSi_{10}^{+}$, less-symmetric non-endohedral structures are clearly favored.[306]

7.4. Investigations using the Electron Localization Function

To gain insight into the chemical bonding of Group 14 and Group 15 element polyanions, electron localization function (ELF) analyses were used.

Particularly interesting results were obtained for some polyphosphides. Species such as the aromatic $[P_4]^{2-}$ anion or the $[P_6]^{4-}$ anion with a formal P–P double bond have been shown to differ quite remarkably in the chemical bonding from their carbon analogues: In $[P_4]^{2-}$, the electron delocalization occurs predominantly in the lone pairs outside of the ring, which led to the term "lone-pair aromaticity" (Figure 18b). The P–P double bond in $[P_6]^{4-}$ also differs from C–C double bonds, as the π part of the bond is again formed by the lone pairs of the phosphorus atoms.[41,42]

The ELF has also been used to describe the bonding situation in homoatomic germanium clusters. The topological analysis of the ELF of the $[Ge_9–Ge_9]^{6-}$ anion (Figure 18c) confirms that localization occurs predominantly in the lone pairs and in the form of a localized two-center bond that links the two Ge_9 units.[140,329] The localization domains of the skeletal framework bonding include three-center bonds, as anticipated. The two-center bond, which links the Ge_9 clusters, is represented by the disynaptic valence basin ② between the two germanium atoms that take part in the intercluster bonding. No monosynaptic valence basins are associated with these *exo*-bonding germanium atoms, and all other germanium atoms of the dimeric anion show monosynaptic valence basins ①.

For the tetrameric $[Ge_9=Ge_9=Ge_9=Ge_9]^{8-}$ anion, the ELF shows a more unusual bonding situation (Figure 18e).[328,329] The bonding between the Ge_9 units is represented by the valence basins ② and ③. The former correspond to the shorter inter-Ge_9 cluster bonds and appear more or less as normal disynaptic valence basins (two-center bonds), while the basins ③ which relate to the longer inter-Ge_9 cluster bonds appear to be between a disynaptic valence basin (two-center bond) and a monosynaptic valence basin (lone pair). Only those germanium atoms that do not take part in inter-Ge_9 cluster contacts have typical monosynaptic valence basins ①.

The ELF has also been helpful for the bond analysis of intermetalloid endohedral clusters. For the rather novel bonding situation for germanium in the pentagonal prismatic cage of $[Co@Ge_{10}]^{3-}$,[250] the ELF (Figure 18d) shows monosynaptic valence basins ① associated with each germanium atom, and disynaptic valence basins occurring between adjacent germanium atoms: both along the edges of the prism base ② and along the prism height ③. The ELF does not show any distinct basins for the bonding between germanium and cobalt. In contrast, a local electron maximum between the central plutonium atom and the lead atoms of the icosahedral cage was found for $[Pu@Pb_{12}]$.[310]

8. From Zintl Ions to Novel Materials: Prospects for Materials Science

Early attempts were made to produce surface-modified solids from K_4Sn_9 solutions by topochemical oxidation,[330] and the synthesis of amorphous metallic spin glasses of the composition M_2SnTe_4 (M = Cr, Mn, Fe, Co) based on the oxidation of the main-group-metal polyanions $[SnTe_4]^{4-}$ by transition-metal cations in solution has been reported.[331]

Recently, the reaction of metal chalcogenides and transition-metal cations was employed to form aerogels using mixed Zintl ions, such as $[ECh_4]^{4-}$, $[E_2Ch_6]^{4-}$,and $[E_4Ch_{10}]^{4-}$ (E = Ge and Sn; Ch = chalcogen atom) as building blocks that are preformed in Zintl phases. Random network aerogels (chalcogels) were obtained by a gradual polymerization of Zintl ions in the presence of Pt^{2+} in solution.[332] The reaction of $[Ge_9]^{4-}$ and $[Sn_9]^{4-}$ clusters with elemental tellurium led to the degradation of the cluster framework and the formation of mixed Ge–Te[333] and Sn–Te polyanions.[334,335]

The bottom-up synthesis of nanostructured semiconductors is a great challenge, and there is a rapidly growing interest in using Zintl anions in these attempted preparations. In particular, dimensionally reduced semiconductor structures are in demand as they can exhibit electronic and optical characteristics similar to those of discrete nanodots. The oxidation of Zintl phases, such as KSi and Mg_2Ge, lead to silicon nanoparticles[336] and mesostructured germanium.[337] Another and possibly more effective way is the application of soluble Zintl ions instead of unsoluble Zintl phases. The principal reaction, which involves the self-oxidation of $[Ge_9]^{4-}$ in ethylenediamine solution and leads to homoatomic dimers, oligomers, and polymers of these units, has been described in Section 3.3. By oxidation with Au^I compounds, a well-defined Ge_{45} cluster could even be obtained.

The process of oxidation of soluble Zintl anions has recently been used to perform cross-linking polymerization reactions of surfactant-templated Ge^{IV} linkers and $[Ge_9]^{4-}$ Zintl anions, thus producing *meso*-structured germanium. Related materials are obtained without additional oxidation agents.[336–339] Oxidation of K_4Ge_9 in ionic liquids produces either clathrate II-type $K_{8.6}Ge_{136}$[340] or even a novel single-crystalline modification of clathrate II-type germanium.[151,341] The reaction of the neat substrate with elemental mercury at 600 °C leads to the ternary phase $K_8Hg_3Ge_{43}$,[342] in contrast to the reaction in solution which affords the polymer $^1_\infty\{[HgGe_9]^{2-}\}$[182] (Figure 12c). In the case of the silicides A_4Si_4 (A = Na, K) oxidation with gaseous HCl leads to clathrate I-type compounds of the composition $A_{8-x}Si_{46}$.[343]

The preservation of the Ge_9 framework during the oxidation process has been anticipated as a matter of principle[8,341] and assumed as an intermediate step during the formation of mesoporous germanium.[337] DFT calculations have shown that polymers that arise from multiple oxidative coupling reactions of $[Ge_9]^{4-}$ have considerable stability. Two-dimensional connection of *nido*-Ge_9 clusters arises in the allotrope $^2_\infty\{[Ge_9]_n\}$ (Figure 19a). Coiling up this sheet results in a $^1_\infty\{[Ge_9]_{24n}\}$ nanotube composed solely of Ge_9 units (Figure 19b) and fullerene-like nanoparticles with the formula $(Ge_9)_{30}$, which are constructed by capping the square faces of a truncated icosidodecahedron with Ge_9 clusters (Figure 19c), are energetically comparable with bulk-like nanostructures of the same size.[344]

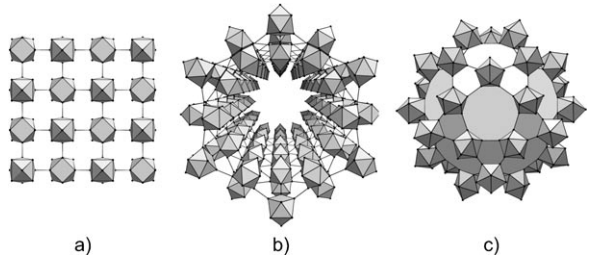

Figure 19. Proposed germanium allotropes based on Ge_9 building units: a) $^2_\infty\{[Ge_9]_n\}$ sheet, b) $^1_\infty\{[Ge_9]_{24n}\}$ nanotube, c) $(Ge_9)_{30}$ cage.[344]

9. Summary and Outlook

The immense progress in the synthesis and isolation of Group 14 and 15 Zintl anions has led to a fast development of their chemistry. A better understanding of the binary Zintl phases makes homoatomic main-group-element clusters and cages available and allows their reactivity to be studied in great detail. Polyhedral clusters and cages serve as ligands in transition-metal complexes and show a large variety of bonding modes reaching from η^1 to η^6 coordination. The addition of organic ligands affords ligand-stabilized main-group-element systems based on small molecules containing Group 14 and 15 elements as starting materials. The functionalized Zintl clusters can serve as building blocks for the directed bottom-up design of semiconducting functional materials in the future. The application of these systems for optoelectronic devices has already been achieved by the oxidation of homoatomic germanium clusters. With the availability of silicon clusters in solution Zintl ion chemistry has reached another milestone, as silicon-based materials will have an even greater impact than germanium-based materials.

The reaction of homoatomic Zintl ions to intermetalloid clusters opens a further direction in this field of chemistry. In analogy to endohedrally filled fullerenes, endohedrally filled Zintl ions can disclose specific properties of the encapsulated metal atom as it has already been demonstrated by the rather sharp signals of the ^{63}Cu NMR of $[Cu@Sn_9]$ and $[Cu@Pb_9]$ owing to the high symmetric coordination environment of the copper atom. In contrast to fullerenes, Zintl ions are available at a larger scale. Applying the oxidation routes that lead in the case of bare germanium clusters to semiconducting materials, the polymerization of intermetalloid clusters might further improve the electrical properties of such materials.

A major step towards the future of a controllable synthesis of main-group cage compounds will be to close the gap between homoatomic Zintl clusters and ligand-stabilized cage molecules experimentally. The formation of bisvinylated clusters $[Ge_9R_2]^{2-}$ from Zintl ions and the tris-silylated clusters $[Ge_9R_3]^{3-}$ using small precursor germanium organyls shows the close relationship, as it does the anion $[(MesCu)_2(Si_4)]^{4-}$, which is an intermediate compound between $[Si_4]^{4-}$ and Si_4R_4 and thus "between Zintl and Wiberg";[35] indeed there is "plenty of room for fantasy".[11]

Appendix: Tables 6 and 7

Table 6: Compounds with Group 14 element polyhedra.

Cluster	Compound	Ref.
$[Si_4]^{4-}$	NaSi	[345]
	KSi	[346, 347]
	RbSi, CsSi	[346]
	$BaSi_2$	[389]
	K_3LiSi_4	[390]
	K_7LiSi_8	[390]
	$Rb_{12}Si_{17}$	[348]
	$A_{12}Si_{17}$ (A = K, Cs)	[34]
$[Si_5]^{2-}$	$[Rb([2.2.2]crypt)]_2Si_5(NH_3)_4$	[60]
$[Si_9]^{2-}$	$[K([2.2.2]crypt)]_2Si_9$	[61]
	$[K([18]crown-6)]_2Si_9(py)$	[61]
$[Si_9]^{3-}$	$[K([2.2.2]crypt)]_3Si_9(NH_3)_8$	[60]
	$[Rb([2.2.2]crypt)]_6Si_9Si_9(NH_3)_{6.3}$	[60]
	$[K([2.2.2]crypt)]_3Si_9(py)_{2.5}$	[60]
$[Si_9]^{4-}$	$Rb_{12}Si_{17}$	[348]
	$A_{12}Si_{17}$ (A = K, Cs)	[34]
	$Rb_4Si_9(NH_3)_{4.75}$	[62]
	$Rb_4Si_9(NH_3)_5$	[391]
	$[Rb([18]crown-6)]Rb_3Si_9(NH_3)_4$	[62]
$[Ge_4]^{4-}$	NaGe	[345]
	KGe, RbGe, CsGe	[346]
	$SrGe_2$, $BaGe_2$	[392]
	$Na_2Cs_2Ge_4$	[393]
	NaK_7Ge_8, $NaPb_7Ge_8$	[394]
	$A_{12}Ge_{17}$ (A = Na, Rb, Cs)	[33, 34]
$[Ge_5]^{2-}$	$[K([2.2.2]crypt)]_2Ge_5(thf)$	[63]
	$[A([2.2.2]\text{-}crypt)]_2Ge_5(NH_3)_4$ (A = K, Rb)	[64]
$[Ge_9]^{2-/4-}$	$[K([2.2.2]crypt)]_6[Ge_9]^{2-}[Ge_9]^{4-}(en)_{2.5}$	[65]
$[Ge_9]^{3-}$	$[K([2.2.2]crypt)]_3Ge_9(PPh_3)$	[66]
	$[K([2.2.2]crypt)]_3Ge_9(en)_{0.5}$	[67]
	$[K([2.2.2]crypt)]_6Ge_9Ge_9(en)_x$ (x = 0.5, 1.5)	[68]
$[Ge_9]^{4-}$	K_4Ge_9	[93]
	Cs_4Ge_9, Rb_4Ge_9	[32]
	$A_{12}Ge_{17}$ (A = Na, Rb, Cs)	[33, 34]
	$Rb_4Ge_9(en)$	[69]
	$Cs_4Ge_9(en)$	[72]
	$K_4Ge_9(NH_3)_9$, $Rb_4Ge_9(NH_3)_5$	[71]
	$[K([2.2]crypt)]K_3Ge_9(en)_2$	[70]
$[Ge_{10}]^{2-}$	$[K([2.2.2]crypt)]_2Ge_{10}$	[73]
$[Sn_4]^{4-}$	NaSn	[349, 350]
	KSn	[349, 351]
	RbSn, CsSn	[351, 352]
	$Na_{12}Sn_{17}$	[34]
	$A_{12}Sn_{17}$ (A = K, Rb, Cs)	[33, 34]
	$A_{52}Sn_{82}$ (A = K, Cs)	[353]
	$Rb_4Sn_4(NH_3)_2$, $Cs_4Sn_4(NH_3)_2$	[31]
	$A_{12}[Sn_4]_2[GeO_4]$ (A = Rb, Cs)	[354]
	$Cs_{20}[Sn_4]_2[SiO_4]_3$	
$[Sn_5]^{2-}$	$[Na([2.2.2]crypt)]_2Sn_5$	[74]
$[Sn_9]^{3-}$	$[K[(2.2.2]crypt)_3Sn_9(en)_{1.5}$	[75]
	$[K([2.2.2]crypt)]_3Sn_9$	[67]
	$[K([2.2.2]crypt)]_3Sn_9(en)_{0.5}$	[77, 78]
	$[K([2.2.2]crypt)]_6Sn_9Sn_9(en)_{1.5}(tol)_{0.5}$	[76]
$[Sn_9]^{4-}$	K_4Sn_9	[92]
	$A_{12}Sn_{17}$ (A = K, Rb, Cs)	[33, 34]
	$Na_4Sn_9(en)_7$	[22]
	$[Li(NH_3)_4]_4Sn_9(NH_3)$	[80]
	$[Na([2.2.2]crypt)]_4Sn_9$	[23]

Table 6: (Continued)

Cluster	Compound	Ref.
	$[K([2.2.2]crypt)]_3KSn_9$	[79]
	$[K([18]crown\text{-}6)]_4Sn_9(en)$	[29]
	$[K([18]crown\text{-}6)]_3KSn_9(en)_{1.5}$	[29]
	$[K([18]crown\text{-}6)]_2K_2Sn_9(en)_{1.5}$	[82]
	$[Rb([18]crown\text{-}6)]_2Rb_2Sn_9(en)_{1.5}$	[81]
	$[K([2.2.2]crypt)]Cs_7Sn_{92}(en)_3$	[84]
	$[K([2.2.2]crypt)]_2Cs_2Sn_9(en)_2$	[83]
$[Pb_4]^{4-}$	NaPb	[30]
	KPb	[351, 355]
	RbPb, CsPb	[351, 356]
	LiK_3Pb_4, $LiRb_3Pb_4$, $LiCs_3Pb_4$, $NaCs_3Pb_4$	[395]
	$Rb_4Pb_4(NH_3)_2$	[31]
	$K_{19}Pb_8O_4(OH)_3$	[355]
$[Pb_5]^{2-}$	$[Na([2.2.2]crypt)]_2Pb_5$	[74, 85]
$[Pb_9]^{3-}$	$[K([2.2.2]crypt)]_3Pb_9$	[86]
	$[K([2.2.2]crypt)]_3Pb_9(en)_{0.5}$	[67]
	$[K([2.2.2]crypt)]_6Pb_9Pb_9(en)_{1.5}(tol)_{0.5}$	[76]
$[Pb_9]^{4-}$	A_4Pb_9 (A = K, Rb)	[34, 94]
	Cs_4Pb_9	[95]
	$K_6Cs_{10}Pb_{36}$	[395]
	$[Li(NH_3)_4]_4[Pb_9](NH_3)$	[80]
	$[K([2.2.2]crypt)]_3KPb_9$	[86]
	$[K([18]crown\text{-}6)]_4Pb_9(en)(tol)$	[87]
	$[K([18]crown\text{-}6)]_2K_2Pb_9(en)_{1.5}$	[88]
$[Pb_{10}]^{2-}$	$[K([2.2.2]crypt)]_2Pb_{10}$	[89]
$[Ge_9\text{–}Ge_9]^{6-}$	$K_4[K([2.2.2]crypt)]_2[Ge_9\text{-}Ge_9](en)_6$	[141]
	$Cs_4[K([2.2.2]crypt)]_2[Ge_9\text{-}Ge_9](en)_6$	[139]
	$[Rb(Benzo[18]crown\text{-}6)]_2Rb_4[Ge_9\text{-}Ge_9](en)_x$ ($x = 4$, 6)	[140]
	$[K([18]crown\text{-}6)]_2K_4[Ge_9\text{-}Ge_9](en)_2$	[140]
	$[K([18]crown\text{-}6)]_3Cs_3[Ge_9\text{-}Ge_9](en)_2$	[140]
	$A_6[Ge_9\text{-}Ge_9](dmf)_{12}$ (A = K, Rb)	[26]
	$K_{2.5}Cs_{3.5}[Ge_9\text{-}Ge_9](dmf)_{12}$	[26]
$[Ge_9{=}Ge_9{=}Ge_9]^{6-}$	$[Rb([2.2.2]crypt)]_6[Ge_9{=}Ge_9{=}Ge_9](en)_3$	[146]
	$[K([18]crown\text{-}6)]_6[Ge_9{=}Ge_9{=}Ge_9](en)_3(tol)$	[147]
$[Ge_9{=}Ge_9{=}Ge_9{=}Ge_9]^{8-}$	$[Rb([18]crown\text{-}6)]_8[Ge_9{=}Ge_9{=}Ge_9{=}Ge_9](en)_x$ ($x = 2$, 6)	[148]
	$[K([18]crown\text{-}6)]_8[Ge_9{=}Ge_9{=}Ge_9{=}Ge_9](en)_8$	[149]
$^1_\infty\{[Ge_9]^{2-}\}$	$[K([18]crown\text{-}6)]_2Ge_9(en)$	[144]
	$[K([2.2]crypt)]KGe_9(en)_3$	[143]
	$[Rb([2.1.1]crypt)]_2Ge_9(en)$	[145]
$[Si_4(SiMe\{CH(SiMe_3)_2\}_2)_3]^-$	$K[Si_4(SiMe\{CH(SiMe_3)_2\}_2)_3]$	[152]
	$[K([18]crown\text{-}6)]\ [Si_4(SiMe\{CH(SiMe_3)_2\}_2)_3](pen)_{0.5}$	[152]
$[Si_4(SiMe\{CH(SiMe_3)_2\}_2)_4]$	$[Si_4(SiMe\{CH(SiMe_3)_2\}_2)_4]\ (C_6H_6)_3$	[152]
$Si_4(tBu_3Si)_4$	$[Si_4(tBu_3Si)_4]_2(tBu_3Si\text{-}SitBu_3)\ (C_6D_6)$	[153]
$Ge_4(SitBu_3)_4$	$[Ge_4(SitBu_3)_4]_2(tBu_3Si\text{-}SitBu_3)$	[154]
$Ge_5\{CH(SiMe_3)_2\}_4$	$Ge_5\{CH(SiMe_3)_2\}_4$	[358]
$Ge_5[2,6\text{-}(2,4,6\text{-}Me_3C_6H_2)_2C_6H_3]_4$	$Ge5\{2,6\text{-}(2,4,6\text{-}Me_3C_6H_2)_2C_6H_3\}_4$	[358]
$Ge_6[2,6\text{-}(2,6\text{-}iPr_2C_6H_3)_2C_6H_3]_2$	$Ge_6\{2,6\text{-}(2,6\text{-}iPr_2C_6H_3)_2\text{-}C_6H_3\}_2$	[176]
$Ge_8[N(SiMe_3)_2]_6$	$Ge_8[N(SiMe_3)_2]_6$	[179]
$Ge_8[(OtBu)_2C_6H_3]_6$	$Ge_8[(OtBu)_2C_6H_3]_6$	[359]
$[Ge_9\text{–}CH_2{=}CH]^{3-}$	$[K([18]crown\text{-}6)]_6K(cp)[Ge_9\text{-}CH{=}CH_2]_2(en)_x$	[170]
$[Ge_9\text{–}SnMe_3]^{3-}$	$[K([2.2.2]crypt)]_3[Ge_9\text{-}SnMe_3]$	[164]
$[Ge_9\text{–}SnPh_3]^{3-}$	$[K([2.2.2]crypt)]_3[Ge_9\text{-}SnPh_3](en)$	[164]
$[Ge_9\text{–}(CH{=}CH_2)_2]^{2-}$	$[K([18]crown\text{-}6)]_2[Ge_9\ (CH{=}CH_2)_2]$	[168]
	$[(CH_3)_4N]_2[Ge_9\text{-}(CH{=}CH_2)_2](en)_{0.5}$	[167]
	$[(CH_3CH_2CH_2)_4N]_2[Ge_9(CH{=}CH_2)_2]$	[167]
	$[K([18]crown\text{-}6)]_2[Ge_9\text{-}CH{=}CH_2)_2](en)$	[167]
$[Ge_9\text{–}(CD{=}CD_2)_2]^{2-}$	$[K([2.2.2]crypt)]_2[Ge_9(CD{=}CD_2)_2]$	[168]
$[Ge_9\text{–}(C(CH_3){=}CH\text{-}CH_{2\_}CH_3))_2]^{2-}$	$[K([2.2.2]crypt)]_2[Ge_9\text{-}(C(CH_3){=}CH\text{-}CH_2CH_3))_2]_{0.5}[Ge_9\text{-}(HC(CH_3CH_2){=}CH\text{-}CH_3)]_{0.5}(bz)$	[168]
$[Ge_9\text{–}(HC(CH_3CH_2){=}CH\text{-}CH_3)]^{2-}$	$[K([2.2.2]crypt)]_2[Ge_9\text{-}(C(CH_3){=}CH\text{-}CH_2CH_3))_2]_{0.5}[Ge_9\text{-}(HC(CH_3CH_2){=}CH\text{-}CH_3)]_{0.5}(bz)$	[168]
$[Ge_9\text{–}(CH_2\text{-}CH(CH_2)_2)_2]^{2-}$	$[K([2.2.2]crypt)]_2[Ge_9(CH_2\text{-}CH(CH_2)_2)_2](en)_3$	[168]
$[Ge_9\text{–}(CH{=}CHFc)_2]^{2-}$	$[K([2.2.2]crypt)]_2[Ge_9(CH{=}CHFc)_2]\ (en)_{0.5}(py)_{1.5}$	[169]

Table 6: (Continued)

Cluster	Compound	Ref.
$[Ph_3Ge{-}Ge_9{-}GePh_3]^{2-}$	$[K([2.2.2]crypt)]_3[Ph_3Ge\text{-}Ge_9\text{-}GePh_3](tol)(en)_{0.5}$	[164]
$[Me_3Sn{-}Ge_9{-}SnMe_3]^{2-}$	$[K([2.2.2]crypt)]_2[Me_3Sn\text{-}Ge_9\text{-}SnMe_3](tol)_{3.5}$	[164]
$[Ph_3Sn{-}Ge_9{-}SnPh_3]^{2-}$	$[K([2.2.2]crypt)]_2[Ph_3Sn\text{-}Ge_9\text{-}SnPh_3]$	[164]
	$[K([18]crown\text{-}6)]_2[Ph_3Sn\text{-}Ge_9\text{-}SnPh_3]([18]crown\text{-}6)_{0.25}(en)_2$	[164]
$[Ph{-}Ge_9{-}SbPh_2]^{2-}$	$[K([2.2.2]crypt)]_2[Ph\text{-}Ge_9\text{-}SbPh_2](tol)$	[163]
$[Ph_2Sb{-}Ge_9{-}SbPh_2]^{2-}$	$[K[2.2.2]crypt)]_2Ge_9(SbPh_2)_2(en)$	[162]
$[Ph_2Bi{-}Ge_9{-}BiPh_2]^{2-}$	$[K[2.2.2]crypt)]_2Ge_9(BiPh_2)_2(en)$	[162]
$[Ge_9\{Si(SiMe_3)_3\}_3]^-$	$[Li(thf)_4][Ge_9\{Si(SiMe_3)_3\}_3](thf)_3$	[171]
$[Ge_9\{Si(SiMe_3)_3\}_3Cr(CO)_5]^-$	$Li(thf)_4[Ge_9\{Si(SiMe_3)_3\}_3Cr(CO)_5]$	[172]
$[Ge_{10}\{Fe(CO)_4\}_8]^{6-}$	$Na_6[Ge_{10}\{Fe(CO)_4\}_8](thf)_{18}$	[173]
$[Ge_{10}(Si\textit{t}Bu_3)_6I]^+$	$[Ge_{10}(Si\textit{t}Bu_3)_6I](B(2,3,5,6\text{-}F_4C_6H)_4)(tol)$	[175]
$[Ge_{10}Si\{Si(SiMe_3)_3\}_4(SiMe_3)_2Me]^-$	$Li(thf)_4[Ge_{10}Si\{Si(SiMe_3)_3\}_4(SiMe_3)_2Me](C_5H_{12})$	[184]
$[Ge_{14}\{Ge(SiMe_3)_3\}_5]^{3-}$	$[Ge(SiMe_3)_4][Li_3(thf)_6][Ge_{14}\{Ge(SiMe_3)_3\}_5]\ (Et_2O)$	[174]
$[\textit{t}BuGe_9{-}Ge_9\textit{t}Bu]^{4-}$	$[K([2.2.2]crypt)]_4[\textit{t}Bu\text{-}Ge_9\text{-}Ge_9\text{-}\textit{t}Bu](en)_7$	[165]
$[Ph_2SbGe_9{-}Ge_9SbPh_2]^{4-}$	$[K([2.2.2]crypt)]_4[Ph_2Sb\text{-}Ge_9\text{-}Ge_9\text{-}SbPh_2](en)_{2.5}$	[163]
$[Ph_3SnGe_9{-}Ge_9SnPh_3]^{4-}$	$[K([2.2.2]crypt)]_4[Ph_3Sn\text{-}Ge_9\text{-}Ge_9SnPh_3](en)_2$	[164]
	$[K([18]crown\text{-}6)]_3[Ge_9\text{-}SnMe_3](thf)(en)_2$	[164]
$Sn_4Ge_2\{2,6\text{-}(2,6\text{-}i\text{Pr}_2\text{-}C_6H_3)_2C_6H_3\}_2$	$Sn_4Ge_2\{2,6\text{-}(2,6\text{-}i\text{Pr}_2\text{-}C_6H_3)_2\text{-}C_6H_3\}_2$	[176]
$[GeSn_8CH{=}CH_2]^{3-}$	$[K([2.2.2]crypt)]_3[GeSn_8\text{-}CH{=}CH_2](en)_3(tol)_3$	[183]
$[GeSn_8(CH{=}CH\textit{c}Pr)]^{3-}$	$[K([2.2.2]crypt)]_3[GeSn_8\text{-}(CH{=}CH\textit{c}Pr)](en)_3$	[183]
$[Ge_2Sn_7(CH{=}CH_2)_2]^{2-}$	$[K([2.2.2]crypt)]_4[Ge_2Sn_7\text{-}(CH{=}CH_2)_2]_2(en)_3$	[183]
	$[Pr_4N]_4[Ge_2Sn_7\text{-}(CH{=}CH_2)_2]_2$	[183]
$[Ge_2Sn_7(CH{=}CHPh)]^{3-}$	$[K([2.2.2]crypt)]_3[Ge_2Sn_7\text{-}(CH{=}CHPh)](en)_2$	[183]
$Sn_7\{2,6\text{-}(2,6\text{-}i\text{Pr}_2C_6H_3)_2C_6H_3\}_2$	$Sn_7\{2,6\text{-}(2,6\text{-}i\text{Pr}_2C_6H_3)_2C_6H_3\}_2(hex)$	[177]
$Sn_7\{GaCl(ddp)\}$	$Sn_7\{GaCl(ddp)\}_2$	[160]
$Sn_8(C_6H_3\text{-}2,6\text{-}(2,4,6\text{-}Me_3C_6H_2)_2)_4$	$Sn_8(C_6H_3\text{-}2,6\text{-}(2,4,6\text{-}Me_3C_6H_2)_2)_4(C_6H_6)_{1.5}$	[178]
$[Sn_8(Si\textit{t}Bu_3)_6]^{2-}$	$[Na(thf)_2]_2[Sn_8(Si\textit{t}Bu_3)_6]$	[159]
$Sn_8(Si\textit{t}Bu_3)_6$	$Sn_8(Si\textit{t}Bu_3)_6$	[159]
$[Sn_9\textit{t}Bu]^{2-}$	$[K([2.2.2]crypt)]_3[Sn_9\text{-}\textit{t}Bu](py)_2$	[181]
$[Sn_9i\text{Pr}]^{3-}$	$[K([2.2.2]crypt)]_3[Sn_9\text{-}i\text{Pr}](py)_2$	[182]
$[Sn_9(CH{=}CH_2)]^{3-}$	$[K([2.2.2]crypt)]_3[Sn_9\text{-}CH\text{-}CH_2](py)_2$	[181]
$[Sn_9(CH{=}CHPh)]^{3-}$	$[K([2.2.2]crypt)]_3[Sn_9\text{-}CH\text{-}CHPh](tol)(py)_{0.75}$	[181]
$[Sn_9SnCy_3]^{3-}$	$[K([2.2.2]crypt)]_3[Sn_9\text{-}SnCy_3](py)_2$	[182]
$Sn_9\{2,6\text{-}(2,4,6\text{-}i\text{Pr}_3C_6H_2)_2C_6H_3\}_3$	$Sn_9\{2,6\text{-}(2,4,6\text{-}i\text{Pr}_3C_6H_2)_2C_6H_3\}_3(thf)_4$	[158]
$[Sn_{10}(2,6\text{-}(2,4,6\text{-}Me_3C_6H_2)_2C_6H_3)_3]^+$	$[Sn_{10}\{2,6\text{-}(2,4,6\text{-}Me_3C_6H_2)_2C_6H_3\}_3][AlCl_4](tol)$	[158]
	$[Sn_{10}\{2,6\text{-}(2,4,6\text{-}Me_3C_6H_2)_2C_6H_3\}_3][GaCl_4](tol)$	[158]
$Sn_{10}\{Si(SiMe_3)_3\}_6$	$Sn_{10}\{Si(SiMe_3)_3\}_6$	[185]
$Sn_{15}(N(2,6\text{-}i\text{Pr}_2C_6H_3)(SiMe_3))_6$	$Sn_{15}\{N(2,6\text{-}i\text{Pr}_2C_6H_3)(SiMe_3)\}_6$	[260]
$Sn_{15}(N(2,6\text{-}i\text{Pr}_2C_6H_3)(SiMe_2Ph))_6$	$Sn_{15}\{N(2,6\text{-}i\text{Pr}_2C_6H_3)(SiMe_2Ph)\}_6$	[260]
$Sn_{17}(GaCl(ddp))_4$	$Sn_{17}\{GaCl(ddp)\}_4$	[160]
$Pb_{10}\{Si(SiMe_3)_3\}_6$	$[Pb_{10}(Si(SiMe_3)_3)_6](C_5H_{12})$	[180]
$Pb_{12}(Si(SiMe_3)_3)_6$	$[Pb_{12}(Si(SiMe_3)_3)_6](C_6H_6)_3$	[180]
$[Si_4(CuMes)_2]^{4-}$	$Rb_{1.54}K_{0.46}[K([18]crown\text{-}6)]_2[Si_4(CuMes)_2](NH_3)_{12}$	[35]
$[Si_9\text{-}Zn(C_6H_5)]^{3-}$	$[K([2.2.2]crypt)]_3[Si_9\text{-}Zn(C_6H_5)](py)_2$	[222]
$[Si_9{-}\{Ni(CO)_2\}_2{-}Si_9]^{8-}$	$Rb_4[K([18]crown\text{-}6)]_2[Rb([18]crown\text{-}6)]_2[Si_9\text{-}\{Ni(CO)_2\}_2\text{-}Si_9](NH_3)_{22}$	[226]
$[Ge_6\{Cr(CO)_5\}_6]^{2-}$	$[PPh_4]_2[Ge_6\{Cr(CO)_5\}_6]$	[209]
$[Ge_6\{Mo(CO)_5\}_6]^{2-}$	$[PPh_4]_2[GE_6\{Mo(CO)_5\}_6]$	[211]
$[Ge_6\{W(CO)_5\}_6]^{2-}$	$[PPh_4]_2[Ge_6\{W(CO)_5\}_6]$	[211]
$[Ge_9\{Si(SiMe_3)_3\}_3Cr(CO)_3]^-$	$Li(THF)_4[Ge_9\{Si(SiMe_3)_3\}_3Cr(CO)_3]^{[a]}$	[172]
$[Ge_9{-}Ni(CO)]^{3-}$	$[K([2.2.2]crypt)]_3[Ge_9\text{-}Ni(CO)]$	[220]
$[Ge_9{-}Pd(PPh_3)]^{3-}$	$[K([2.2.2]crypt)]_3[Ge_9\text{-}Pd(PPh_3)](en)$	[224]
$[Ge_9{-}Cu(PCy_3)]^{3-}$	$[K([2.2]crypt)]_3[Ge_9\text{-}Cu(PCy_3)](dmf)_3$	[221]
$[Ge_9{-}Cu(Pi\text{Pr}_3)]^{3-}$	$[K([2.2.2]crypt)]_3[Ge_9\text{-}Cu(Pi\text{Pr}_3)](NH_3)_{13}$	[221]
$[Ge_9{-}Cu(Ge_9)]^{7-}$	$K_4[K([2.2]crypt)]_3[Ge_9\text{-}Cu(Ge_9)](NH_3)_{21}$	[221]
	$K_5[K([2.2.2]crypt)]_2[Ge_9\text{-}Cu(Ge_9)](NH_3)_{14+x}$	[221]
$[Cu\{Ge_9[Si(SiMe_3)_3]_3\}_2]^-$	$[Li(thf)_6][Cu\{Ge_9[Si(SiMe_3)_3]_3\}_2]$	[231]
$[Ag\{Ge_9[Si(SiMe_3)_3]_3\}_2]^-$	$[Li(thf)_6][Ag\{Ge_9[Si(SiMe_3)_3]_3\}_2]$	[231]
$[Au\{Ge_9[Si(SiMe_3)_3]_3\}_2]^-$	$[Li(thf)_6][Au\{Ge_9[Si(SiMe_3)_3]_3\}_2]$	[230]
$[Ge_9Au_3Ge_9]^{5-}$	$[K([2.2.2]crypt)]_5[Ge_9Au_3Ge_9](sol)$	[229]
$[Au_3Ge_{45}]^{9-}$	$[K([2.2.2]crypt)]_9[Au_3Ge_{45}](sol)_n$	[150]

Table 6: (Continued)

Cluster	Compound	Ref.
$[Ge_9{-}Zn(C_6H_5)]^{3-}$	$[K([2.2.2]crypt)]_3[Ge_9\text{-}Zn(C_6H_5)](en)_2(tol)$	[222]
$[Ge_9{-}Zn(C_3H_7)]^{3-}$	$[K([2.2.2]crypt)]_3[Ge_9\text{-}Zn(C_3H_7)](en)(tol)_2$	[223]
$[Ge_9{-}Zn(C_9H_{11})]^{3-}$	$[K([2.2.2]crypt)]_3[Ge_9\text{-}Zn(C_9H_{11})]$	[223]
$Zn\{Ge_9[Si(SiMe_3)_3]_3\}_2$	$Zn\{Ge_9[Si(SiMe_3)_3]_3\}_2$	[232]
$Cd\{Ge_9[Si(SiMe_3)_3]_3\}_2$	$Cd\{Ge_9[Si(SiMe_3)_3]_3\}_2$	[232]
$Hg\{Ge_9[Si(SiMe_3)_3]_3\}_2$	$Hg\{Ge_9[Si(SiMe_3)_3]_3\}_2$	[232]
$[Hg_3(Ge_9)_4]^{10-}$	$[K([2.2.2]crypt)]_{10}[Hg_3(Ge_9)_4](en)_2(tol)_2$	[228]
$^1_\infty\{[HgGe_9]^{2-}\}$	$[K([2.2.2]crypt)]_2[HgGe_9](en)_2$	[51]
	$[K([2.2]crypt)]_2[HgGe_9](dmf)$	[227]
$[Sn_6Nb(\eta^6\text{-tol})_2]^{2-}$	$[K([2.2.2]crypt)]_2[Sn_6Nb(\eta^6\text{-tol})_2](en)$	[213]
$[Sn_6\{Cr(CO)_5\}_6]^{2-}$	$[K([2.2.2]crypt)]_2[Sn_6\{Cr(CO)_5\}_6]$	[210]
	$[PPh_4]_2[Sn_6\{Cr(CO)_5\}_6]$	[211]
$[Sn_6\{Mo(CO)_5\}_6]^{2-}$	$[PPh_4]_2[Sn_6\{Mo(CO)_5\}_6]$	[211]
$[Sn_6\{W(CO)_5\}_6]^{2-}$	$[PPh_4]_2[Sn_6\{W(CO)_5\}_6]$	[211]
$[Sn_9{-}Cr(CO)_3]^{4-}$	$[K([2.2.2]crypt)]_4[Sn_9\text{-}Cr(CO)_3](en)_n$	[49]
	$[K([2.2.2]crypt)]_4[Sn_9\text{-}Cr(CO)_3](en)_x$ ($x=0$, 1.5)	[216]
$[Sn_9{-}Mo(CO)_3]^{4-}$	$[K([2.2.2]crypt)]_4[Sn_9\text{-}Mo(CO)_3](en)$	[214]
	$[K([2.2.2]crypt)]_4[Sn_9\text{-}Mo(CO)_3](en)_{1.5}$	[216]
	$[K([2.2.2]crypt)]_4[Sn_9\text{-}Mo(CO)_3](en)_2$	[360]
$[Sn_9{-}W(CO)_3]^{4-}$	$[K([2.2.2]crypt)]_4[Sn_9\text{-}W(CO)_3](en)$	[214]
	$[K([2.2.2]crypt)]_4[Sn_9\text{-}W(CO)_3](en)_{1.5}$[a]	[216]
$[Sn_9{-}Ir(cod)]^{3-}$	$[K([2.2.2]crypt)]_3[Sn_9\text{-}Ir(cod)]$	[219]
	$[K([2.2.2]crypt)]_3[Sn_9\text{-}Ir(cod)](en)(tol)$	[219]
	$[K([2.2.2]crypt)]_3[Sn_9\text{-}Ir(cod)](en)_2$	[218]
$[Ag(Sn_9)_2]^{5-}$	$[K([2.2.2]crypt)]_5[Ag(Sn_9)_2](en)(tol)$	[142]
$[Sn_9{-}Zn(C_6H_5)]^{3-}$	$[K([2.2.2]crypt)]_3[Sn_9\text{-}Zn(C_6H_5)](tol)$	[222]
$[Sn_9{-}Zn(C_3H_7)]^{3-}$	$[K([2.2.2]crypt)]_3[Sn_9\text{-}Zn(C_3H_7)](en)_{0.5}$	[223]
$[Sn_9{-}Zn(C_9H_{11})]^{3-}$	$[K([2.2.2]crypt)]_3[Sn_9\text{-}Zn(C_9H_{11})](tol)$	[223]
$[Sn_9{-}Cd(C_6H_5)]^{3-}$	$[K([2.2.2]crypt)]_3[Sn_9\text{-}Cd(C_6H_5)](en)$	[225]
$[Sn_9{-}Cd\{Sn(n\text{Bu})_3\}]^{3-}$	$[K([2.2.2]crypt)]_6[Sn_9\text{-}Cd\{Sn(n\text{Bu})_3\}]_2(tol)_6(py)$	[225]
$[Pb_5\{Mo(CO)_3\}_2]^{4-}$	$K_2[K([2.2]crypt)]_2[Pb_5\{Mo(CO)_3\}_2](en)_3$	[212]
$[Pb_9{-}Cr(CO)_3]^{4-}$	$[K([2.2.2]crypt)]_4[Pb_9\text{-}Cr(CO)_3]$	[215]
$[Pb_9{-}Mo(CO)_3]^{4-}$	$[Mo(CO)_3(en)_2][K([2.2.2]crypt)]_4[Pb_9\text{-}Mo(CO)_3](en)_{2.5}$	[214]
	$[K([2.2.2]crypt)]_4[Pb_9\text{-}Mo(CO)_3]$	[217]
	$[K([2.2.2]crypt)]_4(Pb_9\text{-}Mo(CO)_3]^1$	[217]
$[Pb_9{-}W(CO)_3]^{4-}$	$[W(CO)_3(en)_2][K([2.2.2]crypt)]_4[Pb_9\text{-}W(CO)_3](en)_{2.5}$	[214]
$[Pb_9{-}Ir(cod)]^{3-}$	$[K([2.2.2]crypt)]_3[Pb_9\text{-}Ir(cod)](en)_2$	[218]
$[Pb_9{-}Zn(C_6H_5)]^{3-}$	$[K([2.2.2]crypt)]_6[Pb_9\text{-}Zn(C_6H_5)]_2(en)_2(tol)$	[222]
$[Pb_9{-}Zn(C_7H_3)]^{3-}$	$[K([2.2.2]crypt)]_3[Pb_9\text{-}Zn(C_3H_7)](en)$	[223]
$[Pb_9{-}Zn(C_9H_{11})]^{3-}$	$[K([2.2.2]crypt)]_3[Pb_9\text{-}Zn(C_9H_{11})]$	[223]
$[Pb_9{-}Cd(C_6H_5)]^{3-}$	$[K([2.2.2]crypt)]_6[Pb_9\text{-}Cd(C_6H_5)]_2(en)_2(tol)$	[225]
$[Pb_9{-}Cd{-}Cd{-}Pb_9]^{6-}$	$[K([2.2.2]crypt)]_6[Pb_9\text{-}Cd\text{-}Cd\text{-}Pb_9](en)_2$	[233]
$[Ni@Ge_9]^{3-}$	$[K([2.2.2]crypt)]_6[Ni@Ge_9]_2(en)_3$	[247]
	$[K([2.2.2]crypt)]_3\{[Ni@Ge_9\text{-}Ni(en)]_{0.735}([Ni@Ge_9]en)_{0.265}\}(en)$	[220]
$[Co@Ge_{10}]^{3-}$	$[K([2.2.2]crypt)]_4[Co@Ge_{10}][Co(C_8H_{12})_2](tol)$	[250]
$[Fe@Ge_{10}]^{3-}$	$[K([2.2.2]crypt)]_3[Fe@Ge_{10}](en)_2$	[249]
$[Ni_3@Ge_{18}]^{4-}$	$[K([2.2.2]crypt)]_4[Ni_3@Ge_{18}](tol)_2$	[247]
$[Pd_2@Ge_{18}]^{4-}$	$[K([2.2.2]crypt)]_4[Pd_2@Ge_{18}](tol)_2$	[254]
$[Ni_6Ge_{13}(CO)_5]^{4-}$	$[K([2.2.2]crypt)]_4[Ni_6Ge_{13}(CO)_5]$	[262]
$[Cu@Sn_9]^{3-}$	$[K([2.2.2]crypt)]_3[Cu@Sn_9](dmf)_2$	[248]
$[Ir@Sn_{12}]^{3-}$	$[K([2.2.2]crypt)]_3[Ir@Sn_{12}](en)(tol)_2$	[219]
$[Ni_2Sn_{17}]^{4-}$	$[K([2.2.2]crypt)]_4[Ni_2Sn_{17}](en)$	[253]
$[Pd_2@Sn_{18}]^{4-}$	$[K([2.2.2]crypt)]_4[Pd_2@Sn_{18}](en)_3$	[255, 256]
$[Pt_2@Sn_{17}]^{4-}$	$[K([2.2.2]crypt)]_4[Pt_2@Sn_{17}](en)_3$	[257]
$[Cu@Pb_9]^{3-}$	$[K([2.2.2]crypt)]_3[Cu@Pb_9](dmf)_2$	[248]
$[Ni@Pb_{10}]^{2-}$	$[K([2.2.2]crypt)]_2[Ni@Pb_{10}]$	[251]
$[Ni@Pb_{12}]^{2-}$	$[K([2.2.2]crypt)]_2[Ni@Pb_{12}](en)$	[252]
$[Pd@Pb_{12}]^{2-}$	$[K([2.2.2]crypt)]_2[Pd@Pb_{12}](tol)$	[252]
$[Pt@Pb_{12}]^{2-}$	$[K([2.2.2]crypt)]_2[Pt@Pb_{12}]$	[53]
$[Ni@Ge_9{-}Ni(CO)]^{2-}$	$[K([2.2.2]crypt)]_3[Ni@Ge_9\text{-}Ni(CO)](tol)$	[220]

Table 6: (Continued)

Cluster	Compound	Ref.
$[Ni@Ge_9{-}Ni(PPh_3)]^{2-}$	$[K([2.2.2]crypt)]_2[Ni@Ge_9\text{-}Ni(PPh_3)](en)$	[262]
$[Ni@Ge_9{-}Ni(en)]^{3-}$	$[K([2.2.2]crypt)]_3\{[Ni@Ge_9\text{-}Ni(en)]_{0.735}([Ni@Ge_9]en)_{0.265}\}(en)$	[220]
$[Ni@Ge_9{-}Ni(CCPh)]^{3-}$	$[K([2.2.2]crypt)]_3[Ni@Ge_9\text{-}Ni(CCPh)](en)$	[220]
$[Ni@Ge_9{-}Pd(PPh_3)]^{2-}$	$[K([2.2.2]crypt)]_2[Ni@Ge_9\text{-}Pd(PPh_3)](en)$	[224]
$[Ni@Sn_9{-}Ni(CO)]^{3-}$	$[K([2.2.2]crypt)]_3[Ni@Sn_9\text{-}Ni(CO)](en)(PPh_3)_{0.5}$	[263]
$[Pt@Sn_9{-}Pt(PPh_3)]^{2-}$	$[K([2.2.2]crypt)]_2[Pt@Sn_9\text{-}Pt(PPh_3)](en)$	[263]
	$[K([2.2.2]crypt)]_2[Pt@Sn_9\text{-}Pt(PPh_3)](tol)$	[263]

[a] E_9 coordinated in a η^5 fashion.

Table 7: Compounds with Group 15 element polyhedra.

Cluster	Compound	Ref.
$[P_4]^{2-}$	$Cs_2P_4(NH_3)_2$	[48]
	$[K([18]crown\text{-}6)]_2P_4(NH_3)_2$	[106]
$[P_7]^{3-}$	Li_3P_7	[361]
	Na_3P_7	[10]
	K_3P_7	[10]
	Rb_3P_7	[10]
	Cs_3P_7	[363]
	Sr_3P_{14}	[364]
	Ba_3P_{14}	[364]
	$Rb_3P_7(NH_3)_7$	[42]
	$Cs_3P_7(NH_3)_3$	[115]
	$Ba_3P_{14}(NH_3)_{18}$	[116]
	$[Li(tmeda)]_3P_7$	[357]
	$[K([18]crown\text{-}6)]_3K_3[P_7]_2(NH_3)_{10}$	[42]
	$[Rb([18]crown\text{-}6)]_3[P_7](NH_3)_6$	[42]
	$[NMe_4]_2RbP_7(NH_3)$	[113]
	$[NMe_3Et]Cs_2P_7(NH_3)_2$	[114]
	$[NMeEt_3]Cs_2P_7(NH_3)$	[112]
	$[NEt_4]Cs_2P_7(NH_3)_4$	[112]
$[P_{11}]^{3-}$	Na_3P_{11}	[10]
	K_3P_{11}	[10]
	Rb_3P_{11}	[10]
	Cs_3P_{11}	[10]
	$Cs_3P_{11}(NH_3)_3$	[121]
	$BaCsP_{11}(NH_3)_{11}$	[120]
	$[Li(NH_3)_4]_3P_{11}(NH_3)_5$	[119]
	$[NMeEt_3]CsP_{11}(NH_3)_5$	[118]
	$[NEt_4]Cs_2P_{11}$	[113]
	$[NMe_3Et]_3P_{11}$	[118]
	$[K([18]crown\text{-}6)]_3P_{11}(en)_2$	[396]
$[P_{14}]^{4-}$	$[Li(NH_3)_4]_4P_{14}(NH_3)$	[122]
	$Na_4P_{14}(dme)_{7.5}$	[123]
	$Na_4P_{14}(en)_6$	[123]
$[P_{21}]^{3-}$	$[Li([12]crown\text{-}4)]_3P_{21}(thf)_2$	[124]
$[P_{22}]^{4-}$	$[NEtMe_3]_4P_{22}(NH_3)_2$	[125]
$[P_{26}]^{4-}$	$Li_4P_{26}(thf)_{16}$	[126]
$[As_4]^{2-}$	$[Li(NH_3)_4]_2As_4$	[365]
	$[Na(NH_3)_5]_2As_4(NH_3)_3$	[365]
	$[(K[18]crown\text{-}6)]_2As_4$	[106]
	$[Cs_{0.35}Rb_{0.65}([2.2.2]crypt)]_2As_4(NH_3)_2$	[365]
$[As_6]^{4-}$	$[Rb([18]crown\text{-}6)]_2Rb_2As_6(NH_3)_6$	[41]
$[As_7]^{3-}$	Li_3As_7	[366]
	Na_3As_7	[367]
	K_3As_7	[368]
	Rb_3As_7	[368, 369]
	Cs_3As_7	[368, 370]
	Ba_3As_{14}	[371]
	$[Li(NH_3)_4]_3As_7(NH_3)$	[129]
	$[Li(dme)]_3As_7(Et_2O)$	[132]
	$[Li(tmeda)]_3As_7(Et_2O)$	[131]

Table 7: (Continued)

Cluster	Compound	Ref.
	$[Li(tmeda)]_3As_7(tol)_{1.5}$	[399]
	$[K([2.2.2]Krypt)]_{1.5}K_{1.5}As_7$	[400]
	$[Rb([18]crown\text{-}6)]_3As_7(NH_3)_8$	[129]
	$[NMe_4]_2RbAs_7(NH_3)$	[130]
	$Cs_3As_7(NH_3)$	[397]
	$Cs_3As_7(NH_3)_6$	[129]
	$[PPh_4]_2CsAs_7(NH_3)_5$	[129]
$[As_{11}]^{3-}$	Li_3As_{11}	[372]
	Na_3As_{11}	[372]
	K_3As_{11}	
	Rb_3As_{11}	[373]
	Cs_3As_{11}	[373]
	$[K([2.2.2]crypt)]_3As_{11}$	[133]
	$[Cs([18]crown\text{-}6)]_2CsAs_{11}(NH_3)_8$	[134]
$[As_{14}]^{4-}$	$[Rb([18]crown\text{-}6)]_4As_{14}(NH_3)_6$	[122]
$[As_{22}]^{4-}$	$[K([2.2.2]crypt)]_4As_{22}(dmf)_4$	[135]
	$[Rb([2.2.2]crypt)]_4As_{22}(dmf)$	[135]
$[Sb_4]^{2-}$	$[K([2.2.2]crypt)]_2Sb_4(en)_2$	[107]
$[Sb_5]^{5-}$	$[Li(NH_3)_4]_3[Li_2(NH_3)_2Sb_5](NH_3)_2$	[110]
$[Sb_7]^{3-}$	Cs_3Sb_7	[374]
	$Li_3Sb_7(HNMe_2)_6$	[401]
	$Li_3Sb_7(tmeda)_3(tol)$	[401]
	$Na_3Sb_7(en)_3$	[402]
	$Na_3Sb_7(tmeda)_3(thf)_3$	[399]
	$Na_3Sb_7(pmdeta)_3(tol)$	[403]
	$[Na([2.2.2]crypt)]_3Sb_7$	[398]
	$[K([2.2.2]crypt)]_3Sb_7$	[107]
$[Sb_8]^{8-}$	$K_{17}(Sb_8)_2(NH_2)(NH_3)_{17.5}$	[136]
$[Sb_{11}]^{3-}$	$[Na([2.2.2]crypt)]_3Sb_{11}$	[137]
	$[K([18]crown\text{-}6)(NH_3)_2]Sb_{11}(NH_3)_{5.5}$	[134]
$[Bi_4]^{2-}$	$[K([2.2.2]crypt)]_2Bi_4$	[108]
	$[Rb([2.2.2]crypt)]_2Bi_4$	[109]
AsP_3	AsP_3	[208]
$[In_4Bi_5]^{3-}$	$[Na([2.2.2]crypt)]_3In_4Bi_5$	[205]
	$[K([2.2.2]crypt)]_6[In_4Bi_5]_2(en)_{1.5}(tol)_{0.5}$	[205]
$[InBi_3]^{2-}$	$[K([2.2.2]crypt)]_2[InBi_3](en)$	[205]
	$[Rb([2.2.2]crypt)]_2[InBi_3](en)$	[205]
$[GaBi_3]^{2-}$	$[K([2.2.2]crypt)]_2[GaBi_3](en)$	[205]
$[Sn_2Bi_2]^{2-}$	$[K([2.2.2]crypt)]_2[Sn_2Bi_2](en)$	[375]
$[P_3H_2]^{3-}$	$K_3(P_3H_2)(NH_3)_{2.3}$	[202]
	$Rb_3(P_3H_2)(NH_3)$	[202]
$[P_3H_3]^{2-}$	$[Na(NH_3)_5][Na(NH_3)_3(P_3H_3)]$	[201]
	$[Rb([18]crown\text{-}6)]_2[P_3H_3](NH_3)_{7.5}$	[202]
	$[Cs([18]crown\text{-}6)]_2[P_3H_3](NH_3)_7$	[202]
$[\{(CO)_5W\}_2P_3(Nb\{N[Np]Ar\}_3)]^{-[a]}$	$[Na([12]crown\text{-}4)_2][(\{CO\}_5W)P_3(Nb\{N[Np]Ar\}_3)]$	[240]
	$[Na(Et_2O)][\{(CO)_5W\}_2P_3(Nb\{N[Np]Ar\}_3)](C_6H_6)$	[240]
$(P_3)Mo(N[i\text{Pr}]Ar)_3$	$(P_3)Mo(N[i\text{Pr}]Ar)_3$	[240]
$(\{CO\}_5W)P_3(M\{N[i\text{Pr}]Ar\}_3)$ (M = Mo, W)	$(\{CO\}_5W)P_3(M\{N[i\text{Pr}]Ar\}_3)$ (M = Mo, W)	[240]
$(\{CO\}_5W)(Ph_3SnP_3)(Nb\{N[Np]Ar\}_3)$[a]	$(CO)_5W(Ph_3SnP_3)$ $(Nb\{N[Np]Ar\}_3)(\{Me_3Si\}_2O)$	[240]
Mes*NP(W(CO)$_5$)P$_3$(Nb{N[Np]Ar}$_3$)[a]	Mes*NP(W(CO)$_5$)P$_3$(Nb{N[Np]Ar}$_3$)(Et$_2$O)$_{0.75}$	[240]
{(CO)$_5$W}$_2$AdC(O)P$_3$(Nb{N[Np]Ar}$_3$)[a,b]	{(CO)$_5$W}$_2$AdC(O)P$_3$(Nb{N[Np]Ar}$_3$)(C$_5$H$_{10}$)$_{0.5}$	[240]
$P_4(SiR_2)$	$P_4(SiR_2)$	[187]
$P_4(SiR_2)_2$	$P_4(SiR_2)_2$	[187]
$Cp^*Nb(CO)_2P_4$	$Cp^*Nb(CO)_2P_4$	[241]
$Tl_2[P_4(ArDipp_2)_2]$	$Tl_2[P_4(ArDipp_2)_2]$	[189]
$(CO)_4W[P_4](W(CO)_5)_4$	$(CO)_4W[P_4](W(CO)_5)_4$	[241, 242]
$P_2(CoCp'^*)_2P_4(CoCp^*)$	$P_2(CoCp^*)_2P_4(CoCp^*)$	[199]
$[P_5Ph_2]^+$	$[P_5Ph_2][GaCl_4]$	[188]
$[(\eta^5\text{-}P_5)\{Fe(\eta^5\text{-}C_5Me)\}]$	$[(\eta^5\text{-}P_5)\{Fe(\eta^5\text{-}C_5Me)\}]$	[387]
$[P_3Fe(Cp^*Fe)_3P_6]$	$[P_3Fe(Cp^*Fe)_3P_6](thf)$	[199]
$[(Cp^*Fe)_3P_6]^+$	$[(Cp^*Fe)_3P_6][FeCl_3(thf)]$	[199]
$(Cp'Nb)P_6(NbCp')$	$(Cp'Nb)P_6(NbCp')$	[241]

Table 7: (Continued)

Cluster	Compound	Ref.
$(Cp^*Mo)P_6(MoCp^*)$	$(Cp^*Mo)P_6(MoCp^*)$	[246]
$[P_7Cr(CO)_3]^{3-}$	$[K([2.2.2]crypt)]_3[P_7Cr(CO)_3](en)$	[376]
$[P_7Mo(CO)_3]^{3-}$	$[K([2.2.2]crypt)]_3[P_7Mo(CO)_3](en)$	[376]
$[P_7W(CO)_3]^{3-}$	$[K([2.2.2]crypt)]_3[P_7W(CO)_3](en)$	[376]
$[P_7\{FeCp(CO)_2\}_3]$	$[P_7\{FeCp(CO)_2\}_3](thf)$	[199]
$[P_7Ni(CO)]^{3-}$	$[K([2.2.2]crypt)][(PnBu_4]_2[P_7Ni(CO)]$	[196]
$[P_7InPh_2]^{2-}$	$[K([2.2.2]crypt)]_2[P_7InPh_2]$	[268]
$[HP_7]^{2-}$	$[K([2.2.2]crypt)]_3K(HP_7)_2(en)$	[195]
	$[K([18]crown\text{-}6)]_2(HP_7)$	[195]
	$[K(db\text{-}[18]crown\text{-}6)]_2(HP_7)(tol)$	[195]
	$[PPh_4]_2(HP_7)(NH_3)_3$	[194]
P_7Me_3	P_7Me_3	[191]
$P_7(MMe_3)_3$ (M = Si, Ge, Sn, Pb)	$P_7(MMe_3)_3$ (M = Si, Ge, Sn, Pb)	[191]
$[HP_7Mo(CO)_4]^{2-}$	$[K([2.2.2]crypt)]_2[HP_7Mo(CO)_4](en)$	[377]
$[HP_7W(CO)_4]^{2-}$	$[K([2.2.2]crypt)]_2[HP_7W(CO)_4](en)$	[377]
$[P_7PtH(PPh_3)]^{2-}$	$[K([2.2.2]crypt)]_2[P_7PtH(PPh_3)]$	[196]
$[P_7PH_2]^{2-}$	$[Nb](OC[^2Ad]Mes)_3(P_7PH_2)](C_6H_6)_{0.17}$	[198]
$[P_7H_2]^-$	$[PPh_4](P_7H_2)$	[192]
$[P_7(PhCH)_2]^-$	$[PPh_4][P_7(PhCH)_2]$	[193]
$[P_7Ph_6]^+$	$[P_7Ph_6][Ga_2Cl_7]$	[188]
$[Cp'_4Fe_4(CO)_6P_8]$	$[Cp'_4Fe_4(CO)_6P_8]$	[378]
$[Cp'_4Fe_6(CO)_{13}P_8]$	$[Cp'_4Fe_6(CO)_{13}P_8]$	[378]
$[(Cp^*Ir\{CO\})_2(Cr\{CO\}_5)_3P_8]$	$[(Cp^*Ir\{CO\})_2(Cr\{CO\}_5)_3P_8]$	[379]
$[(SmCp^*_2)_4P_8]$	$[(SmCp^*_2)_4P_8]$	[237]
$[(P_8)(CotBu_3Cp)_3]$	$[(P_8)(CotBu_3Cp)_3]$	[388]
$[HP_{11}]^{2-}$	$[K([2.2.2]crypt)]_2(HP_{11})$	[380]
	$[Sr(NH_3)_8](HP_{11})(NH_3)$	[381]
	$[NBzMe_3]_2(HP_{11})$	[118]
	$[PBzPh_3]_2(HP_{11})$	[118]
$[\{Ni(PBu_3)_2\}_4P_{14}]$	$[\{Ni(PBu_3)_2\}_4P_{14}]$	[199]
$As_3(Co\{CO\}_3)$	$As_3(Co\{CO\}_3)$	[238]
$(CpMo)As_5(MoCp)$	$(CpMo)As_5(MoCp)$	[244]
$[As_7Cr(CO)_3]^{3-}$	$[Rb([2.2.2]crypt)]_3[As_7Cr(CO)_3](tol)_{0.5}$	[50,376]
$[As_7Mo(CO)_3]^{3-}$	$[K([2.2.2]crypt)]_3[As_7Mo(CO)_3]$	[376]
$[As_7W(CO)_3]^{3-}$	$[K([2.2.2]crypt)]_3[As_7W(CO)_3](en)$	[376]
$[As_7PtH(PPh_3)]^{2-}$	$[K([2.2.2]crypt)]_2[As_7PtH\ (PPh_3)]$	[197]
$[R_2As_7]^-$	$[K([2.2.2]crypt)][(PhCH)_2As_7]$	[193]
$Sb_3(MoCp\{CO\}_2)$	$Sb_3(MoCp\{CO\}_2)$	[382]
$Sb_3(MoCp^*\{CO\}_2)$	$Sb_3(MoCp^*\{CO\}_2)$	[382]
$[Sb_3Ni_4(CO)_6]^{3-}$	$[K([2.2.2]crypt)]_4[Bi_3Ni_4(CO)_6](en)(tol)$	[272]
$(Cp'Mo)Sb_5(MoCp')$	$(Cp'Mo)Sb_5(MoCp')$	[245]
$[Sb_7Cr(CO)_3]^{3-}$	$[K([2.2.2]crypt)]_3[Sb_7Cr(CO)_3]$	[376]
$[Sb_7Mo(CO)_3]^{3-}$	$[Na([2.2.2]crypt)]_3[Sb_7Mo(CO)_3]$	[383]
$[Sb_7W(CO)_3]^{3-}$	$[K([2.2.2]crypt)]_3[Sb_7W(CO)_3]$	[376]
$[Sb_7(NiCO)_3]^{3-}$	$[K([2.2.2]crypt)]_3[Sb_7(NiCO)_3](en)$	[236]
$[Bi_3M_2(CO)_6]^{3-}$ (M = Cr, Mo)	$K[K([2.2.2]crypt)]_5[Bi_3M_2(CO)_6]_2(en)_3$	[239]
$[Bi_4Fe_4(CO)_{13}]^{2-}$	$[NEt_4]_2[Bi_4Fe_4(CO)_{13}]$	[243]
$[Bi_4(Fe\{CO\}_3)_3(FeCp'\{CO\}_2)]$	$[Bi_4(Fe\{CO\}_3)_3(FeCp'\{CO\}_2)]$	[384]
$[Bi_3Ni_4(CO)_6]^{3-}$	$[K([2.2.2]crypt)]_4[Bi_3Ni_4(CO)_6](en)(tol)$	[272]
$[Bi_4Ni_4(CO)_6]^{2-}$	$[K([2.2.2]crypt)]_4[Bi_4Ni_4(CO)_6]_2(tol)_{0.5}$	[272]
$[Bi_3Ni_6(CO)_9]^{3-}$	$[K([18]crown\text{-}6)]_3[Bi_3Ni_6(CO)_9](en)(tol)_{0.5}$	[272]
$[Ni_x@Bi_6Ni_6(CO)_8]^{4-}$	$[K([18]crown\text{-}6)]_4[Ni_x@Bi_6Ni_6(CO)_8](en)_3$	[272]
$[Cu(P_4)_2]^+$	$[Cu(P_4)_2][Al(OC(CF_3)_3)_4]$	[235]
$[Ag(P_4)_2]^+$	$[Ag(P_4)_2][Al(OC(CF_3)_3)_4]$	[385]
$[Ti(P_5)_2]^{2-}$	$[K([18]crown\text{-}6)]_2[Ti(P_5)_2]$	[267]
	$[PPh_4]_2[Ti(P_5)_2]$	[267]
	$[PPN]_2[Ti(P_5)_2]$	[267]
$[Zn(P_7)_2]^{4-}$	$[K([2.2.2]crypt)]_4[Zn(P_7)_2]$	[268]
$[Cd(P_7)_2]^{4-}$	$[K([2.2.2]crypt)]_4[Cd(P_7)_2](py)_6$	[268]

Table 7: (Continued)

Cluster	Compound	Ref.
$[(As_6)(As_3)_2\{Co(PEt_2Ph)_6\}]$	$[(As_6)(As_3)_2\{Co(PEt_2Ph)_6\}]$	[199]
$[Cu_2(As_7)_2]^{4-}$	$[K([2.2.2]crypt)]_4[Cu_2(As_7)_2]$	[268]
$[NbAs_8]^{3-}$	$[Rb([2.2.2]crypt)]_2Rb[NbAs_8]$	[265]
$[MoAs_8]^{2-}$	$[K([2.2.2]crypt)]_2[MoAs_8](en)$	[266]
$[Pd_2(As_7)_2]^{4-}$	$[K([2.2.2]crypt)]_4[Pd_{32}As_{14}](en)_5$	[269]
$[Sn(As_7)_2]^{4-}$	$[K([2.2.2]crypt)]_4[SnAs_{14}]$	[135]
$[Pd_7As_{16}]^{4-}$	$[K([2.2.2]crypt)]_8[Pd_7As_{16}]_2(en)_{3.5}$	[269]
$[As@Ni_{12}@As_{20}]^{3-}$	$[PBu_4]_3[As@Ni_{12}@As_{20}]$	[270]
$[Ni_5Sb_{17}]^{4-}$	$[K([2.2.2]crypt)]_4[Ni_5Sb_{17}](en)$	[271]
$[Zn@Zn_8Bi_4@Bi_7]^{5-}$	$[K([2.2.2]crypt)]_5[Zn_9Bi_{11}](en)_2(tol)$	[273]
$[Zn@Zn_5Sn_3Bi_3@Bi_5]^{4-}$	$[K([2.2.2]crypt)]_4[Zn@Zn_5Sn_3Bi_3@Bi_5](en)_{0.5}(tol)_{0.5}$	[274]
$[Eu@Sn_6Bi_8]^{4-}$	$[K([2.2.2]Krypt)]_4[Eu@Sn_6Bi_8](en)_{1.1}$	[362]

[a] Np = neopentyl. [b] Ad = adamantyl.

Acknowledgement

We thank the Deutsche Forschungsgemeinschaft and the Fonds der Chemischen Industrie for their continuous support.

Received: March 18, 2010

[1] H. W. Kroto, J. R. Heath, S. C. O'Brien, R. F. Curl, R. E. Smalley, *Nature* **1985**, *318*, 162.
[2] A. F. Hebard, M. J. Rosseinsky, R. C. Haddon, D. W. Murphy, S. H. Glarum, T. T. M. Palstra, A. P. Ramirez, A. R. Kortan, *Nature* **1991**, *350*, 600.
[3] W. Krätschmer, L. D. Lamb, K. Fostiropoulos, D. R. Huffman, *Nature* **1990**, *347*, 354.
[4] A. Schnepf, H. Schnöckel, *Angew. Chem.* **2001**, *113*, 733; *Angew. Chem. Int. Ed.* **2001**, *40*, 711.
[5] A. Schnepf, H. Schnöckel, *Angew. Chem.* **2002**, *114*, 3682; *Angew. Chem. Int. Ed.* **2002**, *41*, 3533.
[6] H. Schnöckel, *Dalton Trans.* **2008**, 4344.
[7] J. D. Corbett, *Chem. Rev.* **1985**, *85*, 383.
[8] T. F. Fässler, *Coord. Chem. Rev.* **2001**, *215*, 347.
[9] J. D. Corbett, *Struct. Bonding (Berlin)* **1997**, *87*, 158.
[10] H.-G. von Schnering, W. Hönle, *Chem. Rev.* **1988**, *88*, 243.
[11] H.-G. von Schnering, *Angew. Chem.* **1981**, *93*, 44; *Angew. Chem. Int. Ed. Engl.* **1981**, *20*, 33.
[12] S. Scharfe, T. F. Fässler, *Philos. Trans. R. Soc. London Ser. A* **2010**, *328*, 1265.
[13] S. Scharfe, T. F. Fässler, in *Nanoparticles - From Theory to Application Vol. 2* (Ed.: G. Schmid), WILEY-VCH, Weinheim, **2010**, pp. 49.
[14] M. Joannis, *Hebd. Seances Acad. Sci.* **1891**, *113*, 795.
[15] C. A. Kraus, *Trans. Am. Electrochem. Soc.* **1924**, *45*, 175.
[16] F. H. Smyth, *J. Am. Chem. Soc.* **1917**, *39*, 1299.
[17] E. Zintl, J. Goubeau, W. Dullenkopf, *Z. Phys. Chem. Abt. A* **1931**, *154*, 1.
[18] C. A. Kraus, *J. Am. Chem. Soc.* **1922**, *44*, 1216.
[19] E. B. Peck, *J. Am. Chem. Soc.* **1918**, *40*, 335.
[20] E. Zintl, A. Harder, *Z. Phys. Chem. Abt. A* **1931**, *154*, 47.
[21] L. Diehl, K. Khodadadeh, D. Kummer, J. Strähle, *Z. Naturforsch. B* **1976**, *31*, 522.
[22] L. Diehl, K. Khodadadeh, D. Kummer, J. Strähle, *Chem. Ber.* **1976**, *109*, 3404.
[23] J. D. Corbett, P. A. Edwards, *J. Am. Chem. Soc.* **1977**, *99*, 3313.
[24] J. D. Corbett, D. G. Adolphson, D. J. Merryman, P. A. Edwards, F. J. Armatis, *J. Am. Chem. Soc.* **1975**, *97*, 6267.
[25] D. Kummer, L. Diehl, *Angew. Chem.* **1970**, *82*, 881; *Angew. Chem. Int. Ed. Engl.* **1970**, *9*, 895.
[26] A. Nienhaus, S. D. Hoffmann, T. F. Fässler, *Z. Anorg. Allg. Chem.* **2006**, *632*, 1752.
[27] [2.2.2]crypt = 4,7,13,16,21,24-hexaoxa-1,10-diazabicyclo-[8.8.8]hexacosane.
[28] [18]crone-6 = 1,4,7,10,13,16-hexaoxacyclooctadecane.
[29] T. F. Fässler, R. Hoffmann, *Angew. Chem.* **1999**, *111*, 526; *Angew. Chem. Int. Ed.* **1999**, *38*, 543.
[30] R. E. Marsh, D. P. Shoemaker, *Acta Crystallogr.* **1953**, *6*, 197.
[31] K. Wiesler, K. Brandl, A. Fleischmann, N. Korber, *Z. Anorg. Allg. Chem.* **2009**, *635*, 508.
[32] V. Quéneau, S. C. Sevov, *Angew. Chem.* **1997**, *109*, 1818; *Angew. Chem. Int. Ed. Engl.* **1997**, *36*, 1754.
[33] H.-G. von Schnering, M. Baitinger, U. Bolle, W. Carrillo-Cabrera, J. Curda, Y. Grin, F. Heinemann, J. Llanos, K. Peters, A. Schmeding, M. Somer, *Z. Anorg. Allg. Chem.* **1997**, *623*, 1037.
[34] C. Hoch, M. Wendorff, C. Röhr, *J. Alloys Compd.* **2003**, *361*, 206.
[35] M. Waibel, F. Kraus, B. Wahl, S. Scharfe, T. F. Fässler, *Angew. Chem.* **2010**, *122*, 6761; *Angew. Chem. Int. Ed.* **2010**, *49*, 6611.
[36] E. Zintl, H. Kaiser, *Z. Anorg. Allg. Chem.* **1933**, *211*, 113.
[37] B. Eisenmann, *Angew. Chem.* **1993**, *105*, 1764; *Angew. Chem. Int. Ed. Engl.* **1993**, *32*, 1693.
[38] E. Zintl, W. Dullenkopf, *Z. Phys. Chem. Abt. B* **1932**, *16*, 183.
[39] W. Hönle, H.-G. von Schnering, A. Schmidpeter, G. Burget, *Angew. Chem.* **1984**, *96*, 796; *Angew. Chem. Int. Ed. Engl.* **1984**, *23*, 817.
[40] H.-G. von Schnering, T. Meyer, W. Hönle, W. Schmettow, U. Hinze, W. Bauhofer, G. Kliche, *Z. Anorg. Allg. Chem.* **1987**, *553*, 261.
[41] F. Kraus, T. Hanauer, N. Korber, *Angew. Chem.* **2005**, *117*, 7366; *Angew. Chem. Int. Ed.* **2005**, *44*, 7200.
[42] F. Kraus, N. Korber, *Chem. Eur. J.* **2005**, *11*, 5945.
[43] M. Baudler, H. Ternberger, W. Faber, J. Hahn, *Z. Naturforsch. B* **1979**, *34*, 1690.
[44] M. Baudler, R. Heumüller, *Z. Naturforsch. B* **1984**, *39*, 1306.
[45] M. Baudler, *Angew. Chem.* **1987**, *99*, 429; *Angew. Chem. Int. Ed. Engl.* **1987**, *26*, 419.
[46] M. Baudler, R. Heumüller, *Z. Anorg. Allg. Chem.* **1988**, *559*, 49.
[47] M. Baudler, P. Winzek, *Z. Anorg. Allg. Chem.* **1999**, *625*, 417.
[48] F. Kraus, J. C. Aschenbrenner, N. Korber, *Angew. Chem.* **2003**, *115*, 4162; *Angew. Chem. Int. Ed.* **2003**, *42*, 4030.

[49] B. W. Eichhorn, R. C. Haushalter, *J. Am. Chem. Soc.* **1988**, *110*, 8704.
[50] B. W. Eichhorn, R. C. Haushalter, J. C. Huffman, *Angew. Chem.* **1989**, *101*, 1081; *Angew. Chem. Int. Ed. Engl.* **1989**, *28*, 1032.
[51] A. Nienhaus, R. Hauptmann, T. F. Fässler, *Angew. Chem.* **2002**, *114*, 3352; *Angew. Chem. Int. Ed.* **2002**, *41*, 3213.
[52] M. J. Moses, J. C. Fettinger, B. W. Eichhorn, *Science* **2003**, *300*, 778.
[53] E. N. Esenturk, J. Fettinger, Y.-F. Lam, B. W. Eichhorn, *Angew. Chem.* **2004**, *116*, 2184; *Angew. Chem. Int. Ed.* **2004**, *43*, 2132.
[54] T. F. Fässler, S. D. Hoffmann, *Angew. Chem.* **2004**, *116*, 6400; *Angew. Chem. Int. Ed.* **2004**, *43*, 6242.
[55] K. Wade, *Nucl. Chem. Lett.* **1972**, *8*, 559.
[56] K. Wade, *Adv. Inorg. Chem. Radiochem.* **1976**, *18*, 1.
[57] J. D. Corbett, *Prog. Inorg. Chem.* **1976**, *21*, 129.
[58] J. Rosdahl, T. F. Fässler, L. Kloo, *Eur. J. Inorg. Chem.* **2005**, 2888.
[59] R. W. Rudolph, W. L. Wilson, F. Parker, R. C. Taylor, D. C. Young, *J. Am. Chem. Soc.* **1978**, *100*, 4629.
[60] J. M. Goicoechea, S. C. Sevov, *J. Am. Chem. Soc.* **2004**, *126*, 6860.
[61] J. M. Goicoechea, S. C. Sevov, *Inorg. Chem.* **2005**, *44*, 2654.
[62] S. Joseph, C. Suchentrunk, F. Kraus, N. Korber, *Eur. J. Inorg. Chem.* **2009**, 4641.
[63] J. Campbell, G. J. Schrobilgen, *Inorg. Chem.* **1997**, *36*, 4078.
[64] C. Suchentrunk, N. Korber, *New J. Chem.* **2006**, *30*, 1737.
[65] C. H. E. Belin, J. D. Corbett, A. Cisar, *J. Am. Chem. Soc.* **1977**, *99*, 7163.
[66] V. Angilella, C. Belin, *J. Chem. Soc. Faraday Trans.* **1991**, *87*, 203.
[67] T. F. Fässler, M. Hunziker, *Inorg. Chem.* **1994**, *33*, 5380.
[68] T. F. Fässler, U. Schütz, *Inorg. Chem.* **1999**, *38*, 1866.
[69] M. Somer, W. Carrillo-Cabrera, E. M. Peters, K. Peters, H.-G. von Schnering, *Z. Anorg. Allg. Chem.* **1998**, *624*, 1915.
[70] C. Downie, J.-G. Mao, A. M. Guloy, *Inorg. Chem.* **2001**, *40*, 4721.
[71] C. Suchentrunk, J. Daniels, M. Somer, W. Carrilo-Cabrera, N. Korber, *Z. Naturforsch. B* **2005**, *60*, 277.
[72] W. Carrillo-Cabrera, U. Aydemir, M. Somer, A. Kircali, T. F. Fässler, S. D. Hoffmann, *Z. Anorg. Allg. Chem.* **2007**, *633*, 1575.
[73] C. Belin, H. Mercier, V. Angilella, *New J. Chem.* **1991**, *15*, 931.
[74] P. A. Edwards, J. D. Corbett, *Inorg. Chem.* **1977**, *16*, 903.
[75] S. C. Critchlow, J. D. Corbett, *J. Am. Chem. Soc.* **1983**, *105*, 5715.
[76] T. F. Fässler, M. Hunziker, *Z. Anorg. Allg. Chem.* **1996**, *622*, 837.
[77] T. F. Fässler, R. Hoffmann, *Z. Kristallogr. New Cryst. Struct.* **2000**, *215*, 139.
[78] L. Yong, S. D. Hoffmann, T. F. Fässler, *Z. Kristallogr. New Cryst. Struct.* **2005**, *220*, 49.
[79] R. Burns, J. D. Corbett, *Inorg. Chem.* **1985**, *24*, 1489.
[80] N. Korber, A. Fleischmann, *J. Chem. Soc. Dalton Trans.* **2001**, 383.
[81] R. Hauptmann, T. F. Fässler, *Z. Anorg. Allg. Chem.* **2002**, *628*, 1500.
[82] R. Hauptmann, T. F. Fässler, *Z. Kristallogr. New Cryst. Struct.* **2003**, *218*, 458.
[83] R. Hauptmann, T. F. Fässler, *Z. Kristallogr. New Cryst. Struct.* **2003**, *218*, 455.
[84] R. Hauptmann, R. Hoffmann, T. F. Fässler, *Z. Anorg. Allg. Chem.* **2001**, *627*, 2220.
[85] J. D. Corbett, P. A. Edwards, *J. Chem. Soc. Chem. Commun.* **1975**, 984.
[86] J. Campbell, D. A. Dixon, H. P. A. Mercier, G. J. Schrobilgen, *Inorg. Chem.* **1995**, *34*, 5798.
[87] T. F. Fässler, R. Hoffmann, *J. Chem. Soc. Dalton Trans.* **1999**, 3339.
[88] L. Yong, S. D. Hoffmann, T. F. Fässler, *Inorg. Chim. Acta* **2006**, *359*, 4774.
[89] A. Spiekermann, S. D. Hoffmann, T. F. Fässler, *Angew. Chem.* **2006**, *118*, 3538; *Angew. Chem. Int. Ed.* **2006**, *45*, 3459.
[90] S.-J. Kim, S. D. Hoffmann, T. F. Fässler, *Angew. Chem.* **2007**, *119*, 3205; *Angew. Chem. Int. Ed.* **2007**, *46*, 3144.
[91] T. F. Fässler, H.-J. Muhr, M. Hunziker, *Eur. J. Inorg. Chem.* **1998**, 1433.
[92] C. Hoch, M. Wendorff, C. Rohr, *Acta Crystallogr. Sect. C* **2002**, *58*, i45.
[93] S. Ponou, T. F. Fässler, *Z. Anorg. Allg. Chem.* **2007**, *633*, 393.
[94] V. Quéneau, S. C. Sevov, *Inorg. Chem.* **1998**, *37*, 1358.
[95] E. Todorov, S. C. Sevov, *Inorg. Chem.* **1998**, *37*, 3889.
[96] A. F. Hollemann, E. Wiberg, N. Wiberg, *Lehrbuch der Anorganischen Chemie*, 101 ed., De Gruyter, Berlin, **1995**.
[97] [2.2]crypt = 1,7,10,16-tetraoxa-4,13-diazacyclooctadecane.
[98] T. F. Fässler, M. Hunziker, M. Spahr, H. Lueken, *Z. Anorg. Allg. Chem.* **2000**, *626*, 692.
[99] L. F. Cui, X. Huang, L. M. Wang, D. Y. Zubarev, A. I. Boldyrev, J. Li, L. S. Wang, *J. Am. Chem. Soc.* **2006**, *128*, 8390.
[100] L. F. Cui, X. Huang, L. M. Wang, J. Li, L. S. Wang, *J. Phys. Chem. A* **2006**, *110*, 10169.
[101] J. D. Corbett, *Inorg. Chem.* **1968**, *7*, 198.
[102] B. Krebs, M. Mummert, C. Brendel, *J. Less-Common Met.* **1986**, *116*, 159.
[103] T. Hanauer, N. Korber, *Z. Anorg. Allg. Chem.* **2004**, *630*, 2532.
[104] L. Xu, S. Bobev, J. El-Bahraoui, S. C. Sevov, *J. Am. Chem. Soc.* **2000**, *122*, 1838.
[105] M. Baudler, S. Akpapoglou, D. Ouzounis, F. Wasgestian, B. Meinigke, H. Budzikiewicz, H. Münster, *Angew. Chem.* **1988**, *100*, 288; *Angew. Chem. Int. Ed. Engl.* **1988**, *27*, 280.
[106] F. Kraus, T. Hanauer, N. Korber, *Inorg. Chem.* **2006**, *45*, 1117.
[107] S. C. Critchlow, J. D. Corbett, *Inorg. Chem.* **1984**, *23*, 770.
[108] A. Cisar, J. D. Corbett, *Inorg. Chem.* **1977**, *16*, 2482.
[109] A. E. Kuznetsov, T. F. Fässler, *Z. Anorg. Allg. Chem.* **2002**, *628*, 2537.
[110] N. Korber, F. Richter, *Angew. Chem.* **1997**, *109*, 1575; *Angew. Chem. Int. Ed. Engl.* **1997**, *36*, 1512.
[111] K. Pfisterer, Diploma thesis, Universität Regensburg (Regensburg), **1999**.
[112] N. Korber, J. Daniels, *J. Chem. Soc. Dalton Trans.* **1996**, 1653.
[113] N. Korber, H.-G. von Schnering, *Chem. Ber.* **1996**, *129*, 155.
[114] N. Korber, J. Daniels, *Acta Crystallogr. Sect. C* **1996**, *52*, 2454.
[115] N. Korber, J. Daniels, *Helv. Chim. Acta* **1996**, *79*, 2083.
[116] N. Korber, J. Daniels, *Z. Anorg. Allg. Chem.* **1999**, *625*, 189.
[117] N. Korber, J. Daniels, *Polyhedron* **1996**, *15*, 2681.
[118] N. Korber, J. Daniels, H.-G. von Schnering, *Angew. Chem.* **1996**, *108*, 1188; *Angew. Chem. Int. Ed. Engl.* **1996**, *35*, 1107.
[119] N. Korber, F. Richter, *Chem. Commun.* **1996**, 2023.
[120] N. Korber, J. Daniels, *Z. Anorg. Allg. Chem.* **1996**, *622*, 1833.
[121] D. Knettel, M. Reil, N. Korber, *Z. Naturforsch. B* **2001**, *56*, 965.
[122] T. Hanauer, J. C. Aschenbrenner, N. Korber, *Inorg. Chem.* **2006**, *45*, 6723.
[123] V. Miluykov, A. Kataev, O. Sinyashin, P. Lönnecke, E. Hey-Hawkins, *Z. Anorg. Allg. Chem.* **2006**, *632*, 1728.
[124] G. Fritz, H. W. Schneider, W. Hönle, H.-G. von Schnering, *Z. Anorg. Allg. Chem.* **1988**, *43*, 561.
[125] N. Korber, *Phosphorus Sulfur Silicon Relat. Elem.* **1997**, *125*, 339.
[126] K. F. Tebbe, M. Feher, M. Baudler, *Z. Kristallogr.* **1985**, *170*, 180.
[127] T. Hanauer, F. Kraus, N. Korber, *Monatsh. Chem.* **2005**, *136*, 119.
[128] N. Korber, M. Reil, *Chem. Commun.* **2002**, 84.

[129] T. Hanauer, M. Grothe, M. Reil, N. Korber, *Helv. Chim. Acta* **2005**, *88*, 950.
[130] N. Korber, H.-G. von Schnering, *Z. Kristallogr. New Cryst. Struct.* **1997**, *212*, 85.
[131] M. Driess, K. Merz, H. Pritzkow, R. Janoschek, *Angew. Chem.* **1996**, *108*, 2688; *Angew. Chem. Int. Ed. Engl.* **1996**, *35*, 2507.
[132] K. Hübler, G. Becker, *Z. Anorg. Allg. Chem.* **1998**, *624*, 483.
[133] C. H. E. Belin, *J. Am. Chem. Soc.* **1980**, *102*, 6036.
[134] T. Hanauer, N. Korber, *Z. Anorg. Allg. Chem.* **2006**, *632*, 1135.
[135] R. C. Haushalter, B. W. Eichhorn, A. L. Rheingold, S. Geib, *J. Chem. Soc. Chem. Commun.* **1988**, 1027.
[136] M. Reil, N. Korber, *Z. Anorg. Allg. Chem.* **2007**, *633*, 1599.
[137] U. Bolle, W. Tremel, *J. Chem. Soc. Chem. Commun.* **1992**, 91.
[138] G. Fritz, H. W. Schneider, W. Hönle, H.-G. von Schnering, *Z. Naturforsch. B* **1988**, *43*, 561.
[139] L. Xu, S. C. Sevov, *J. Am. Chem. Soc.* **1999**, *121*, 9245.
[140] R. Hauptmann, T. F. Fässler, *Z. Anorg. Allg. Chem.* **2003**, *629*, 2266.
[141] R. Hauptmann, T. F. Fässler, *Z. Kristallogr. New Cryst. Struct.* **2003**, *218*, 461.
[142] J.-Q. Wang, B. Wahl, T. F. Fässler, *Angew. Chem.* **2010**, *122*, 6742; *Angew. Chem. Int. Ed.* **2010**, *49*, 6592.
[143] C. Downie, J.-G. Mao, H. Parmar, A. M. Guloy, *Inorg. Chem.* **2004**, *43*, 1992.
[144] C. Downie, Z. Tang, A. M. Guloy, *Angew. Chem.* **2000**, *112*, 346; *Angew. Chem. Int. Ed.* **2000**, *39*, 337.
[145] A. Ugrinov, S. C. Sevov, *C. R. Chim.* **2005**, *8*, 1878.
[146] A. Ugrinov, S. C. Sevov, *J. Am. Chem. Soc.* **2002**, *124*, 10990.
[147] L. Yong, S. D. Hoffmann, T. F. Fässler, *Z. Anorg. Allg. Chem.* **2005**, *631*, 1149.
[148] A. Ugrinov, S. C. Sevov, *Inorg. Chem.* **2003**, *42*, 5789.
[149] L. Yong, S. D. Hoffmann, T. F. Fässler, *Z. Anorg. Allg. Chem.* **2004**, *630*, 1977.
[150] A. Spiekermann, S. D. Hoffmann, T. F. Fässler, I. Krossing, U. Preiss, *Angew. Chem.* **2007**, *119*, 5404; *Angew. Chem. Int. Ed.* **2007**, *46*, 5310.
[151] A. M. Guloy, R. Ramlau, Z. Tang, W. Schnelle, M. Baitinger, Y. Grin, *Nature* **2006**, *443*, 320.
[152] M. Ichinohe, M. Toyoshima, R. Kinjo, A. Sekiguchi, *J. Am. Chem. Soc.* **2003**, *125*, 13328.
[153] N. Wiberg, C. M. M. Finger, K. Polborn, *Angew. Chem.* **1993**, *105*, 1140; *Angew. Chem. Int. Ed. Engl.* **1993**, *32*, 1054.
[154] N. Wiberg, W. Hochmuth, H. Nöth, A. Appel, M. Schmidt-Amelunxen, *Angew. Chem.* **1996**, *108*, 1437; *Angew. Chem. Int. Ed. Engl.* **1996**, *35*, 1333.
[155] S. C. Sevov, J. M. Goicoechea, *Organometallics* **2006**, *25*, 5678.
[156] A. Schnepf, *Chem. Soc. Rev.* **2007**, *36*, 745.
[157] M. Weidenbruch, *Angew. Chem.* **1993**, *105*, 574; *Angew. Chem. Int. Ed. Engl.* **1993**, *32*, 545.
[158] A. F. Richards, B. E. Eichler, M. Brynda, M. M. Olmstead, P. P. Power, *Angew. Chem.* **2005**, *117*, 2602; *Angew. Chem. Int. Ed.* **2005**, *44*, 2546.
[159] N. Wiberg, H.-W. Lerner, S. Wagner, H. Nöth, *Z. Naturforsch. B* **1999**, *54*, 877.
[160] G. Prabusankar, A. Kempter, C. Gemel, M.-K. Schröter, R. A. Fischer, *Angew. Chem.* **2008**, *120*, 7344; *Angew. Chem. Int. Ed.* **2008**, *47*, 7234.
[161] A. Schnepf, *Eur. J. Inorg. Chem.* **2008**, 1007.
[162] A. Ugrinov, S. C. Sevov, *J. Am. Chem. Soc.* **2002**, *124*, 2442.
[163] A. Ugrinov, S. C. Sevov, *J. Am. Chem. Soc.* **2003**, *125*, 14059.
[164] A. Ugrinov, S. C. Sevov, *Chem. Eur. J.* **2004**, *10*, 3727.
[165] M. W. Hull, A. Ugrinov, I. Petrov, S. C. Sevov, *Inorg. Chem.* **2007**, *46*, 2704.
[166] C. B. Benda, J.-Q. Wang, B. Wahl, T. F. Fässler, **2011**, unpublished results.
[167] M. W. Hull, S. C. Sevov, *Inorg. Chem.* **2007**, *46*, 10953.
[168] M. W. Hull, S. C. Sevov, *J. Am. Chem. Soc.* **2009**, *131*, 9026.
[169] M. W. Hull, S. C. Sevov, *Angew. Chem.* **2007**, *119*, 6815; *Angew. Chem. Int. Ed.* **2007**, *46*, 6695.
[170] C. Benda, Diploma thesis, TU München (Garching), **2009**.
[171] A. Schnepf, *Angew. Chem.* **2003**, *115*, 2728; *Angew. Chem. Int. Ed.* **2003**, *42*, 2624.
[172] C. Schenk, A. Schnepf, *Chem. Commun.* **2009**, 3208.
[173] A. Schnepf, C. Schenk, *Angew. Chem.* **2006**, *118*, 5499; *Angew. Chem. Int. Ed.* **2006**, *45*, 5373.
[174] A. Schnepf, C. Schenk, *Chem. Commun.* **2008**, 4643.
[175] A. Sekiguchi, Y. Ishida, Y. Kabe, M. Ichinohe, *J. Am. Chem. Soc.* **2002**, *124*, 8776.
[176] A. F. Richards, H. Hope, P. P. Power, *Angew. Chem.* **2003**, *115*, 4205; *Angew. Chem. Int. Ed.* **2003**, *42*, 4071.
[177] E. Rivard, J. Steiner, J. C. Fettinger, J. R. Giuliani, M. P. Augustine, P. P. Power, *Chem. Commun.* **2007**, 4919.
[178] B. E. Eichler, P. P. Power, *Angew. Chem.* **2001**, *113*, 818; *Angew. Chem. Int. Ed.* **2001**, *40*, 796.
[179] A. Schnepf, R. Köppe, *Angew. Chem.* **2003**, *115*, 940; *Angew. Chem. Int. Ed.* **2003**, *42*, 911.
[180] K. W. Klinkhammer, Y. Xiong, S. Yao, *Angew. Chem.* **2004**, *116*, 6328; *Angew. Chem. Int. Ed.* **2004**, *43*, 6202.
[181] D. J. Chapman, S. C. Sevov, *Inorg. Chem.* **2008**, *47*, 6009.
[182] F. S. Kocak, P. Y. Zavalij, Y. F. Lam, B. W. Eichhorn, *Chem. Commun.* **2009**, 4197.
[183] M. M. Gillett-Kunnath, I. Petrov, S. C. Sevov, *Inorg. Chem.* **2010**, *49*, 721.
[184] A. Schnepf, *Chem. Commun.* **2007**, 192.
[185] C. Schrenk, I. Schellenberg, R. Pöttgen, A. Schnepf, *Dalton Trans.* **2010**, *39*, 1872.
[186] M. Peruzzini, L. Gonsalvi, A. Romerosa, *Chem. Soc. Rev.* **2005**, *34*, 1038.
[187] Y. Xiong, S. Yao, M. Brym, M. Driess, *Angew. Chem.* **2007**, *119*, 4595; *Angew. Chem. Int. Ed.* **2007**, *46*, 4511.
[188] J. J. Weigand, M. Holthausen, R. Fröhlich, *Angew. Chem.* **2009**, *121*, 301; *Angew. Chem. Int. Ed.* **2009**, *48*, 295.
[189] A. R. Fox, R. J. Wright, E. Rivard, P. P. Power, *Angew. Chem.* **2005**, *117*, 7907; *Angew. Chem. Int. Ed.* **2005**, *44*, 7729.
[190] M. Baudler, *Angew. Chem.* **1982**, *94*, 520; *Angew. Chem. Int. Ed. Engl.* **1982**, *21*, 492.
[191] G. Fritz, K. D. Hoppe, W. Hönle, D. Weber, D. Mujica, V. Manriquez, H. G. von Schnering, *J. Organomet. Chem.* **1983**, *249*, 63.
[192] N. Korber, H.-G. von Schnering, *J. Chem. Soc. Chem. Commun.* **1995**, 1713.
[193] S. P. Mattamana, K. Promprai, J. C. Fettinger, B. W. Eichhorn, *Inorg. Chem.* **1998**, *37*, 6222.
[194] J. C. Aschenbrenner, N. Korber, *Z. Anorg. Allg. Chem.* **2004**, *630*, 31.
[195] F. R. Dai, L. Xu, *Inorg. Chim. Acta* **2006**, *359*, 4265.
[196] S. Charles, J. C. Fettinger, S. G. Bott, B. W. Eichhorn, *J. Am. Chem. Soc.* **1996**, *118*, 4713.
[197] B. Kesanli, S. Charles, Y. F. Lam, S. G. Bott, J. C. Fettinger, B. W. Eichhorn, *J. Am. Chem. Soc.* **2000**, *122*, 11101.
[198] B. M. Cossairt, C. C. Cummins, *Angew. Chem.* **2008**, *120*, 175; *Angew. Chem. Int. Ed.* **2008**, *47*, 169.
[199] R. Ahlrichs, D. Fenske, K. Fromm, H. Krautscheid, U. Krautscheid, O. Treutler, *Chem. Eur. J.* **1996**, *2*, 238.
[200] W. Hönle, H.-G. von Schnering, *Z. Anorg. Allg. Chem.* **1978**, *440*, 171.
[201] N. Korber, J. C. Aschenbrenner, *J. Chem. Soc. Dalton Trans.* **2001**, 1165.
[202] F. Kraus, J. C. Aschenbrenner, T. Klamroth, N. Korber, *Inorg. Chem.* **2009**, *48*, 1911.
[203] R. W. Rudolph, W. L. Wilson, R. C. Taylor, *J. Am. Chem. Soc.* **1981**, *103*, 2480.
[204] S. C. Critchlow, J. D. Corbett, *Inorg. Chem.* **1985**, *24*, 979.
[205] L. Xu, S. C. Sevov, *Inorg. Chem.* **2000**, *39*, 5383.

[206] R. C. Burns, J. D. Corbett, *J. Am. Chem. Soc.* **1982**, *104*, 2804.
[207] B. M. Cossairt, C. C. Cummins, *J. Am. Chem. Soc.* **2009**, *131*, 15501.
[208] B. M. Cossairt, M. C. Diawara, C. C. Cummins, *Science* **2009**, *323*, 602.
[209] P. Kircher, G. Huttner, K. Heinze, G. Renner, *Angew. Chem.* **1998**, *110*, 1754; *Angew. Chem. Int. Ed.* **1998**, *37*, 1664.
[210] B. Schiemenz, G. Huttner, *Angew. Chem.* **1993**, *105*, 295; *Angew. Chem. Int. Ed. Engl.* **1993**, *32*, 297.
[211] G. Renner, P. Kircher, G. Huttner, P. Rutsch, K. Heinze, *Eur. J. Inorg. Chem.* **2001**, 973.
[212] L. Yong, S. D. Hoffmann, T. F. Fässler, S. Riedel, M. Kaupp, *Angew. Chem.* **2005**, *117*, 2129; *Angew. Chem. Int. Ed.* **2005**, *44*, 2092.
[213] B. Kesanli, J. Fettinger, B. W. Eichhorn, *Angew. Chem.* **2001**, *113*, 2364; *Angew. Chem. Int. Ed.* **2001**, *40*, 2300.
[214] J. Campbell, H. P. A. Mercier, H. Franke, D. P. Santry, D. A. Dixon, G. J. Schrobilgen, *Inorg. Chem.* **2002**, *41*, 86.
[215] B. W. Eichhorn, R. C. Haushalter, *J. Chem. Soc. Chem. Commun.* **1990**, 937.
[216] B. Kesanli, J. Fettinger, B. W. Eichhorn, *Chem. Eur. J.* **2001**, *7*, 5277.
[217] L. Yong, S. D. Hoffmann, T. F. Fässler, *Eur. J. Inorg. Chem.* **2005**, 3663.
[218] D. O. Downing, P. Zavalij, B. W. Eichhorn, *Eur. J. Inorg. Chem.* **2010**, 890.
[219] J.-Q. Wang, S. Stegmaier, B. Wahl, T. F. Fässler, *Chem. Eur. J.* **2010**, *16*, 1793.
[220] J. M. Goicoechea, S. C. Sevov, *J. Am. Chem. Soc.* **2006**, *128*, 4155.
[221] S. Scharfe, T. F. Fässler, *Eur. J. Inorg. Chem.* **2010**, 1207.
[222] J. M. Goicoechea, S. C. Sevov, *Organometallics* **2006**, *25*, 4530.
[223] B. Zhou, M. S. Denning, C. Jones, J. M. Goicoechea, *Dalton Trans.* **2009**, 1571.
[224] Z.-M. Sun, Y.-F. Zhao, J. Li, L.-S. Wang, *J. Cluster Sci.* **2009**, *20*, 601.
[225] B. Zhou, M. S. Denning, T. A. D. Chapman, J. M. Goicoechea, *J. Am. Chem. Soc.* **2009**, *131*, 2899.
[226] S. Joseph, M. Hamberger, F. Mutzbauer, O. Härtl, M. Meier, N. Korber, *Angew. Chem.* **2009**, *121*, 8926; *Angew. Chem. Int. Ed.* **2009**, *48*, 8770.
[227] M. B. Boeddinghaus, S. D. Hoffmann, T. F. Fässler, *Z. Anorg. Allg. Chem.* **2007**, *633*, 2338.
[228] M. S. Denning, J. M. Goicoechea, *Dalton Trans.* **2008**, 5882.
[229] A. Spiekermann, S. D. Hoffmann, F. Kraus, T. F. Fässler, *Angew. Chem.* **2007**, *119*, 1663; *Angew. Chem. Int. Ed.* **2007**, *46*, 1638.
[230] C. Schenk, A. Schnepf, *Angew. Chem.* **2007**, *119*, 5408; *Angew. Chem. Int. Ed.* **2007**, *46*, 5314.
[231] C. Schenk, F. Henke, G. Santiso-Quinones, I. Krossing, A. Schnepf, *Dalton Trans.* **2008**, 4436.
[232] F. Henke, C. Schenk, A. Schnepf, *Dalton Trans.* **2009**, 9141.
[233] B. Zhou, M. S. Denning, T. A. D. Chapman, J. E. McGrady, J. M. Goicoechea, *Chem. Commun.* **2009**, 7221.
[234] O. J. Scherer, *Angew. Chem.* **2000**, *112*, 1069; *Angew. Chem. Int. Ed.* **2000**, *39*, 1029.
[235] G. Santiso-Quiñones, A. Reisinger, J. Slattery, I. Krossing, *Chem. Commun.* **2007**, 5046.
[236] S. Charles, B. W. Eichhorn, S. G. Bott, *J. Am. Chem. Soc.* **1993**, *115*, 5837.
[237] S. N. Konchenko, N. A. Pushkarevsky, M. T. Gamer, R. Köppe, H. Schnöckel, P. W. Roesky, *J. Am. Chem. Soc.* **2009**, *131*, 5740.
[238] A. S. Foust, M. S. Foster, L. F. Dahl, *J. Am. Chem. Soc.* **1969**, *91*, 5631.
[239] L. Xu, A. Ugrinov, S. C. Sevov, *J. Am. Chem. Soc.* **2001**, *123*, 4091.
[240] N. A. Piro, C. C. Cummins, *J. Am. Chem. Soc.* **2008**, *130*, 9524.
[241] O. J. Scherer, J. Vondung, G. Wolmershauser, *Angew. Chem.* **1989**, *101*, 1395; *Angew. Chem. Int. Ed. Engl.* **1989**, *28*, 1355.
[242] M. Scheer, E. Herrmann, J. Sieler, M. Oehme, *Angew. Chem.* **1991**, *103*, 1023; *Angew. Chem. Int. Ed. Engl.* **1991**, *30*, 969.
[243] K. H. Whitmire, M. R. Churchill, J. C. Fettinger, *J. Am. Chem. Soc.* **1985**, *107*, 1056.
[244] A. L. Rheingold, M. J. Foley, P. J. Sullivan, *J. Am. Chem. Soc.* **1982**, *104*, 4727.
[245] H. J. Breunig, N. Burford, R. Rösler, *Angew. Chem.* **2000**, *112*, 4320; *Angew. Chem. Int. Ed.* **2000**, *39*, 4148.
[246] O. J. Scherer, H. Sitzmann, G. Wolmershauser, *Angew. Chem.* **1985**, *97*, 358; *Angew. Chem. Int. Ed. Engl.* **1985**, *24*, 351.
[247] J. M. Goicoechea, S. C. Sevov, *Angew. Chem.* **2005**, *117*, 4094; *Angew. Chem. Int. Ed.* **2005**, *44*, 4026.
[248] S. Scharfe, T. F. Fässler, S. Stegmaier, S. D. Hoffmann, K. Ruhland, *Chem. Eur. J.* **2008**, *14*, 4479.
[249] B. Zhou, M. S. Denning, D. L. Kays, J. M. Goicoechea, *J. Am. Chem. Soc.* **2009**, *131*, 2802.
[250] J.-Q. Wang, S. Stegmaier, Thomas F. Fässler, *Angew. Chem.* **2009**, *121*, 2032; *Angew. Chem. Int. Ed.* **2009**, *48*, 1998.
[251] E. N. Esenturk, J. Fettinger, B. W. Eichhorn, *Chem. Commun.* **2005**, 247.
[252] E. N. Esenturk, J. Fettinger, B. W. Eichhorn, *J. Am. Chem. Soc.* **2006**, *128*, 9178.
[253] E. N. Esenturk, J. C. Fettinger, B. W. Eichhorn, *J. Am. Chem. Soc.* **2006**, *128*, 12.
[254] J. M. Goicoechea, S. C. Sevov, *J. Am. Chem. Soc.* **2005**, *127*, 7676.
[255] F. S. Kocak, P. Zavalij, Y.-F. Lam, B. W. Eichhorn, *Inorg. Chem.* **2008**, *47*, 3515.
[256] Z. M. Sun, H. Xiao, J. Li, L. S. Wang, *J. Am. Chem. Soc.* **2007**, *129*, 9560.
[257] B. Kesanli, J. E. Halsig, P. Zavalij, J. C. Fettinger, Y. F. Lam, B. W. Eichhorn, *J. Am. Chem. Soc.* **2007**, *129*, 4567.
[258] S. Scharfe, PhD thesis, TU München (Garching), **2010**.
[259] C. Schrodt, F. Weigend, R. Ahlrichs, *Z. Anorg. Allg. Chem.* **2002**, *628*, 2478.
[260] M. Brynda, R. Herber, P. B. Hitchcock, M. F. Lappert, I. Nowik, P. P. Power, A. Protchenko, V. , A. Ruzicka, J. Steiner, *Angew. Chem.* **2006**, *118*, 4439; *Angew. Chem. Int. Ed.* **2006**, *45*, 4333.
[261] T. F. Fässler, S. Hoffmann, C. Kronseder, *Z. Anorg. Allg. Chem.* **2001**, *627*, 2486.
[262] E. N. Esenturk, J. Fettinger, B. W. Eichhorn, *Polyhedron* **2006**, *25*, 521.
[263] B. Kesanli, J. Fettinger, D. R. Gardner, B. W. Eichhorn, *J. Am. Chem. Soc.* **2002**, *124*, 4779.
[264] X. Zhang, G. Li, Z. Gao, *Rapid Commun. Mass Spectrom.* **2001**, *15*, 1573.
[265] H.-G. von Schnering, J. Wolf, D. Weber, R. Ramirez, T. Meyer, *Angew. Chem.* **1986**, *98*, 372; *Angew. Chem. Int. Ed. Engl.* **1986**, *25*, 353.
[266] B. W. Eichhorn, S. P. Mattamana, D. R. Gardner, J. C. Fettinger, *J. Am. Chem. Soc.* **1998**, *120*, 9708.
[267] E. Urnezius, W. W. Brennessel, C. J. Cramer, J. E. Ellis, P. von R. Schleyer, *Science* **2002**, *295*, 832.
[268] C. Knapp, B. Zhou, M. S. Denning, N. H. Rees, J. M. Goicoechea, *Dalton Trans.* **2010**, *39*, 426.
[269] M. J. Moses, J. Fettinger, B. W. Eichhorn, *J. Am. Chem. Soc.* **2002**, *124*, 5944.
[270] The term "discrete" denotes here anions or clusters in solids without intercluster bonding and irrespective of the contacts to alkali or alkaline-earth metal atoms.
[271] M. J. Moses, J. C. Fettinger, B. W. Eichhorn, *Inorg. Chem.* **2007**, *46*, 1036.
[272] J. M. Goicoechea, M. W. Hull, S. C. Sevov, *J. Am. Chem. Soc.* **2007**, *129*, 7885.

[273] J. M. Goicoechea, S. C. Sevov, *Angew. Chem.* **2006**, *118*, 5271; *Angew. Chem. Int. Ed.* **2006**, *45*, 5147.
[274] F. Lips, S. Dehnen, *Angew. Chem.* **2009**, *121*, 6557; *Angew. Chem. Int. Ed.* **2009**, *48*, 6435.
[275] B. Wrackmeyer, *Annual Reports on NMR Spectroscopy*, *Vol. 47*, Academic Press, **2002**, p. 1.
[276] B. Wrackmeyer, G. A. Webb, *Annual Reports on NMR Spectroscopy*, *Vol. 38*, Academic Press, **1999**, p. 203.
[277] L. J. Guggenberger, E. L. Muetterties, *J. Am. Chem. Soc.* **1976**, *98*, 7221.
[278] W. L. Wilson, R. W. Rudolph, L. L. Lohr, F. Parker, R. C. Taylor, D. C. Pyykkö, *Inorg. Chem.* **1986**, *25*, 1535.
[279] F. Teixidor, M. L. Luetkens, R. W. Rudolph, *J. Am. Chem. Soc.* **1983**, *105*, 149.
[280] M. L. Luetkens Jr. , F. Teixidor, R. W. Rudolph, *Inorg. Chim. Acta* **1984**, *83*, L13.
[281] M. Baudler, K. Glinka, *Chem. Rev.* **1993**, *93*, 1623.
[282] M. Baudler, K. Glinka, *Chem. Rev.* **1994**, *94*, 1273.
[283] M. Baudler, D. Düster, K. Langerbeins, J. Germeshausen, *Angew. Chem.* **1984**, *96*, 309; *Angew. Chem. Int. Ed. Engl.* **1984**, *23*, 317.
[284] M. Baudler, R. Heumüller, K. Langerbeins, *Z. Anorg. Allg. Chem.* **1984**, *514*, 7.
[285] S. Charles, J. C. Fettinger, B. W. Eichhorn, *J. Am. Chem. Soc.* **1995**, *117*, 5303.
[286] J. Schmedt auf der Günne, S. Kaczmarek, L. van Wüllen, H. Eckert, D. Paschke, A. J. Foecker, W. Jeitschko, *J. Solid State Chem.* **1999**, *147*, 341.
[287] F. Kraus, J. Schmedt auf der Günne, B. F. DiSalle, N. Korber, *Chem. Commun.* **2006**, 218.
[288] D. M. P. Mingos, R. L. Johnston, *Struct. Bonding (Berlin)* **1987**, *68*, 29.
[289] D. M. P. Mingos, T. Slee, L. Zhenyang, *Chem. Rev.* **1990**, *90*, 383.
[290] K. Wade, *J. Chem. Soc. D* **1971**, 792.
[291] R. B. King, I. Silaghi-Dumitrescu, *Dalton Trans.* **2008**, 6083.
[292] W. A. de Heer, *Rev. Mod. Phys.* **1993**, *65*, 611.
[293] A. J. Stone, *Inorg. Chem.* **1981**, *20*, 563.
[294] A. J. Stone, *Mol. Phys.* **1980**, *41*, 1339.
[295] A. J. Stone, *Polyhedron* **1984**, *3*, 1299.
[296] A. Hirsch, Z. Chen, H. Jiao, *Angew. Chem.* **2000**, *112*, 4079; *Angew. Chem. Int. Ed.* **2000**, *39*, 3915.
[297] A. Hirsch, Z. Chen, H. Jiao, *Angew. Chem.* **2001**, *113*, 2916; *Angew. Chem. Int. Ed.* **2001**, *40*, 2834.
[298] A. J. Stone, D. J. Wales, *Mol. Phys.* **1987**, *61*, 747.
[299] Z. Lin, T. Slee, D. M. P. Mingos, *Chem. Phys.* **1990**, *142*, 321.
[300] D.-L. Chen, W. Q. Tian, W.-C. Lu, C.-C. Sun, *J. Chem. Phys.* **2006**, *124*, 154313.
[301] R. B. King, I. Silaghi-Dumitrescu, *Inorg. Chem.* **2003**, *42*, 6701.
[302] R. B. King, *Chem. Rev.* **2001**, *101*, 1119.
[303] Z. Chen, R. B. King, *Chem. Rev.* **2005**, *105*, 3613.
[304] P. von R. Schleyer, C. Maerker, A. Dransfeld, H. Jiao, N. J. R. v. E. Hommes, *J. Am. Chem. Soc.* **1996**, *118*, 6317.
[305] Z. Chen, C. S. Wannere, C. Corminboeuf, R. Puchta, P. von R. Schleyer, *Chem. Rev.* **2005**, *105*, 3842.
[306] Z. Chen, S. Neukermans, X. Wang, E. Janssens, Z. Zhou, R. E. Silverans, R. B. King, P. von R. Schleyer, P. Lievens, *J. Am. Chem. Soc.* **2006**, *128*, 12829.
[307] R. B. King, T. Heine, C. Corminboeuf, P. von R. Schleyer, *J. Am. Chem. Soc.* **2004**, *126*, 430.
[308] R. B. King, I. Silaghi-Dumitrescu, M. M. Uta, *Dalton Trans.* **2007**, 364.
[309] L.-F. Cui, X. Huang, L.-M. Wang, J. Li, L.-S. Wang, *Angew. Chem.* **2007**, *119*, 756; *Angew. Chem. Int. Ed.* **2007**, *46*, 742.
[310] J. P. Dognon, C. Clavaguera, P. Pyykkö, *Angew. Chem.* **2007**, *119*, 1449; *Angew. Chem. Int. Ed.* **2007**, *46*, 1427.
[311] A. D. Zdetsis, *J. Chem. Phys.* **2007**, *127*, 244308.
[312] N. Shao, S. Bulusu, X. C. Zeng, *J. Chem. Phys.* **2008**, *128*, 154326.
[313] D.-L. Chen, W. Q. Tian, J.-K. Feng, C.-C. Sun, *J. Phys. Chem. A* **2007**, *111*, 8277.
[314] S. Neukermans, E. Janssens, Z. F. Chen, R. E. Silverans, P. von R. Schleyer, P. Lievens, *Phys. Rev. Lett.* **2004**, *92*, 163401.
[315] A. D. Zdetsis, *J. Chem. Phys.* **2007**, *127*, 014314.
[316] R. B. King, I. Silaghi-Dumitrescu, M.-M. Uta, *Inorg. Chem.* **2006**, *45*, 4974.
[317] D.-L. Chen, W. Q. Tian, C.-C. Sun, *Phys. Rev. A* **2007**, *75*, 013201.
[318] V. Kumar, Y. Kawazoe, *Appl. Phys. Lett.* **2003**, *83*, 2677.
[319] C. Rajesh, C. Majumder, *J. Chem. Phys.* **2008**, *128*, 024308.
[320] C. Rajesh, C. Majumder, *Chem. Phys. Lett.* **2006**, *430*, 101.
[321] V. Kumar, Y. Kawazoe, *Appl. Phys. Lett.* **2002**, *80*, 859.
[322] J. Lu, S. Nagase, *Chem. Phys. Lett.* **2003**, *372*, 394.
[323] S. Neukermans, X. Wang, N. Veldeman, E. Janssens, R. E. Silverans, P. Lievens, *Int. J. Mass Spectrom.* **2006**, *252*, 145.
[324] S. Schäfer, R. Schäfer, *ChemPhysChem* **2008**, *9*, 1925.
[325] A. D. Zdetsis, *Phys. Rev. B* **2007**, *75*, 085409.
[326] R. B. King, I. Silaghi-Dumitrescu, M.-M. Uta, *Chem. Eur. J.* **2008**, *14*, 4542.
[327] R. B. King, I. Silaghi-Dumitrescu, M. M. Uta, *J. Phys. Chem. A* **2008**, *113*, 527.
[328] S. Stegmaier, T. F. Fässler, **2010**, unpublished results.
[329] S. Stegmaier, Diploma thesis, TU München (Garching), **2007**.
[330] R. C. Haushalter, *Angew. Chem.* **1983**, *95*, 560; *Angew. Chem. Int. Ed. Engl.* **1983**, *22*, 558.
[331] R. C. Haushalter, C. M. O'Connor, J. P. Haushalter, A. M. Umarji, G. K. Shenoy, *Angew. Chem.* **1984**, *96*, 147; *Angew. Chem. Int. Ed. Engl.* **1984**, *23*, 169.
[332] S. Bag, I. U. Arachchigea, M. G. Kanatzidis, *J. Mater. Chem.* **2008**, *18*, 3628.
[333] Q. Zhang, C. D. Malliakas, M. G. Kanatzidis, *Inorg. Chem.* **2009**, *48*, 10910.
[334] T. F. Fässler, U. Schütz, *J. Organomet. Chem.* **1997**, *541*, 269.
[335] J.-Q. Wang, V. Hlukhyy, T. F. Fässler, *Z. Naturforsch. B* **2009**, *64*, 1319.
[336] M. G. Kanatzidis, G. S. Armatas, *Science* **2006**, *313*, 817.
[337] G. S. Armatas, M. G. Kanatzidis, *Adv. Mater.* **2008**, *20*, 546.
[338] D. Sun, A. E. Riley, A. J. Cadby, E. K. Richmann, S. D. Korlann, S. H. Tolbert, *Nature* **2006**, *441*, 1126.
[339] A. P. Z. Clark, K.-F. Shen, Y. F. Rubin, S. H. Tolbert, *Nano Lett.* **2005**, *5*, 1647.
[340] A. M. Guloy, Z. Tang, R. Ramlau, B. Böhme, M. Baitinger, Y. Grin, *Eur. J. Inorg. Chem.* **2009**, 2455.
[341] T. F. Fässler, *Angew. Chem.* **2007**, *119*, 2624; *Angew. Chem. Int. Ed.* **2007**, *46*, 2572.
[342] A. Kaltzoglou, S. Ponou, T. F. Fässler, *Eur. J. Inorg. Chem.* **2008**, 4507.
[343] B. Böhme, A. Guloy, Z. Tang, W. Schnelle, U. Burkhardt, M. Baitinger, Y. Grin, *J. Am. Chem. Soc.* **2007**, *129*, 5348.
[344] A. J. Karttunen, T. F. Fässler, M. Linnolahti, T. A. Pakkanen, *ChemPhysChem* **2010**, *11*, 1944.
[345] J. Witte, H.-G. von Schnering, *Z. Anorg. Allg. Chem.* **1964**, *327*, 260.
[346] E. Busmann, *Z. Anorg. Allg. Chem.* **1961**, *313*, 90.
[347] R. Schäfer, W. Klemm, *Z. Anorg. Allg. Chem.* **1961**, *312*, 214.
[348] V. Quéneau, E. Todorov, S. C. Sevov, *J. Am. Chem. Soc.* **1998**, *120*, 3263.
[349] Y. Grin, M. Baitinger, R. Kniep, H.-G. von Schnering, *Z. Kristallogr. New Cryst. Struct.* **1999**, *214*, 453.
[350] W. Müller, K. Volk, *Z. Naturforsch. B* **1977**, *32*, 709.
[351] I. F. Hewaidy, E. Busmann, W. Klemm, *Z. Anorg. Allg. Chem.* **1964**, *328*, 283.
[352] M. Baitinger, Y. Grin, R. Kniep, H.-G. von Schnering, *Z. Kristallogr. New Cryst. Struct.* **1999**, *214*, 457.

[353] C. Hoch, M. Wendorff, C. Röhr, *Z. Anorg. Allg. Chem.* **2003**, *629*, 2391.
[354] C. Hoch, C. Röhr, *Z. Anorg. Allg. Chem.* **2002**, *628*, 1541.
[355] C. Röhr, *Z. Naturforsch. B* **1995**, *50*, 802.
[356] M. Baitinger, K. Peters, M. Somer, W. Carrillo-Cabrera, Y. Grin, R. Kniep, H.-G. von Schnering, *Z. Kristallogr. New Cryst. Struct.* **1999**, *214*, 455.
[357] W. Hönle, H. G. von Schnering, A. Schmidpeter, G. Burget, *Angew. Chem.* **1984**, *96*, 796; *Angew. Chem. Int. Ed.* **1984**, *23*, 817.
[358] A. F. Richards, M. Brynda, M. M. Olmstead, P. P. Power, *Organometallics* **2004**, *23*, 2841.
[359] A. Schnepf, C. Drost, *Dalton Trans.* **2005**, 3277.
[360] L. Yong, S. D. Hoffmann, T. F. Fässler, *Z. Kristallogr. New Cryst. Struct.* **2005**, *220*, 53.
[361] V. Manriquez, W. Hönle, H.-G. von Schnering, *Z. Anorg. Allg. Chem.* **1986**, *539*, 95.
[362] F. Lips, R. Clérac, S. Dehnen, *Angew. Chem.* **2011**, *123*, 991; *Angew. Chem. Int. Ed.* **2011**, *50*, 960.
[363] T. Meyer, W. Hönle, H.-G. von Schnering, *Z. Anorg. Allg. Chem.* **1987**, *552*, 81.
[364] W. Dahlmann, H.-G. von Schnering, *Naturwissenschaften* **1973**, *60*, 429.
[365] T. Hanauer, F. Kraus, M. Reil, N. Korber, *Monatsh. Chem.* **2006**, *137*, 147.
[366] W. Hönle, J. Buresch, K. Peters, J. H. Chang, H.-G. von Schnering, *Z. Kristallogr. New Cryst. Struct.* **2002**, *217*, 485.
[367] W. Hönle, J. Buresch, K. Peters, J. H. Chang, H.-G. von Schnering, *Z. Kristallogr. New Cryst. Struct.* **2002**, *217*, 487.
[368] F. Emmerling, C. Röhr, *Z. Naturforsch. B* **2002**, *57*, 963.
[369] W. Hönle, J. Buresch, J. Wolf, D. Peters, J. H. Chang, H.-G. von Schnering, *Z. Kristallogr. New Cryst. Struct.* **2002**, *217*, 489.
[370] M. Somer, W. Hönle, H.-G. von Schnering, *Z. Naturforsch. B* **1989**, *44*, 296.
[371] W. Schmettow, H.-G. von Schnering, *Angew. Chem.* **1977**, *89*, 895; *Angew. Chem. Int. Ed. Engl.* **1977**, *16*, 857.
[372] H.-G. von Schnering, M. Somer, G. Kliche, W. Hönle, T. Meyer, J. Wolf, L. Ohse, P. B. Kempa, *Z. Anorg. Allg. Chem.* **1991**, *601*, 13.
[373] F. Emmerling, C. Röhr, *Z. Anorg. Allg. Chem.* **2003**, *629*, 467.
[374] C. Hirschle, C. Röhr, *Z. Anorg. Allg. Chem.* **2000**, *626*, 1992.
[375] S. C. Critchlow, J. D. Corbett, *Inorg. Chem.* **1982**, *21*, 3286.
[376] S. Charles, B. W. Eichhorn, A. L. Rheingold, S. G. Bott, *J. Am. Chem. Soc.* **1994**, *116*, 8077.
[377] S. Charles, J. C. Fettinger, B. W. Eichhorn, *Inorg. Chem.* **1996**, *35*, 1540.
[378] M. E. Barr, B. R. Adams, R. R. Weller, L. F. Dahl, *J. Am. Chem. Soc.* **1991**, *113*, 3052.
[379] M. Scheer, U. Becker, E. Matern, *Chem. Ber.* **1996**, *129*, 721.
[380] Y. Z. Ye, L. Xu, *Chin. J. Struct. Chem.* **2008**, *27*, 75.
[381] N. Korber, J. Daniels, *Inorg. Chem.* **1997**, *36*, 4906.
[382] H. J. Breunig, R. Rösler, E. Lork, *Angew. Chem.* **1997**, *109*, 2941; *Angew. Chem. Int. Ed. Engl.* **1997**, *36*, 2819.
[383] U. Bolle, W. Tremel, *J. Chem. Soc. Chem. Commun.* **1994**, 217.
[384] T. Gröer, M. Scheer, *Organometallics* **2000**, *19*, 3683.
[385] I. Krossing, *J. Am. Chem. Soc.* **2001**, *123*, 4603.
[386] D. Rios, S. C. Sevov, *Inorg. Chem.* **2010**, *49*, 6396.
[387] O. J. Scherer, T. Brück, *Angew. Chem.* **1987**, *99*, 59; *Angew. Chem. Int. Ed. Engl.* **1987**, *26*, 59.
[388] O. J. Scherer, G. Berg, G. Wolmershauser, *Chem. Ber.* **1996**, *129*, 53.
[389] K. H. Janzon, H. Schäfer, A. Weiss, *Z. Anorg. Allg. Chem.* **1970**, *372*, 325.
[390] H. G. von Schnering, M. Schwarz, R. Nesper, *Angew. Chem.* **1986**, *98*, 558; *Angew. Chem. Int. Ed. Engl.* **1986**, *25*, 566.
[391] J. Suchentrunk, N. Korber, *Z. Naturforsch. B* **2010**, *65*, 1059.
[392] A. Betz, H. Schäfer, A. Weiss, *Z. Naturforsch. B* **1968**, *23*, 878.
[393] H. G. von Schnering, J. Llanos, Y. Grin, W. Carillo-Cabrera, E. M. Peters, K. Peters, *Z. Krist. NCS*, **1998**, 213.
[394] J. Llanos, R. Nesper, H. G. von Schnering, *Angew. Chem.* **1983**, *95*, 1026; *Angew. Chem. Int. Ed. Engl.* **1983**, *22*, 998.
[395] S. Bobev, S. C. Sevov, *Polyhedron* **2002**, *21*, 641.
[396] F. R. Dai, L. Xu, *Chin. J. Struct. Chem.* **2007**, *26*, 45.
[397] M. Somer, W. Hönle, H. G. von Schnering, *Z. Naturfosch. B* **1989**, *44*, 296.
[398] D. G. Adolphson, J. D. Corbett, D. J. Merryman, *J. Am. Chem. Soc.* **1976**, *98*, 7234.
[399] A. Bashall, M. A. Beswick, N. Choi, A. D. Hopkins, S. J. Kidd, Y. G. Lawson, M. E. G. Mosquera, M. McPartlin, P. R. Raithby, A. Wheatley, J. A. Wood, D. S. Wright, *Dalton Trans.* **2000**, 479.
[400] A. W. Castleman, S. N. Khanna, A. Sen, A. C. Reber, M. Qian, K. M. Davis, S. J. Peppernick, A. Ugrinov, M. D. Merrit, *Nano Lett.* **2007**, *7*, 2734.
[401] M. A. Beswick, N. Choi, C. N. Harmer, A. D. Hopkins, M. McPartlin, D. S. Wright, *Science* **1998**, *281*, 1500.
[402] L. Diehl, K. Khodadadeh, D. Kummer, J. Strähle, *Z. Naturforsch. B* **1976**, *31*, 522.
[403] H. J. Breunig, M. E. Ghesner, E. Lork, *Z. Anorg. Allg. Chem.* **2005**, *631*, 851.

